OF-ETWI-1987-1

Hydrogeologic Characterization of the Saline Aquifers, East Texas Basin--Implications to Nuclear Waste Storage in East Texas Salt Domes

by

Charles W. Kreitler, Edward W. Collins, Graham E. Fogg,

Martin Jackson, and Steven J. Seni

assisted by

P. Brock, E. Duncan, D. Miser,

B. Richter, R. Senger, and H. V. Wuerch

This work was supported by U.S. Department of Energy

under Contract No. DE-AC97-80ET46617

Bureau of Economic Geology

W. L. Fisher, Director

The University of Texas at Austin

Austin, Texas 78713

CONTENTS

FIGURES

TABLES

APPENDICES

The raw data displayed in Appendix B were purchased as Proprietary Data under agreement with Petroleum Information Corporation and cannot be shown in the final report. However, interpretations of these data are included in the body of this report. For further information contact the Bureau of Economic Geology.

ABSTRACT

Ground waters in the deep aquifers (Nacatoch to Travis Peak) range in salinity from 20,000 to over 200,000 mg/l. Based on their isotopic compositions, they were originally recharged as continental meteoric waters. Recharge probably occurred predominantly during Cretaceous time; therefore, the waters are very old. Because the basin has not been uplifted, and faulting of the northern and western sides, there are no extensive recharge or discharge zones. The flanks of domes and radial faults associated with domes may function as localized discharge points. Both the water chemistry and the hydraulic pressures for the aquifers suggest that the basin can be subdivided into two major aquifer systems: (1) the upper Cretaceous aquifers (Woodbine and shallower) which are hydrostatic to subhydrostatic and (2) the deep lower Cretaceous and deeper formations (Glen Rose, Travis Peak, and older units), which are slightly overpressured.

The source of sodium and chloride in the saline waters is considered to be from salt dome dissolution. Most of the dissolution occurred during the Cretaceous. Chlorine-36 analyses suggest that dome solution is not presently occurring. Salinity cross sections across individual domes do not indicate that ongoing solution is an important process.

The major chemical reactions in the saline aquifers are dome dissolution, albitization, and dedolomitization. Albitization and dedolomitization are important only in the deeper formations. The high Na concentrations in the deeper aquifers system results in the alteration of plagioclase to albite and the release of Ca into solution. The increase in Ca concentrations causes a shift in the calcite/dolomite equilibrium. The increase in Mg results from dissolution of dolomite.

The critical hydrologic factors in the utilization of salt domes for disposal of high-level nuclear waste are whether the wastes could leak from a candidate dome and where they would migrate. The following conclusions are applicable to the problem of waste isolation in salt domes.

(1) Salt domes in the East Texas Basin have extensively dissolved. The NaCl in the saline aquifers is primarily from this process. Major dissolution, however, probably occurred in the Cretaceous time. There is little evidence for ongoing salt dome dissolution in the saline aquifers.

(2) If there was a release to a saline aquifer, waste migration would either be along the dome flanks or laterally away from the dome. If there is a permeability conduit along the dome flanks, then contaminants could migrate to the fresh-water aquifers provided an upward hydraulic gradient exists. Calculation of performance assessment scenarios must take into account whether there is potential for upward flow between saline aquifers at repository level and the fresh water aquifers. If an upward flow potential exists, upward leakage along the dome flanks should be used as the worst-case scenario.

INTRODUCTION

The suitability of salt domes in the East Texas Basin, Texas, for long-term isolation of nuclear wastes is, in part, dependent on the hydrologic stability of the salt domes and the hydrogeologic conditions around the domes. The two prime hydrogeologic issues can be defined as follows: (1) Can salt dissolution breach a dome and permit a repository leak during the life of the repository? and (2) What is the regional aquifer hydrology which determines where radionuclides would migrate (Kreitler, 1979; Fogg and Kreitler, 1981)?

In the studies of the Bureau of Economic Geology on the East Texas Basin much of the emphasis on these two primary issues has been in the shallow fresh ground water aquifers that surround the candidate domes. These shallow aquifers, the Wilcox-Carrizo and Queen City aquifers, represent a major water supply for the region (Fogg and Kreitler, 1982; Fogg, Seni, and Kreitler, 1983). These units have an abundance of data to interpret the physical hydrology and hydrogeochemistry.

The fresh-water aquifers, however, represent only a thin upper layer (maximum thickness of 2,000 ft) to a basin that contains up to 15,000 ft of sedimentary rocks. These deeper formations contain saline waters and constitute another hydrologic system that is separate from the fresh-water aquifers. A potential nuclear waste repository would be located at a depth which would be either transitional between fresh and saline ground-water systems or completely within the saline system. The two issues of dome dissolution and radionuclide migration that have been addressed for the fresh-water aquifers must similarly be addressed for the saline aquifers. This report addresses these problems in the saline aquifers of the East Texas Basin.

This report addresses the general characteristics of deep-basin hydrology. Site-specific studies of candidate domes are not conducted, because of the lack of detailed data surrounding any one dome. The availability of hydraulic and geochemistry data is much more limited than for the fresh-water aquifers. Because the Wilcox-Carrizo, Queen City aquifers are major water suppliers for the region, an extensive data base has been collected by state agencies over the years. In contrast, study of the saline aquifers is dependent on data available from oil and gas wells which are much more limited.

Based on the data from previously analyzed oil field samples and samples collected specifically for this study, the following approach has been taken to address these two prime issues. One is to determine the source of the water by isotopic analyses. The hydrogen and oxygen isotopic values can be used to indicate whether the basinal water originated as oceanic waters or were meteoric waters recharged on the continent. Two is to determine whether the domes are the source of salinity in the saline formations. Salinities in these deep formations range from 20,000 to over 200,000 mg/l. Is the source of this salinity from salt dome dissolution over the history of the basin? Mass-balance approaches can help define where and when the salt was dissolved. Three is to determine the important geochemical reactions that occur in the basin. The chemical composition of these waters varies from Na-Cl type to Na-Ca-Cl type. The three geochemical reactions of salt dissolution, albitization and dedolomitization appear to control the chemical composition. By understanding the evolution of the water chemistry it is possible to delineate major hydrologic systems in the basin. Four is to determine the major hydrologic systems from the pressure data of available drill-stem tests. With the information and interpretations from these sections, preliminary conclusions can be drawn on the hydrologic characteristics of the saline aquifers and whether dome dissolution and radionuclide transport are critical problems in the deep saline aquifers.

REGIONAL GEOLOGIC SETTING OF EAST TEXAS BASIN

The East Texas Basin is one of three inland Mesozoic salt basins in Texas, Louisiana, and Mississippi that flank the northern Gulf of Mexico (fig. 1). About 5,791 m (19,000 ft) of Mesozoic and Tertiary strata are preserved in the central parts of the East Texas Basin. These rocks overlie metamorphosed Paleozoic Ouachita strata, which are probably a continuation of the Appalachian foldbelt (Lyons, 1957; Wood and Walper, 1974; McGookey, 1975).

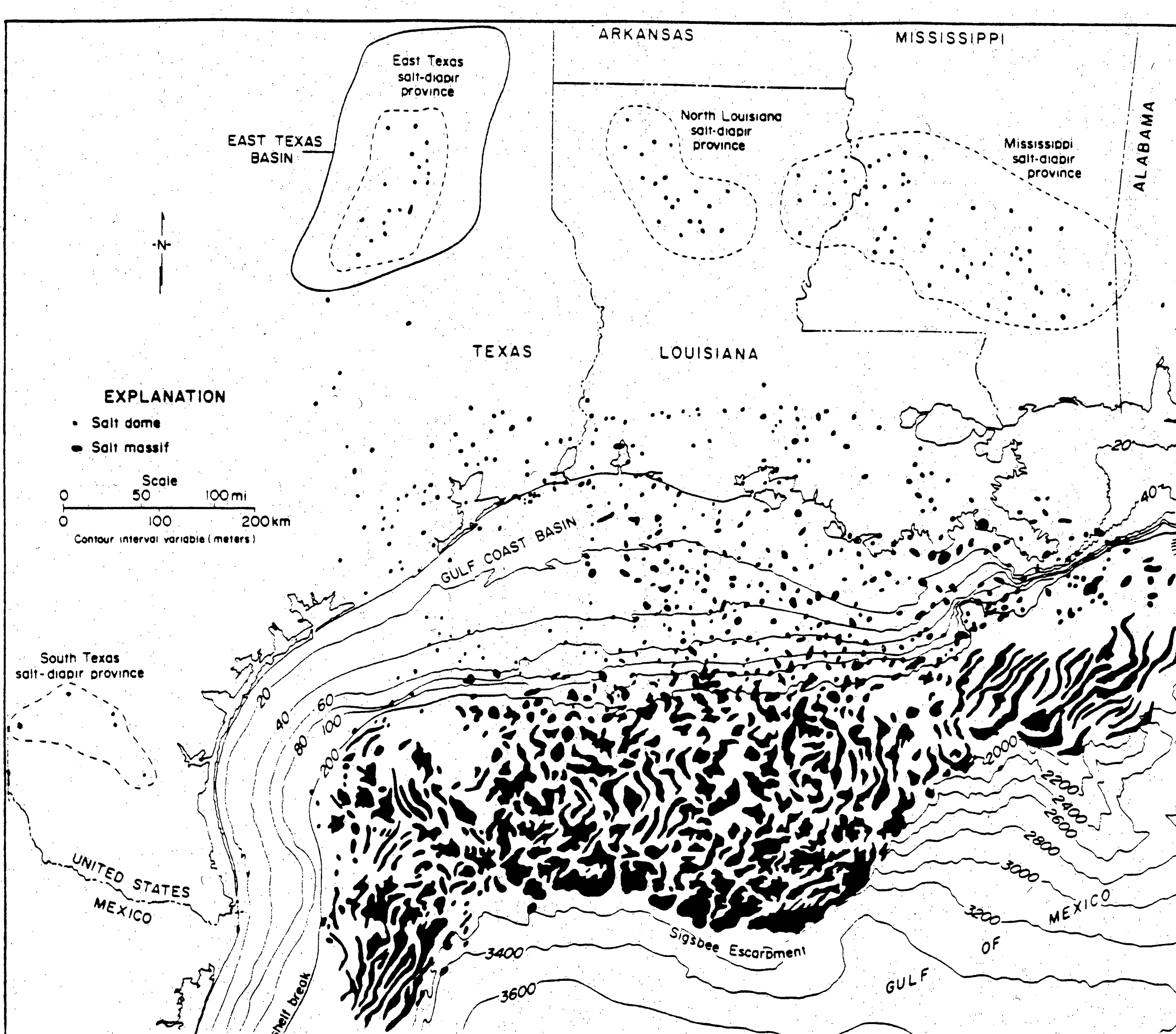

Figure 1. Map showing the East Texas Basin, Gulf Coast Basin, location of inland salt-diapir provinces and salt domes (after Martin, 1978).

The general stratigraphy (fig. 2) and structure of the East Texas Basin (fig. 3) have been summarized in many articles (e.g., Eaton, 1956; Granata, 1963; Bushaw, 1968; Nichols and others, 1968; Kreitler and others, 1980, 1981; Wood and Guevara, 1981; Jackson, 1980; and Jackson and Seni, 1983).

Basin Stratigraphy

The evolution of this basin is briefly summarized by Jackson and Seni (in press, 1983). The Jurassic Louann Salt was deposited on a planar angular unconformity across Triassic rift fill and Paleozoic basement (fig. 4). The early post-Louann history of the basin was dominated by slow progradation of platform carbonates and minor evaporites during Smackover to Gilmer time. After this phase of carbonate-evaporite deposition, massive progradation of Schuler-Hosston siliciclastics took place in the Late Jurassic-Early Cretaceous. Subsequent sedimentation comprised alternating periods of marine carbonate and siliciclastic accumulation. By Oligocene time subsidence in the East Texas Basin had ceased, and major depocenters shifted to the Gulf of Mexico. Paleocene and Eocene strata crop out in most of the basin, indicating that net erosion charcterized the last 40 million years.

Agagu and others (1980) in a more detailed discussion characterized the basin infilling as six regional depositional sequences and is quoted below.

The Eagle Mills-Louann sequence (Upper Triassic-Middle Jurassic).--This sequence was initiated by deposition of the undated continental Eagle Mills red beds. The Eagle Mills red beds are composed of red-brown shales, sandstones, and unfossiliferous limestones, which are unconformably overlain by the Werner Formation. Lower sections of the Werner consist of conglomerates and fine- to coarse-grained sandstones that grade upward into finer clastics and evaporites in the upper part of the formation. Halite interbeds in the Werner progressively increase volumetrically toward the top of the formation and are transitional into the conformably overlying Louann Salt (Nichols and others, 1968).

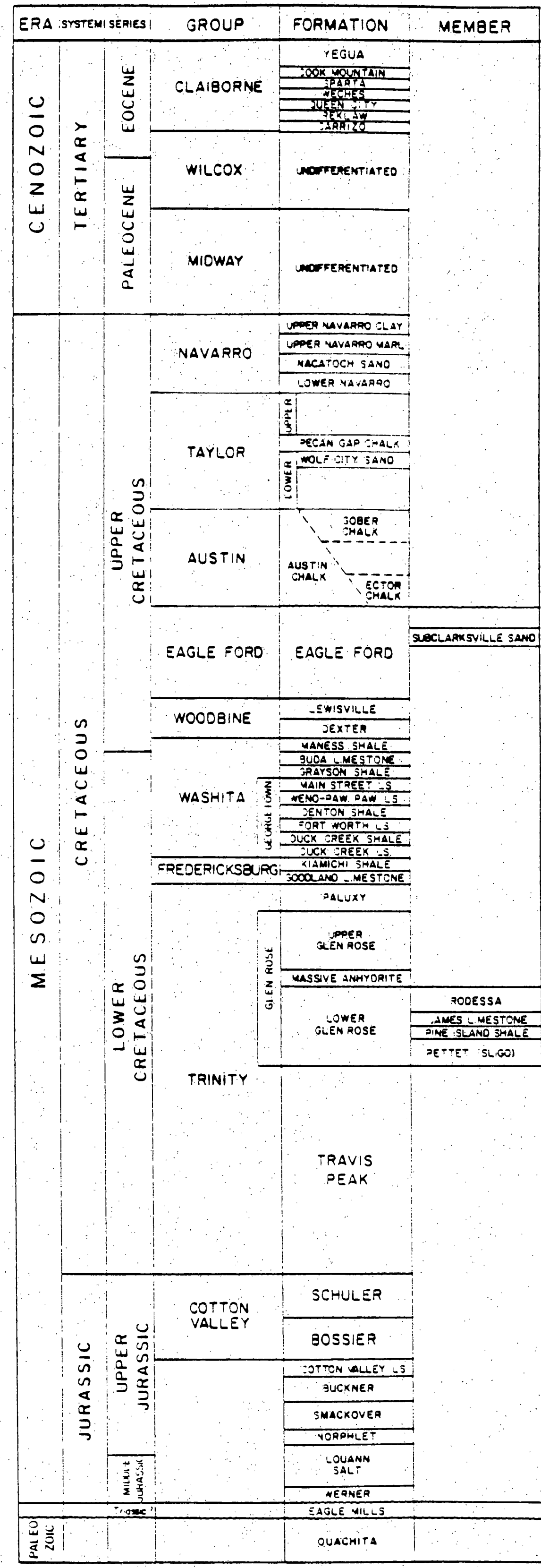

Figure 2. Stratigraphic column of East Texas Basin (from Wood and Guevara, 1978).

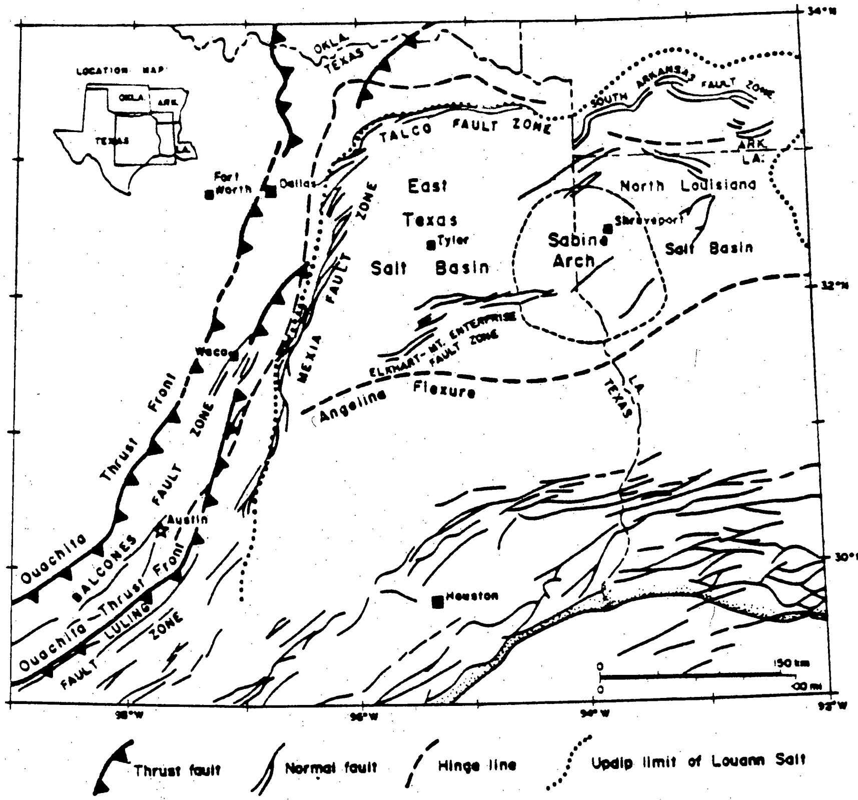

Figure 3. Regional tectonic setting of the East Texas Basin (from Jackson, 1982).

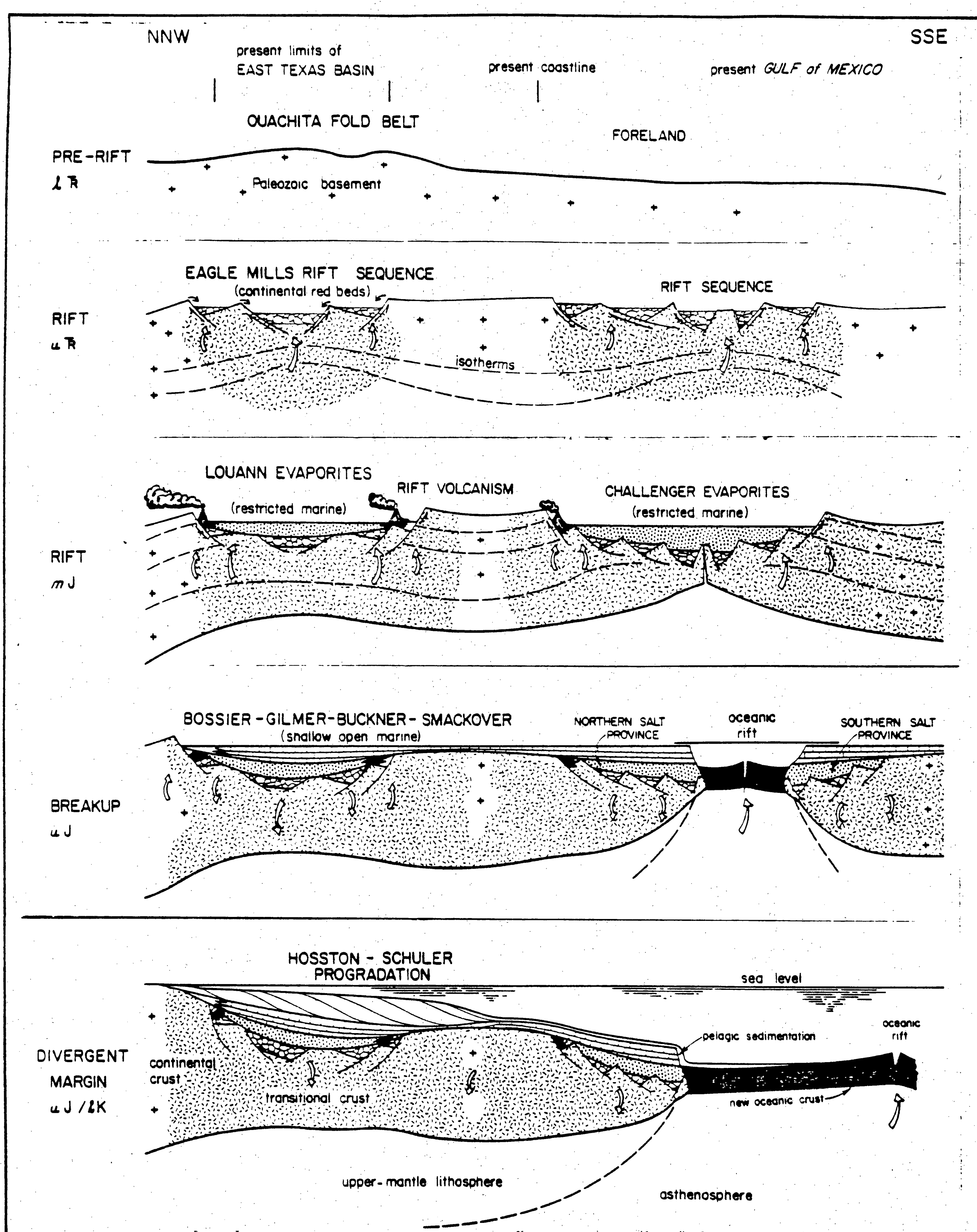

Figure 4a. Schematic northwest-southeast sections showing evolutionary stages in the forming of the East Texas Basin and adjoining Gulf of Mexico (from Jackson and Seni, 1983).

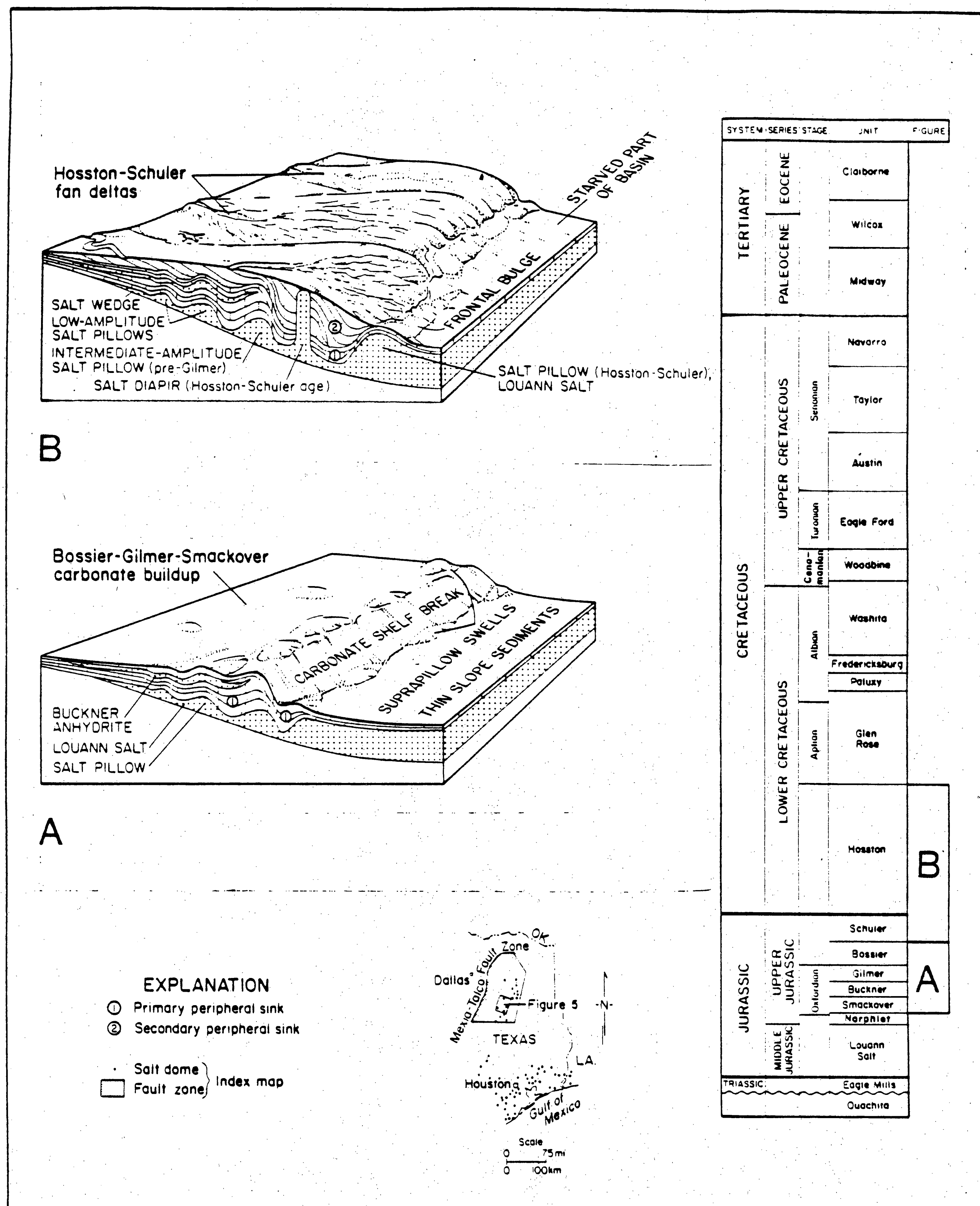

Figure 4b. Schematic block diagram showing relationships between salt flow and sediment accumulation during early period of evolution of the East Texas Basin. A. Initiation of salt flow in Late Jurassic. B. Initiation of Group 1 diapirs in Late Jurassic-Early Cretaceous (after Jackson and Seni, 1983).

The Louann Salt consists of white, gray to blue halite with minor amounts of anhydrite. Upper parts of the formation exhibit some red plastic shales transitional into the conformably overlying Norphlet Formation (Nichols and others, 1968). The partially restricted nature of the East Texas Basin during its initial stages of formation (Wood and Walper, 1974) provided an ideal setting for large-scale evaporitic processes, which have not been repeated in the basin.

Norphlet-Bossier sequence (Upper Jurassic).--The Norphlet Formation consists of sandstones, siltstones, and red shales. The basal part contains halite, anhydrite, and dolomite transitional into the subjacent Louann evaporites (Nichols and others, 1968). The relatively thin Norphlet Formation is conformably overlain by the Smackover Formation, which documents a regressive phase between deposition of the Louann Salt and the Smackover Limestone.

The Smackover Limestone here consists of a basal laminated micrite that grades upward into a pelletal micrite and ultimately into a coated grainstone. The Smackover Limestone is overlain by and is in part correlative with the Buckner Formation, which contains red sandstones in the western and northern margins of the basin and grades basinward into evaporites, shales, dolomites, and limestones (Nichols and others, 1968). The Smackover-Buckner strata document a shoaling sequence from subtidal in the lower Smackover Limestone to supratidal conditions in the Buckner Formation. The Cotton Valley Limestone and Bossier Formation are deeper water, gray, micritic limestones and gray to black shales (Nichols and others, 1968) that onlap the Buckner supratidal facies, an indication of a minor sequence boundary above the Smackover Formation.

Schuler-Glen Rose sequence (Upper Jurassic-Lower Cretaceous).--The Schuler and Travis Peak Formations attest to the high rate of terrigenous clastic influx during Late Jurassic and the Early Cretaceous. They compose a thick sequence (900 m, 3,000 ft) predominantly of sandstones interbedded with dull red and green-gray shales (Nichols and others, 1968). The Schuler-Travis Peak sequence onlaps the subjacent marine units despite its strongly terrigenous character and is probably an example of coastal onlap.

The Glen Rose Group consists of a thick (750 m, 2,500 ft) sequence of shallow marine, micritic, pelletal, oolitic, and shelly limestones interbedded with dark-gray shales and anhydrites (Nichols and others, 1968). The predominantly calcareous units, such as the Pettet, James, and Rodessa Members and much of the Upper Glen Rose Formation, are deeper water facies. Sandy shale units, such as the Pine Island Shale, and evaporites, such as the Massive Anhydrite, were deposited during minor influxes of fine, terrigenous sediment and deposition in supratidal environments, respectively. Terrigenous facies dominate, especially along the north and northwestern flanks of the basin.

Paluxy-Washita sequence (Lower Cretaceous).--The Paluxy Formation consists of interbeds of sandstones and shales, and rare conglomerates lie in the northern half of the East Texas Basin. Basinward, toward the south, the Paluxy gradually changes into dark-gray shales and micritic limestones (Nichols and others, 1968). The volume of terrigenous clastic sediment (up to 135 m, 450 ft) and the high rate of deposition indicate that a major though short-lived phase of fluvial-deltaic clastic influx occurred. Limestone and shales of the Fredericksburg and Washita Groups in East Texas document the Early Cretaceous sea-level high that drowned the Paluxy deltas.

Woodbine-Midway sequence (Upper Cretaceous-Paleocene).--Spasmodic uplift of the marginal areas of the East Texas Basin during Late Cretaceous to Paleocene times, accompanied by possible lowering of relative sea level, resulted in the terrigenous clastic influx marked by the Woodbine and Eagle Ford Groups. The Woodbine Group, composed mainly of fluvial and deltaic sandstone and subordinate shales, marks the peak of clastic sedimentation during this phase. The Eagle Ford Group, consisting primarily of shelf and slope shales and minor sandstones, documents the waning phase of clastic deposition.

The Austin Group initiated the transgressive and submergent phase that terminated in the Paleocene. During this depositional phase, up to 244 m (800 ft) of shelf chalks, shales, and marls were deposited with rare clastic facies that define minor variations in this sequence.

Tertiary Clastics.--The Tertiary stratigraphic sequence in the East Texas Basin is a complex unit mainly composed of fluvio-deltaic sandstones and shales. The Wilcox Group is a thick (up to 900 m, 3,000 ft) unit of fluvial and deltaic sands, clays, lignites, and marls. The Claiborne Group is similar to the Wilcox Group, but it displays some shaly, glauconitic, fossiliferous shelf/embayment units (Reklaw Formation, Weches Formation, and Cook Mountain) that alternate regionally with more sandy fluvial-deltaic units (Carrizo, Queen City, Sparta, and Yegua Formations). The entire Tertiary section constitutes a major regressive phase.

The permeable saline formations in the East Texas Basin are the Nacatoch, Eagle Ford, Woodbine, Paluxy, Glen Rose (including Rodessa and Pettet), Travis Peak (Hosston), and Cotton Valley (Schuler). These formations are considered permeable and are called saline aquifers in the text because they are oil-producing formations and not because aquifer tests were conducted to determine their permeable nature. It is implied that these formations have some permeability because they produce hydrocarbons. A more rigorous site-specific study of a candidate dome will require hydrologic testing of these deep saline aquifers to obtain accurate hydrologic properties. For this reconnaissance study of the East Texas Basin hydrology, it is sufficient to say that these formations have the potential for transmitting water.

Structural Framework

The structural framework of the East Texas Basin is summarized by Jackson (1982).

A map of the tectonic setting of the East Texas Basin (fig. 3) reveals that the western and northern margins of the basin coincide with other geologic structures varying from Pennsylvanian to Tertiary age. The Pennsylvanian Ouachita fold and thrust belt crops out in Arkansas and Oklahoma and extends to southwest Texas beneath Mesozoic cover (Thomas, 1976). Stratal shortening of Ouachita marine deposits generated northwest-converging folds and thrusts. Early Mesozoic continental rifting of this Paleozoic terrane can be inferred from the confinement of the Triassic Eagle Mills rift clastics to grabens and half grabens parallel to the Ouachita trends (Salvador and Green, 1980). Further subsidence allowed marine incursions that deposited the evaporitic Louann Salt on an eroded post-rift, pre-breakup terrane. The updip limit of the Louann Salt (fig. 4) is also parallel to the Ouachita trends, which indicates that during the Jurassic the Ouachita area was still elevated with respect to the subsiding East Texas Basin. A poorly defined monoclinal hinge line is present updip of the Louann Salt (fig. 3), but is too weak to delineate the western and northern margins of the basin. This part of the basin margin is therefore defined by the Mexia-Talco Fault Zone, a peripheral graben system active from the Jurassic to the Eocene that coincides with the updip limit of the Louann Salt (Jackson, 1982).

The Sabine Arch, a broad structural dome, forms the eastern margin of the basin. The southern margin of the basin is defined by the Angelina Flexure, a hinge line that is generally monoclinal at its ends and anticlinal in the middle. The Elkhart-Mount Enterprise Fault Zone extends from just north of the western end of the Angelina Flexure to the center of the Sabine Arch (fig. 3) (Jackson, 1982).

History of Salt Movement

Seni and Jackson (1983) described the evolution of salt structures in the East Texas Basin and is summarized as following.

The present distribution and morphology of salt structures in the East Texas Basin are shown in Figure 5. A broad amphitheater of undeformed salt, 2.7 to 4.6 km deep and 225 km long, encircles a heterogenous array of salt structures. In much of the basin center the Louann Salt is absent or so thin as to be seismically unresolvable. The salt masses can be resolved into geometric groups, each of which defines a province (fig. 5) (Jackson and Seni, 1983). (1) An outermost salt wedge consists of apparently undeformed salt ranging from 0 to 340-640 m thick. Its updip pinchout coincides with the Mexia-Talco fault zone, a symmetrical peripheral graben apparently formed by basinward creep of the Louann Salt and the post-Louann section over a décollement zone of salt (Cloos, 1968; Jackson, 1982). (2) Periclinal salt structures with low amplitude/wavelength ratios are called low amplitude salt pillows. These pillows are flanked by

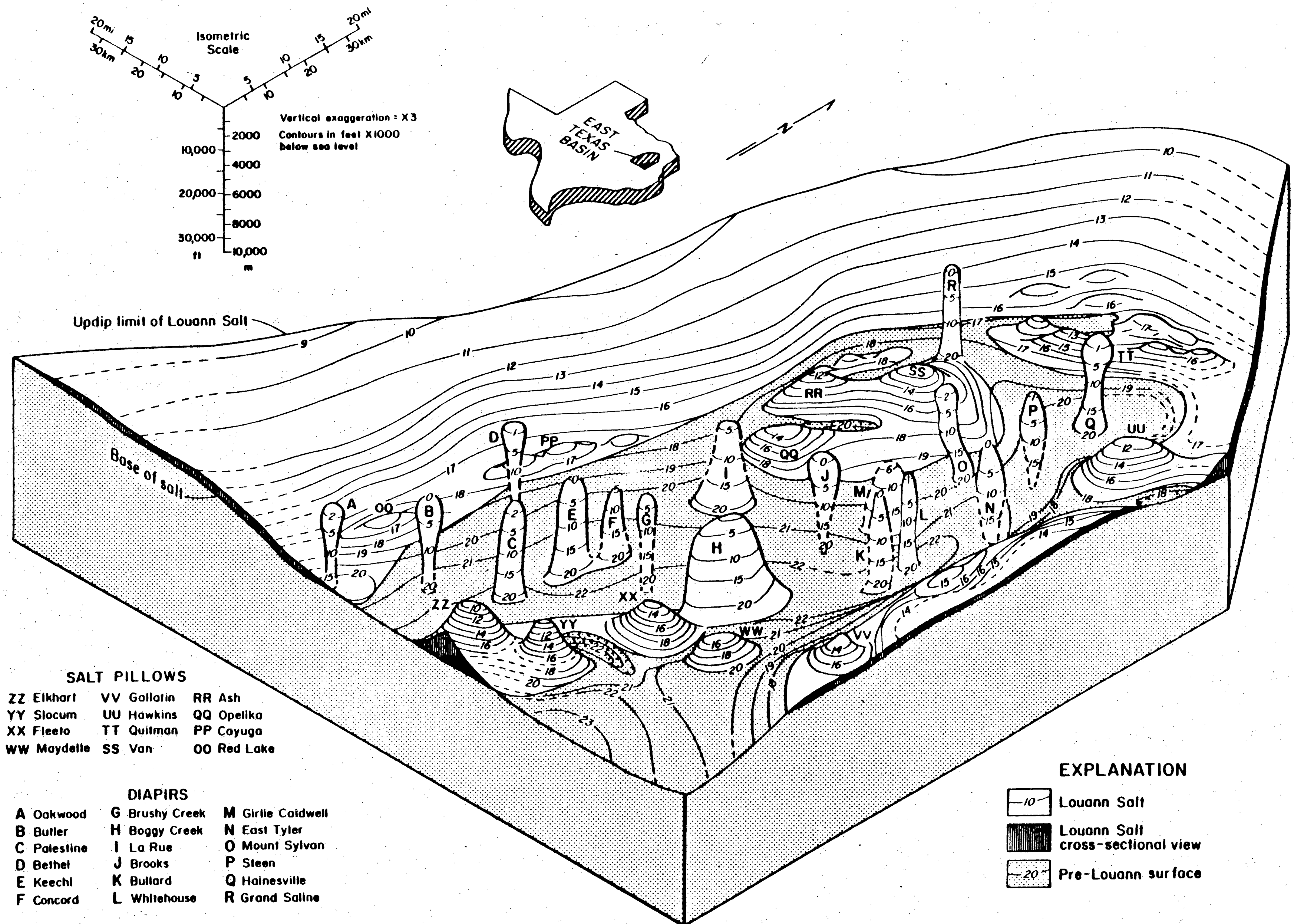

Figure 5. Isometric block diagram of the East Texas Basin showing the three-dimensional configuration of structure contours on top of Louann Salt, or, where salt is absent, on top of basement (from Jackson and Seni, 1983).

synclines of Louann Salt. The Louann Salt was originally at least 550 to 625 m thick before deformation; 600 m is therefore suggested as the approximate minimum thickness of mother salt required to allow formation of salt structures in the East Texas Basin. Overburden thickness was about 500 m throughout provinces 1 through 3 at the start of salt movement. (3) Intermediate-amplitude salt pillows are commonly separated by synclines evacuated of salt and are larger than pillows of province 2. Original thickness of the salt source layer here is estimated as 550 to > 760 meters. (4) The salt diapirs of the diapir province in the basin center are the most mature salt structures. They have all partially "pierced" their overburden and have risen to within 23 m (Steen Dome) to about 2,000 m (Girlie Caldwell Dome) of the present surface.

The earliest record of movement in the Louann Salt is in the overlying shallow-marine interval below the top of the Upper Jurassic Gilmer Limestone. This seismic unit thins over salt anticlines of province 2, indicating the growth of low-amplitude salt pillows in pre-Gilmer time (Jackson and Harris, 1981). The overlying Upper Jurassic marine strata formed an aggrading, slowly prograding, carbonate wedge (Bishop, 1968) that loaded the salt fairly uniformly (fig. 4b).

In Late Jurassic and Early Cretaceous time the Schuler-Travis Peak clastics prograded rapidly across the carbonate platform as coalescing sand-rich deltas. Progradation slowed on crossing the shelf break, but the thick deltas continued to advance as a linear front into the previously starved basn (fig. 4b). Loading of the pre-Schuler substrate by the advancing linear depocenters would have squeezed salt ahead as a frontal bulge to form a salt anticline (cf. Ramberg, 1981, p. 282-286). Increase in sediment supply for progradational rate would bury the frontal anticline, thereby initiating a parallel, but more distal, salt anticline. These anticlines, which may have been formed partly by gravity gliding as well as differential loading, were ridges of source rock from which the salt diapirs grew by budding upward.

The evolution of many of the salt pillows to salt diapirs started by mid-Early Cretaceous time when salt diapirs were growing in three areas around the periphery of the diapir province, starting at about 130 m.y. ago (Seni and Jackson, 1983). At least two areas coincide with the clastic depocenters described above. These early diapirs thus appear to have been localized by loading on the salt-cored anticlines in front of the prograding Schuler-Travis Peak deltas.

By the mid-Cretaceous when maximum sedimentation was taking place in the basin center, a second generation of diapirs evolved, via a pillow stage, from the thick salt layer there. Sites of diapir initiation migrated from the basin center northward along the basin axis.

The diapirs on the northern and western margin of the diapir province had an entirely different origin. In Late Cretaceous time, subsidence of the East Texas Basin had declined exponentially to relatively low rates. Tilting of the basin margins by loading of the basin center would have encouraged basin-edge erosion. Local unconformities exist over Hainesville Dome (Loocke, 1978), and 150 to 200 km^3 of salt are calculated to be missing. The precursor salt pillow was breached by erosion; salt withdrawal through extrusion formed an enormous secondary peripheral sink, the largest in the East Texas Basin. Erosional breaching of the faulted crests of salt pillows might also have initiated diapirism of the first and second generations of diapirs, but we have no unequivocal evidence for this hypothesis.

All the east Texas domes have risen very slowly since the end of the Mesozoic (mean net rate = 35 m/m.y.). No effects of salt withdrawal have been transmitted to the surface since the Paleocene; the diapirs are thus inferred to have risen by basal necking in the Tertiary.

ORIGIN OF WATERS IN THE SALINE AQUIFERS, EAST TEXAS BASIN

Introduction--Summary

Based on hydrogen and oxygen isotopic data, the saline waters in the East Texas Basin appear to have a continental meteoric origin. If there were oceanic waters originally present, they have been flushed by meteoric water. The presence of meteoric water does not, however, imply that these waters are geologically young. The addition of meteoric water has probably been ongoing since early Cretaceous time.

Procedures

Fifty water samples were collected and analyzed for $\delta^{18}O$ and $\delta^{2}H$ (fig. 6 and table 1). Analyses were performed by Global Geochemistry Corporation. For $\delta^{18}O$ measurements brine samples were distilled before equilibration with carbon dioxide. Table 1 shows the error based on replication of samples.

Fourteen samples are not included in further analysis of data because these samples were not considered as representative of natural subsurface conditions. This is based on the extremely low Na, Cl, Ca, Br concentrations for their respective depths (table 2). (See p. 89 and tables 2 and 2a for more complete discussion.)

Definition of Terms

Several terms are used in this paper that are used in various ways in the scientific literature. It is therefore appropriate to define these terms to avoid ambiguity.

Meteoric water: Meteoric waters are surface waters or shallow ground waters. They have not undergone significant isotopic changes of the $\delta^{2}H$ or $\delta^{18}O$ values because of rock-water geochemical reactions. The ratio of $\delta^{2}H$ and $\delta^{18}O$ compositions of waters world-wide plots on a straight line with the equation $\delta^{2}H = 8\delta^{18}O + 10$ (Craig, 1961).

Marine water: Oceanic waters are the ultimate source for nearly all the waters of the hydrosphere. Marine water has a $\delta^{2}H$ and $\delta^{18}O$ composition of approximately 0°/oo, 0°/oo, respectively. The isotopic composition of an average ocean water (SMOW--standard mean ocean water) does not plot on the meteoric water line because of a small isotopic fraction that results from the evaporation of sea water. Marine waters with this 0, 0 isotopic composition are expected to be trapped with marine sediments during deposition and burial.

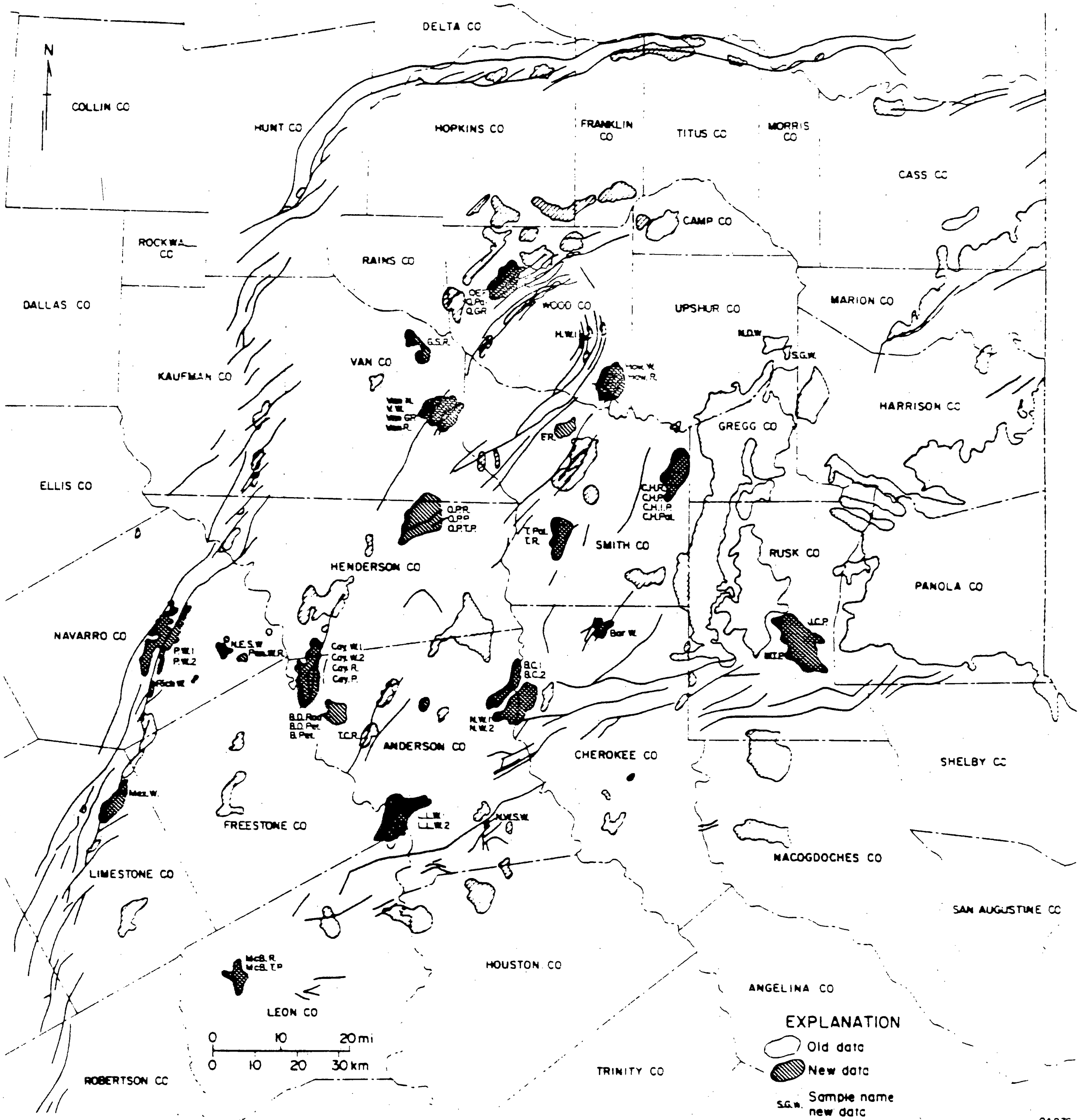

Figure 6. Location map of oil and gas fields where water samples were collected. Map indicates where both analyses from this study and previously published analyses were collected. Data in Table 1 and Appendix A.

Table 1. Chemical and isotopic composition of samples collected for this study between February and July, 1982.

Sample No.	Formation	Depth	Na	K	Ca	Mg	Cl	SO_4	HCO_3	Br	I	Al	Fe	SiO_2	H_2S
Van N	Nacatoch	1,200	7,240	24	300	86	10,950	29	439	55	13	0.235	6.69	22.5	<1
QEF	Eagle Ford	4,210	23,800	81.4	1,030	203	40,400	<4.5	187	262	29	<0.2	0.145	25.7	<0.1
B.C.1	Woodbine	3,600	37,900	125	3,250	465	65,500	120	160	140	42	<0.2	21	16	<0.1
B.C.2	Woodbine	3,600	38,300	122	3,070	500	64,000	130	170	150	40	<0.1	17	15	<0.1
C.W.1	Woodbine	4,404	35,100	112	3,400	530	61,200	90	120	150	24	<0.2	102	27	<1
N.W.1	Woodbine	4,704	35,500	169	3,190	543	62,100	110	160	150	38	<0.2	8.6	18	<1
N.W.2	Woodbine	4,704	35,700	168	3,200	545	62,100	90	150	170	39	<0.2	11	19	<1
CAY W.1	Woodbine	4,030	29,300	73	1,200	210	48,200	120	170	73	31	<0.2	0.74	24	<1
CAY W.2	Woodbine	4,030	29,600	70	1,200	210	48,500	120	160	64	31	<0.2	0.22	24	<1
BAR. W.	Woodbine	4,259	29,400	76	1,400	210	49,300	270	230	83	35	<0.2	17	20	<1
L.L.W.1	Woodbine	5,272	36,400	83	2,400	280	62,200	110	170	110	33	<0.2	1.4	26	<1
L.L.W.2	Woodbine	5,272	35,600	88	2,300	280	58,900	110	180	90	34	<0.2	6.4	28	<1
P.W.1	Woodbine	3,000	4,400	24	74.5	27	6,500	60	350	32	5	<0.1	0.10	30	<1
P.W.2	Woodbine	3,000	5,070	26	86.6	28	7,700	55	340	38	5	<0.1	0.04	30	<1
V.W	Woodbine	2,900	25,100	110	1,160	290	43,100	60	120	250	27	<0.2	0.38	24	<1
N.W.S.W.	Woodbine	5,400	32,500	170	2,700	460	58,100	73	98	280	37	<0.2	11	35	<1
N.E.S.W.	Woodbine	3,390	11,200	41	220	70	17,900	58	300	25	12	<0.2	0.04	24	<1
HAW.W.	Woodbine	4,531	35,200	99	2,300	290	59,500	250	170	120	33	<0.2	2.7	26	<1

Table 1. (cont.)

Sample No.	Sr	Ba	Ti	Cu	Mn	Zn	Pb	Li	F	B	Br/Cl $x10^{-4}$	δ^2H	$\delta^{18}O$
Van N	26.3	17.6	0.055	<0.01	0.281	0.022	<0.1	0.675	0.4	9.89	50.22	-30	-3.83
QEF	224	25.7	<0.05	0.022	0.913	<0.02	<0.2	1.08	0.6	11.6	64.9	-27	-1.75
B.C.1	550	3.5	<0.05	<0.02	2.4		<0.2	3.0	0.8	25	21.4	-33	0.03
B.C.2	550	3.6	<0.03	<0.01	2.3		<0.1	2.5	0.6	21	23	-31	0.00
C.W.1	510	5.8	<0.05	1.6	3.9		<0.2	3.4	1.3	30	24.5	-33,-31	-1.57
N.W.1	620	4.3	<0.05	<0.02	1.8		<0.2	3.7	0.8	34	24.2	-31,-29	0.87
N.W.2	620	4.3	<0.05	<0.02	1.8		<0.2	3.9	0.9	35	27.4	-31,-30	0.63
CAY W.1	300	2.7	<0.05	<0.02	0.71	<0.02	<0.2	2.4	0.9	19	15.1	-34	0.10
CAY W.2	300	2.5	<0.05	<0.02	0.39	<0.02	<0.2	2.4	0.9	19	13.2	-29	0.29
BAR.W.	340	1.7	<0.05	<0.02	0.74	<0.02	<0.2	2.6	1.1	21	16.8	-22	-0.56
L.L.W.1	510	3.4	<0.05	<0.02	1.6	<0.02	<0.2	3.4	0.9	19	17.7	-33	0.70
L.L.W.2	510	5.0	<0.05	<0.02	1.1	<0.02	<0.2	3.9	1.0	19	15.2	-29	0.78
P.W.1	13	9.2	<0.03	<0.01	0.06	0.02	<0.1	0.54	1.2	22	49	-28	-3.81
P.W.2	15	8.8	<0.03	<0.01	0.06	<0.01	<0.1	0.56	1.0	23	49	-29	-3.70
V.W	280	4.3	<0.05	<0.02	0.77	<0.02	<0.2	2.1	0.7	18	58	-32	-1.30
N.W.S.W.	660	8.8	<0.05	<0.02	2.0	<0.02	<0.2	5.5	0.7	29	48.2	-30	1.16
N.E.S.W.	54	6.8	<0.05	<0.02	0.08	<0.02	<0.2	1.0	1.2	23	14	-29	-2.03
HAW.W.	430	2.6	<0.05	<0.02	1.4	<0.02	<0.2	3.4	1.0	20	20.2	-29	0.17

Table 1. (cont.)

Sample No.	Formation	Depth	Na	K	Ca	Mg	Cl	SO_4	HCO_3	Br	I	Al	Fe	SiO_2	H_2S
MEX. W	Woodbine	3,100	12,270	44	570	142	20,300	<6	263	124	19	0.236	0.041	22.2	<1
RICH. W	Woodbine	3,300	5,285	22	94	29	8,280	<6	350	39	7	0.246	0.047	24.8	<1
S.G.W.	Woodbine	3,800	19,100	76	1,620	235	33,200	<6	150	155	37	0.475	8.37	41.2	<1
N.D.W	Woodbine	3,700	21,800	69	835	215	36,200	<6	280	233	32	0.470	0.109	24.7	<1
C.H. Pal.	Paluxy	5,600	28,700	67.4	1,680	256	48,000	800	164	173	33	<0.2	0.239	23.4	<0.1
Q. Pal.	Paluxy	6,230	39,000	159	9,540	936	81,300	389	54	1,160	24	0.436	6.46	23.0	<0.1
QGR	Glen Rose	7,320	50,200	147	11,700	1,008	103,500	286	53	470	44	0.452	32.3	28.6	<0.1
B.D.ROD.	Rodessa	10,100	70,900	2,350	31,500	1,800	169,000	15	43	1,700	40	<0.2	110	36	<0.1
HAW.R.	Rodessa	8,300	27,300	540	24,100	1,300	90,300	85	51	710	34	0.50	160	12	<1
T.C.R.	Rodessa	9,000	42,490	250	14,160	1,540	87,900	132	31	597	40	0.599	113	26.0	<1
McB.R.	Rodessa	8,790	50,600	1,200	13,300	712	101,000	269	83	460	47	0.578	1.60	51.5	<1
PAN.W.R.	Rodessa	6,460	65,900	390	24,350	2,674	147,000	225	18	1,800	35	0.721	27.3	20.7	<1
C.H.R	Rodessa	7,680	53,800	318	28,000	2,140	127,000	160	23	1,200	32	0.986	52.2	72.0	<0.1
G.S.R	Rodessa	8,200	68,200	736	20,000	2,014	165,000	83	0	2,290	31	1.05	184	48.4	<0.1

Table 1. (cont.)

Sample No.	Sr	Ba	Ti	Cu	Mn	Zn	Pb	Li	F	B	Br/Cl x10-4	δ^2H	$\delta^{18}O$
MEX. W	115	58.6	0.052	<0.01	0.479	0.029	<0.1	1.0	0.6	21.3	61.1	-33	-2.30
RICH. W.	17	24	0.059	<0.02	0.083	0.017	<0.1	0.415	1.5	18.5	47	-40	-4.15
S.G.W.	280	20	0.102	<0.02	1.53	0.038	<0.2	1.068	6.1	18.8	46.7	-26	-2.03
N.D.W	336	161	0.105	<0.02	1.88	0.030	<0.2	1.30	1.2	20.9	64.4	-31	-2.13
C.H. Pal.	158	5.10	<0.05	0.084	0.891	0.028	<0.2	1.97	0.9	30.9	36.0	-26	1.67
Q. Pal.	526	2.57	0.068	0.037	3.59	0.142	<0.2	6.53	1.4	42.6	142.7	-24,-25	0.43
Q GR	636	1.15	0.08	0.033	0.589	0.097	<0.2	6.52	2.4	58.4	45.4	-26	2.82
B.D.ROD.	3,000	53	<0.05	<0.02	26	.	<0.2	75	6.4	51	100.6	-31	2.83
HAW.R.	1,700	36	<0.05	<0.02	61	23	<0.2	25	1.4	13	78.6	-32	-2.24
T.C.R.	980	6	0.136	0.163	1.07	0.068	<0.2	19.5	7.5	67.4	67.9	-23	7.11
McB.R.	903	1.76	0.392	<0.02	0.180	0.045	<0.2	70.3	7.5	149	45.5	-27	8.95
PAN.W.R	1,270	2.19	0.150	<0.02	0.452	0.423	<0.2	15.1	5.4	45.9	122.4	-24	1.56
C.H.R	1,174	3.87	0.152	0.077	1.92	2.14	<0.4	16.1	4.2	72.0	94.5	-11	5.88
G.S.R	1,700	8.46	0.197	0.111	8.77	7.34	<0.4	19.3	2.0	48.4	138.8	-18	2.60

Table 1. (cont.)

Sample No.	Formation	Depth	Na	K	Ca	Mg	Cl	SO_4	HCO_3	Br	I	Al	Fe	SiO_2	H_2S
VAN.R.	Rodessa	5,220	23,400	130	7,530	890	50,000	18	130	600	12	0.587	589	9.6	<1
B.Pet.	Pettet	9,500-10,500	69,900	2,000	25,800	1,690	154,000	70	39	1,400	50	<0.2	49	34	<0.1
JCP	Pettet	7,200	46,400	773	13,100	749	99,600	82	30	746	23	0.503	315	17.8	<0.1
McB. T.P	Travis Peak	11,200	56,700	3,340	12,700	452	108,000	214	20	801	56	0.545	37.2	78.6	<1
OP.T.P	Travis Peak	10,000	52,800	2,580	17,800	1,230	111,000	89	23	1,540	22	0.625	132	47.4	<1
MTP	Travis Peak	7,300	60,600	1,730	18,100	1,200	133,000	217	27	1,230	22	0.783	118	32.9	<0.1

Table 1. (cont.)

Sample No.	Sr	Ba	Ti	Cu	Mn	Zn	Pb	Li	F	B	Br/Cl $x10^{-4}$	$\delta^{2}H$	$\delta^{18}O$
VAN.R.	306	39	0.127	<0.02	5.71	0.040	<0.2	4.04	0.4	29.2	120	-35	-2.04
B.Pet.	2,100	33	<0.05	<0.02	9.0		<0.2	52	4.5	58	90.9	-34	4.48
JCP	840	7.79	0.093	0.061	6.26	0.037	<0.2	24.4	1.0	44.2	74.9	-22	1.49
McB. T.P	976	11.4	0.129	<0.02	3.31	0.046	<0.2	35.8	214	37.2	74.2	-24	3.17
OP.T.P	1,140	12.7	0.151	<0.02	8.86	4.93	<0.2	22.4	89	132	138	-21	0.63
MTP	1,180	12.8	0.125	0.060	11.1	7.93	0.713	48.6	0.8	61.4	92.5	-19	2.73

Table 2. Chemical analyses of deleted data.

Sample No.	Formation	Depth	Na	K	Ca	Mg	Cl	SO_4	HCO_3	Br	I	Al	Fe	SiO_2	H_2S
H.W.I	Woodbine	9,776	67	1.1	45	1.9	126	3	52	7.5	3.8	<0.1	41	7.7	<1
T.Pal.	Paluxy	7,500	8,000	7,210	1,130	151	21,800	<4.5	69	32	10	<0.1	103	16.5	<0.1
Van GR	Glen Rose	7,230	4,400	24	74.5	27	6,500	60	350	32	5	<0.1	0.10	30	<1
CAY.R	Rodessa	7,460	11.2	0.89	4.45	0.79	24	<6	14	1.4	1.8	0.256	0.765	1.40	<1
OP.R	Rodessa	8,630	705	112	586	25	2,220	7	72	25	4	0.165	158	2.6	<1
T.R.	Rodessa	9,600	15,000	47.2	2,810	288	29,600	<4.5	109	106	20	0.237	115	13.0	<0.1
F.R.	Rodessa	10,660	5,600	397	3,510	1,060	19,500	286	0	42	1.8	0.274	1,180	3.6	<0.1
VAN.R.	Rodessa	5,220	23,400	130	7,530	890	50,000	18	130	600	12	0.587	589	9.6	<1
B.Pet.	Pettet	≈ 9,500-10,500	69,900	2,000	25,800	1,690	154,000	70	39	1,400	50	<0.2	49	34	<0.1
B.D.Pet.	Pettet	10,300	1,650	48	610	48	4,760	1	24	49	2.4	<0.1	190	4.6	3.4
CAY.P.	Pettet	7,550	56	1.02	6.5	10.2	92	<6	39	2.5	2	0.252	0.158	<1	<1
OP.P.	Pettet	8,900	25	1.6	27.5	1.15	72.7	<6	24	<0.5	1	0.268	0.036	<1	<1
CH.P.	Pettet	8,000	137	2.15	41.6	3.00	327	<4.5	22	2.1	0.9	<0.1	0.372	0.777	<0.1
CH.T.P	Travis Peak	8,350	36,100	649	15,800	942	90,200	77	3	895	13	0.571	170	14.9	<0.1

Table 2. (cont.)

Sample No.	Sr	Ba	Ti	Cu	Mn	Zn	Pb	Li	F	B	Br/Cl $\times 10^{-4}$	δ^2H	$\delta^{18}O$
H.W.I	3.2	0.30	<0.025	<0.01	1.1		<0.1	<0.01	0.1	1.4	595.2	-30,-32	0.38
T.Pal.	63.4	0.727	<0.025	0.020	2.39	0.027	<0.1	0.539	0.4	5.86	14.7	-32	0.05
Van GR	13	9.2	<0.03	<0.01	0.06	0.02	<0.1	0.54	1.2	22	49	-36	1.43
CAY.R	0.26	0.04	0.056	<0.01	0.270	0.014	<0.1	0.019	0.2	1.25	583	-26	2.48
OP.R.	19.6	3.8	0.038	<0.01	1.45	0.024	<0.1	0.327	<0.2	<1	112	-24	-0.30
T.R.	188	2.39	<0.05	0.030	1.78	0.034	<0.2	2.01	1.0	14.2	35.8	-34	0.22
F.R.	29.2	4.98	0.04	0.026	25.8	0.066	0.105	1.55	1.7	5.15	21.5	-31	4.30
VAN.R.	306	39	0.127	<0.02	5.71	0.040	<0.2	4.04	0.4	29.2	120	-35	-2.04
B.Pet.	2,100	33	<0.05	<0.02	9.0		<0.2	52	4.5	58	90.9	-34	4.48
B.D.Pet.	47	45	<0.03	<0.01	1.7		<0.1	0.88	0.2	7.8	102	-43	0.10
CAY.P.	0.76	0.105	0.05	<0.01	0.357	0.016	<0.1	0.01	<0.2	<1	271	-15	-0.09
OP.P.	0.7	0.081	0.054	<0.01	0.198	0.014	<0.1	0.024	<0.2	<1	70	-24,-25	1.98
CH.P.	2.47	0.282	<0.025	0.01	0.511	<0.01	<0.1	0.042	<0.2	1.15	70	-17	1.54
CH.T.P	945	8.78	0.101	0.059	13.3	4.19	<0.2	15.2	1.6	33.2	99.2	-14	-3.72

Table 2a. Type of Well and Collection Points for Deleted Data

Name	Type	Collection Point
HWI	oil	separator
T. Pal	oil	storage tank
Van GR	oil	well head
Cay, R	gas	storage tank
Op. R	oil	storage tank
T.R	gas	separator
F.R	oil	separator
B.D Det	gas	separator
Cay, P	gas	storage
OP.P	gas	storage
CH.P	oil	storage
CH.T.D.	gas	storage

Continental meteoric water: Continental meteoric waters are those waters that result from atmospheric precipitation on the continents. Generally they are on the meteoric water line but are isotopically depleted in δ^2H and $\delta^{18}O$ relative to sea water and follow the meteoric water line, as defined by the equation $\delta^2H = 8\delta^{18}O + 10$.

Isotopic Trends

Three isotopic trends are observed: $\delta^{18}O$ vs. δ^2H (fig. 7), $\delta^{18}O$ vs. depth (fig. 8), $\delta^{18}O$ vs. Cl (fig. 9).

$\delta^{18}O$ versus δ^2H (fig. 7)

$\delta^{18}O$ and δ^2H values range from -6°/oo ($\delta^{18}O$) and -20°/oo (δ^2H) to +6°/oo($\delta^{18}O$) and -15°/oo (δ^2H). The trend approaches the meteoric water line at the same $\delta^{18}O$ value expected for meteoric water in East Texas. $\delta^{18}O$ of ground water samples from the Wilcox around Oakwood dome was -4.9.

$\delta^{18}O$ versus depth (fig. 8)

The $\delta^{18}O$ values increase with depth. The $\delta^{18}O$ values from shallow waters are approximately the same as the $\delta^{18}O$ values of meteoric water in the region ($\delta^{18}O \simeq$ -5°/oo). The $\delta^{18}O$ values increase to +9°/oo. This trend is consistent for all formations sampled.

$\delta^{18}O$ versus chlorinity (fig. 9)

The $\delta^{18}O$ values increase with increasing chlorinity.

Discussion of Isotopic Values

The saline waters in the Nacatoch, Eagle Ford, Woodbine, Paluxy, Glen Rose, Rodessa, Pettet, and Travis Peak Formations all appear to have a continental meteoric water origin. The basin has been flushed of any original oceanic waters and has been replaced by meteoric water.

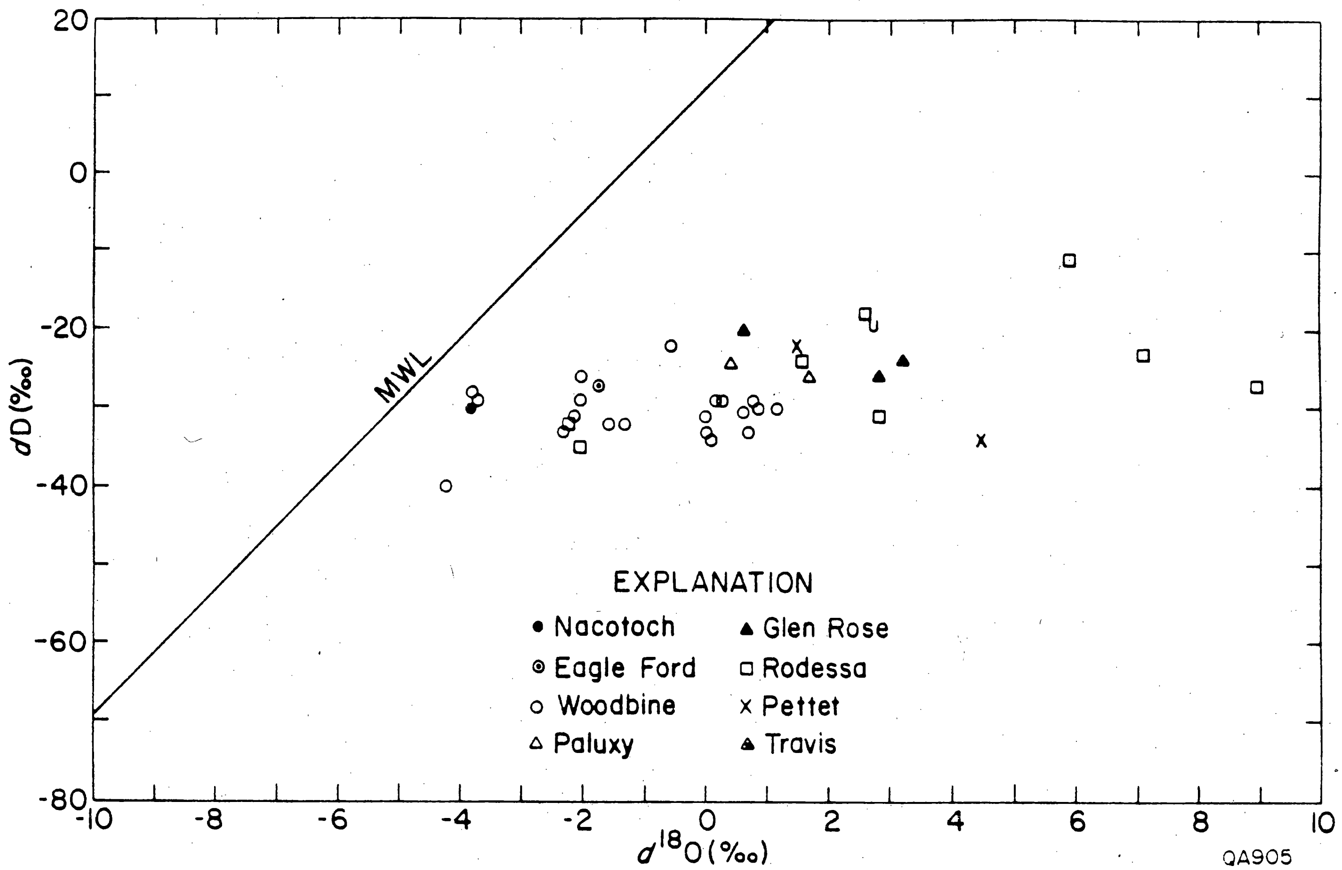

Figure 7. Hydrogen and oxygen isotopic composition of saline waters, East Texas Basin. Table 1 includes isotopic values.

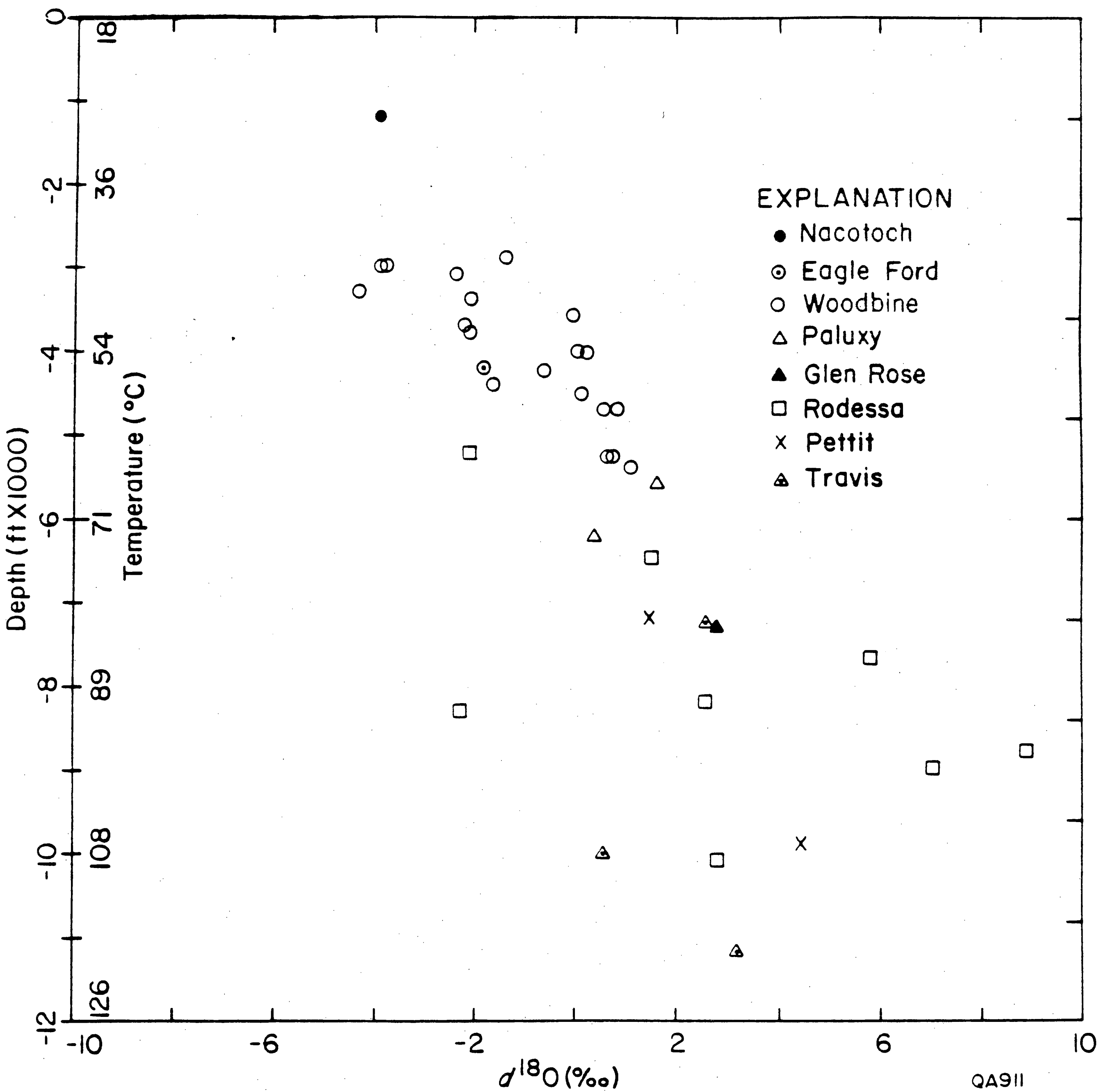

Figure 8. $\delta^{18}O$ values of saline waters, East Texas Basin versus depth (temperature). Note enrichment in $\delta^{18}O$ with increased depth (temperature). (Temperature based on average geothermal gradient of 0.9°C per 100 ft.) Isotopic analyses in Table 1.

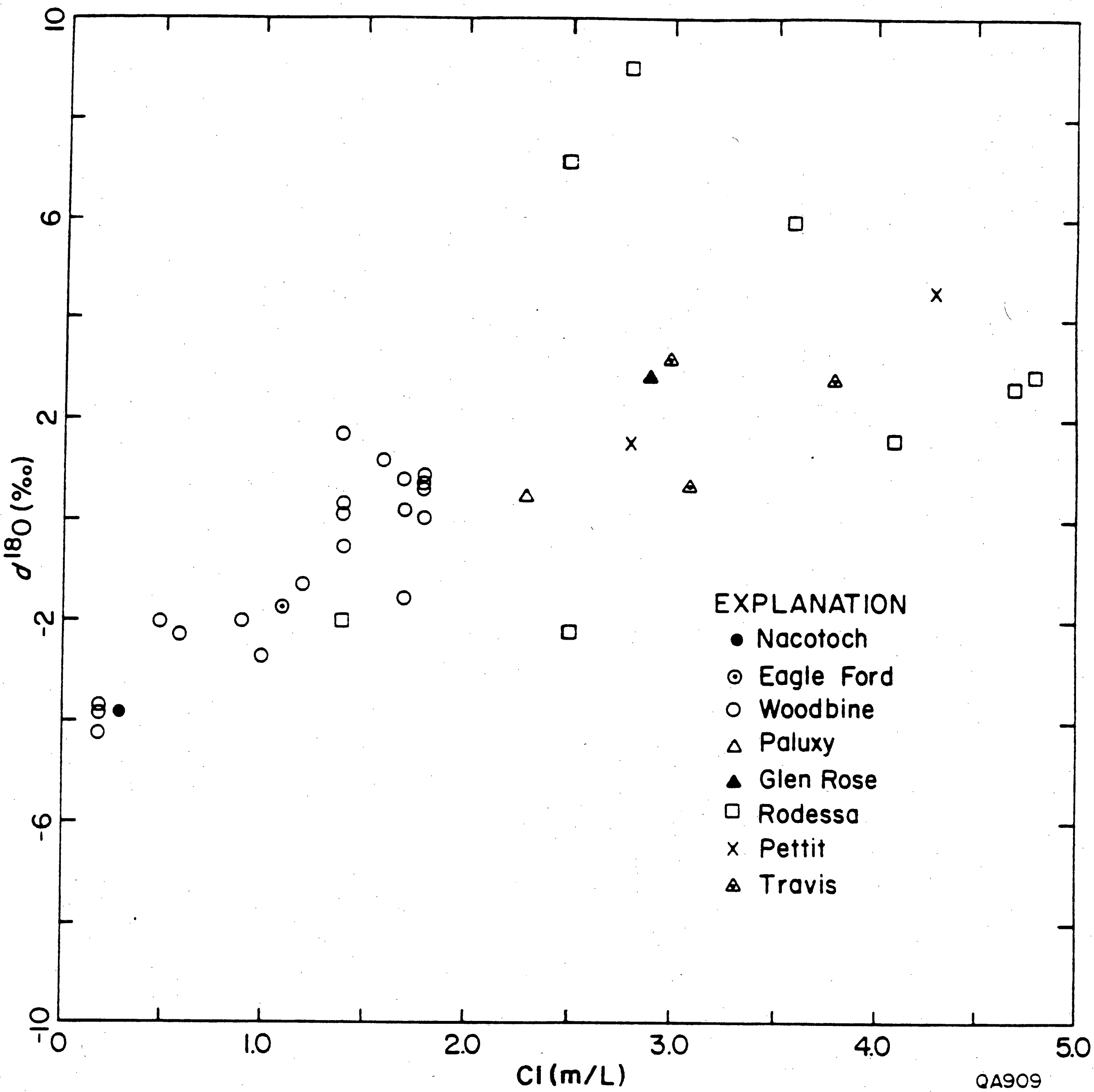

Figure 9. $\delta^{18}O$ values of saline waters versus chlorinity. Data in Table 1.

The presence of meteoric water does not, however, imply that these waters are geologically young. The flushing process was probably predominant in Cretaceous time.

These conclusions are based on the following lines of evidence. The scattergram of $\delta^{18}O$ versus $\delta^{2}H$ (fig. 7) trends back to the original isotopic composition of the meteoric water before the waters equilibrated with the sediments in the basin. With increasing depths (and temperatures) the waters reequilibrate with the oxygen in the carbonate minerals causing an enrichment of ^{18}O in the waters (a reaction documented by Clayton, 1959, 1961). The $\delta^{2}H$ values range between -20 to -30°/oo, the approximate hydrogen isotope composition of meteoric water for this region. Land and Prezbindowski (1981) found that the $\delta^{2}H$ of meteoric waters in Central Texas ranged from -20 to -30°/oo. Knauth and others (1980) found meteoric water in northern Louisiana (≈ 150 km east of East Texas Basin) with a $\delta^{2}H$ value of -30°/oo. A slight enrichment of $\delta^{2}H$ with increased $\delta^{18}O$ could be interpreted for the East Texas Basin data. Because of the minimal isotopic variation in the $\delta^{2}H$ values, regardless of enrichment of the $\delta^{18}O$, the initial $\delta^{2}H$ composition of the basinal waters was approximately -20°/oo to -30°/oo. In contrast marine waters have a δ value of approximately 0°/oo. The hydrogen data, therefore, suggest that the deep basin water originated as a continental meteoric water rather than an oceanic water entrapped during sedimentation and burial.

Clayton and others (1966) observed similar relationships for the Illinois, Michigan, and Alberta sedimentary basins. Isotopic data for each basin trended back to the isotopic composition of surface water and shallow ground water of the area. An enrichment of $\delta^{18}O$ with depth (temperature) was also observed for each basin, as was observed in the East Texas Basin (fig. 8). They attributed this enrichment with increased temperature to a shift in isotopic equilibria for the temperature dependent isotopic reaction between calcite and water. Clayton (1959, 1961) presents the experimental data that documents this isotopic reaction.

Salinity increases as $\delta^{18}O$ values become enriched. This relationship appears coincidental rather than resulting from any mutual dependent geochemical reactions. Clayton and others (1966) also observed an increase in $\delta^{18}O$ with salinity but offered no explanation for this relationship. This increased salinity with depth and oxygen isotope composition will be discussed under Source of NaCl.

Degen and others (1964) suggested that the oxygen isotope shift resulted from mixing of meteoric waters with marine waters. The isotopic data for the East Texas Basin do not agree with this interpretation. The δ^2H remains constant over the range of $\delta^{18}O$ values. If mixing was the mechanism, then there should be an isotopic shift in δ^2H as well as $\delta^{18}O$.

The isotopic shift observed by Clayton and others (1965) for the Alberta, Illinois, and Michigan basins is approximately 0.2 $^o/oo$ ($\delta^{18}O$)/°C. The isotopic shift for the waters in the East Texas Basin is 0.16$^o/oo$ ($\delta^{18}O$/°C, similar to the range observed by Clayton (table 3). For the $\delta^{18}O$ values for the different basins, the initial meteoric waters for the East Texas Basin are isotopically heavier than the other basins and have $\delta^{18}O$ values in the deep basin for similar temperature ranges which are also more enriched. This enriched isotopic range is consistent with the proximal position of the East Texas Basin to the coast in comparison to the other basins. If Degen and others' (1964) mixing model is correct, then the slope of the isotopic shift per temperature rise would not remain constant for all the basins. In contrast the $\delta^{18}O$ of the deep basin waters (the initial sea water end members) should remain constant for all basins, which it doesn't. A model requiring mixing of continental meteoric and original oceanic waters is not considered realistic for the East Texas Basin.

The presence of meteoric water through the basin does not infer that the flushing is recent or is occurring at a rapid hydrologic rate. The timing of fluid movement in the basin is interesting but not resolvable at this point. A brief review of geologic history of the basin points to hydrogeologic complexity. During Travis Peak time (Early Cretaceous) thick alluvial fan delta sediments were deposited. These rocks may have been flushed by continental meteoric waters and never contained oceanic waters. From Glen Rose to Nacatoch time (Cretaceous) the major rock units were marine and therefore contained marine waters. During this time the continental waters in the underlying Travis Peak may have been replaced by waters with a marine origin. From the Tertiary to present the basin was being infilled by

Table 3. Oxygen Isotope and Temperature Ranges of Waters from Four Interior Sedimentary Basins

Basin	Temperature Range (°C)	$\delta^{18}O$ Range (o/oo)	$\delta^{18}O$ (o/oo)/°C
Alberta[1]	30-95 (65°)	-8, +4 (12)	0.18
Illinois[1]	10-60 (50°)	-8, +2 (10)	0.2
Michigan[1]	10-60 (50°)	-9, +3 (12)	0.24
East Texas[2]	45-108 (63°)	-5, +5 (10)	0.16

[1]from Clayton and others (1965)

[2]from this study

primarily continental terrigenous sediments that were subaerially exposed. Minor marine sandstones and shales were deposited during Tertiary time but are considered insignificant in the overall character of the basin.

Incorporation of meteoric water into the different formations of the East Texas Basin may have occurred at different times in the geologic history of the basin. The isotopic data does not indicate when the water was added, just that it had a continental meteoric origin.

SOURCE OF NaCl IN THE DEEP-BASIN BRINE AQUIFERS, EAST TEXAS BASIN

Introduction--Summary

The source of dissolved sodium and chlorides in saline to brine concentrations in deep-basinal formations is enigmatic, primarily because of (1) the high solubility of halite, (2) the multiple sources (evaporites, ocean water) or methods in which brines can be concentrated (ultra-filtration), (3) the lack of a distinguishing tracer that could separate different chloride sources, and (4) our generally poor understanding of hydrologic and geochemical processes in the deep subsurface. Researchers have suggested that the elevated NaCl concentrations have resulted from at least 5 sources or mechanisms: (1) "connate waters" (original sea water) (White, 1965), (2) ultra-filtration (reverse osmosis, e.g., the trapping of dissolved species on the high pressure side of a semipermeable membrane (Graf et al., 1965; Hanshaw and Coplen, 1973), (3) drainage of bittern brine pockets entrapped in the original bedded Louann salt (Carpenter, 1978), (4) brine leaking up from an unknown or external source (Land and Prezbindowski, 1981), or (5) dissolution of halite as either bedded or domal salt (Bassett and Bentley, 1982).

This study has concluded that the source of dissolved NaCl in the saline aquifers of the East Texas Basin is the result of (5) dissolution of halite as domal salt. This conclusion is based on two different approaches: (1) a comparison of the halite that has been lost (original volume of Louann Salt minus present volume in basin) with the dissolved NaCl in the aquifers and (2) a comparison of the amount of halite that was dissolved to accumulate the volume of cap rock in salt domes with the dissolved NaCl in the deep-basin aquifers. Both approaches indicate that more halite is missing than can be accounted for by present dissolved NaCl. All the NaCl that is presently in solution can, therefore, result from dissolution of halite.

This approach does not prove that dome dissolution is the major contributor of NaCl, but does demonstrate that dome salt is a feasible source for the basin's salinity. Previous studies on the origin of saline waters have not been able to document a salt source (occult salt) or mechanism for concentrating NaCl to brine concentrations.

Dissolved NaCl in Deep-Basin Aquifers

The total volume of dissolved salt in the saline part of the East Texas Basin is estimated at 298 km^3 (table 4). This estimate is based on the sum of the average salinity times the average porosity of individual volumes of the Woodbine, Paluxy, Glen Rose, and Travis Peak formations, the units considered as the important saline aquifers in the basin.

Salt Loss

1. Approach 1. Original salt volume versus present salt volume

Comparison of the halite still in the basin (domal, anticlinal, and wedge halite) with estimated original Louann salt indicates that approximately 40 percent of the original halite is missing (6000 km^3). Salt loss is predominantly from the diapirs. Approximately 70 percent of the salt originally in the diapir province is calculated to be missing. Salt was lost by both surface extrusion and subaerial erosion, and subsurface dissolution of salt at diapir crests and flanks.

A. Present Volume of Salt

Present volume of salt in the East Texas Basin (table 5) was calculated by planimetry of a hand-drawn salt isopach map. Four sources of data were used to construct the isopach map.

(1) 740 km of regional and local depth-converted seismic lines;

Table 4

Saline Aquifer	Average Salinity (mg/L)[1]	Volume of Formation (km^3)[2]	Average Porosity (%)[3]	Volume Dissolved Salt (km^3)[4]
WOODBINE	67,500	4,600	25.0	35.2
PALUXY	70,000	3,300	12.0	12.7
GLEN ROSE	165,000	15,000	8.5	95.3
TRAVIS PEAK	200,000	24,500	7.0	155.0
				298.2

[1]Determined from resistivity curves and Schlumberger charts.

[2]Determined from isopach maps for individual formations.

[3]Determined from sonic and density logs.

[4]Density of halite = 2.1 gm/cm^3

1 km^3 halite = 2.16×10^{15}gm

Table 5

Salt Structure Province	Area (km2)	Present Volume (km^3)	Original Volume (km^3)	Volume Loss (km^3)	Percent Volume Loss	Original Maximum Thickness (m)	Techniques
Salt Wedge (Western Area)	7,810	2,110	2,360	250	11	340-640	A Centripetal rate of thickness increase
Salt Pillow (Western Area)	4,070	2,260	2,700	440	16	640-750	A Centripetal rate of thickness increase
			2,620	360	14	620-730	C Wavelength theory
Salt Diapir (1/2 total)	2,520	950	3,200	2,250	70	1,784	Mean
			2,840	1,890	67	1,500	A Centripetal rate of thickness increase
			2,920	1,970	67	1,570	B_1 Sediment thickening around Hainesville Dome
			3,560	2,610	73	2,070	B_2 Sediment thinning around Hainesville Dome
			4,660	3,710	80	1,580-1,850 range	C Wavelength theory
						1,850 best	
			3,380	2,430	72	1,290-3,060 range	D Dome diameter theory
						1,930 mean	
TOTAL (for 1/2 basin)	14,400	5,120	8,450	3,130	37	1,500-2,070 range	

Conversion of volume to mass

Density salt = 2,100 kg/m^3

(2) Basinwide residual-gravity map;

(3) Salt structure maps of all 15 shallow diapirs from gravity models; and

(4) 4,600 geophysical logs.

There are four salt provinces in the East Texas Basin: (1) salt wedge; (2) low-amplitude salt pillow; (3) intermediate-amplitude salt pillow; and (4) salt diapir (Jackson and Seni, 1983). For the present study, provinces 2 and 3 are combined. Present salt volume, original salt volume, and original maximum salt thickness were calculated for each province. The distribution of regional seismic coverage restricted calculations of salt volume and thickness to the western half of the basin in the wedge and pillow provinces. Therefore, to facilitate comparisons, the area and volume of the diapir province were reduced by one-half. In areas of the diapir province where the salt is too thin for its upper and lower contacts to be resolved it is likely to have a finite thickness of up to one-quarter wavelength of the seismic impulse; at about 6 km depth this is approximately 80 m thickness. Using this upper estimate of present thickness conservative estimates of salt loss can be determined. Volumes and areas in table 5 should be doubled to obtain values for the entire basin.

B. <u>Original Volume of Salt (table 5)</u>

The five techniques employed for calculation of the original maximum thickness and original volume of Louann Salt in different provinces of the East Texas Basin are:

(1) Centripetal rate of salt thickness increase

(2) Original volume of salt pillow determined by sediment thickening during diapirism;

(3) Original volume of salt pillow determined by sediment thinning during pillow growth;

(4) Wavelength of present and Jurassic salt ridges; and

(5) Dome diameter.

<u>Centripetal Rate of Thickness Increase</u>--This technique was applied to salt wedge, salt pillow, and salt diapir provinces. Present salt thickness and geometry were calculated from

regional seismic control (Jackson and Seni, 1983). Original maximum salt thickness was determined by a straight-line extrapolation of present average rate of increase of the salt thickness in the wedge province to the axis of the diapir province (table 5). Seismic data shows no evidence of post-depositional thickness changes in the wedge province. But if the wedge had thinned uniformly by dissolution or flow, the processes would leave little trace. The extrapolation technique, therefore, yields conservative thickness estimates. Using the centripetal method of calculation, calculated original volumes of salt for the western salt wedge, western salt pillow and western half of the salt diapir province were 2,360 km^3, 2,200 km^3, and 3,200 km^3, respectively. This technique is advantageous because it is applicable to all provinces and can be used in conjunction with other techniques that are appropriate only for the pillow or diapir provinces.

Hainesville Pillow Reconstruction--This technique is applicable to the original salt volume and thickness in the Hainesville dome region. Hainesville Dome was selected for analysis because seismic data are available down to Louann Salt. Present geometry of Hainesville stock and surrounding strata was determined from a 25 km-long Exxon seismic line (Loocke, 1978) and from 153 logs for three-dimensional control. All thickness variations in strata surrounding the dome are inferred to be salt-induced and synsedimentary because of the absence of basement structure and the inability of structural distortion to account for the magnitude of observed thickness variations (Seni and Jackson, in press).

Sediment Thickening During Diapirism at Hainesville Dome--The shallower seismic-stratigraphic units thicken progressively toward Hainesville Dome. The volume of strata thicker than regional norms defines the salt withdrawal basin. This volume, termed the collapse volume, is the volume of salt evacuated from the collapsing pillow during deposition of the overlying units. If the collapse volume equals the present diapir volume, salt loss was zero. The collapse volume minus the volume of salt in the present diapir indicates the amount of salt lost from the Hainesville structure. In the case of Hainesville Dome, 67 percent of the original volume has been lost. Next Hainesville dome is assumed to be representative of other domes in the basin in terms of its salt budget. The original volume of salt in the whole diapir province can be calculated by analogy (1):

$$(1) \quad \text{Original volume of salt in diapir province} = \frac{\text{Present salt volume}}{\text{1-fractional volume loss}}$$

This approach estimates that the original volume of salt in the entire diapir province was 5,840 km^3 and the original maximum thickness was 1,570 m (table 5).

Sediment Thinning During Pillow Growth at Hainesville Dome--The deeper units surrounding Hainesville dome thin progressively toward the dome as a result of syndepositional uplift of the original Hainesville pillow below them. The amount of thinning along each seismic-stratigraphic unit defines the vertical component of growth of the pillow during deposition of that unit. This thinning can be quantified in the vertical section as the rise area, which is the area lost due to thinning. The area of the pillow in the vertical section is equivalent to the rise area of units deposited during pillow growth. Assuming axial symmetry, the volume of the pillow is derived from the geometry of a right circular cone and frustum of a cone. Subtracting the present volume of Hainesville salt stock from the volume of the reconstructed Hainesville salt pillow yields volume of salt lost. Using equation (1), the original salt volume in the entire diapir province is estimated at 7,120 km^3 with a maximum original thickness of 2,070 m (table 5).

Wavelength of Present and Jurassic Salt Ridges--Ramberg (1981) showed experimentally and theoretically that the wavelength of buoyant salt ridges (salt pillows) is a function of the thickness of the initial buoyant source layer and the density contrast and the viscosity contrast betwen source layer and overburden (Ramberg, 1981, Table 7.5). In the pillow province these Jurassic ridges evolved into salt pillows by segmentation of salt ridges. In the diapir province Jurassic ridges evolved into diapirs. The mean wavelength between 10 salt pillows in the western half of the East Texas Basin is 7 km (standard deviation = 2 km). Using Ramberg's table 7.5, for systems with a buoyant source layer and overburden, a density difference (P_o-P_s/P_o) of 0.1, and viscosity contrast of 3,800 yields original salt thickness of 640 to 750 ma.

The location and orientation of ancestral Jurassic salt ridges on the diapir province was inferred from linear dome families, structural mapping of salt-withdrawal basins, and distribution of salt pillows. The mean wavelength of the seven mapped Jurassic salt ridges within the diapir province is 18 km (standard deviation = 4 km). Using Ramberg's table 7.5, this wavelength yields original maximum salt volumes and thickness of 9,320 km^3 and 1,850 m in the entire diapir province.

Dome Diameter--Parker and McDowell (1955) showed empirically with model domes and Ramberg (1981) confirmed theoretically that dome diameter equals the thickness of the salt source layer. Salt structure contours from twelve East Texas diapirs were used to define the minimum dome diameter. The maximum diameter of the dome is controlled by lateral spreading at the level of the salt overhang. As overhang diameter is dependent on other variables as well as source layer thickness, it was ignored. Diameters of conical diapirs were also not calculated, for such structures are immature. Mean dome diameter yields original salt thickness of 1,930 m and original volume of 6,760 km^3 in the entire diapir province.

The different techniques for calculating original salt thickness all indicate salt loss in the salt wedge, salt pillow, and salt diapir province with the greatest loss in the diapir province. More than 6,000 km^3 of salt in the total basin are calculated to have been lost. This is approximately 20 times more NaCl than presently is in solution. This mass balance calculation indicates that all NaCl in solution in the saline aquifers can easily be accommodated by dome dissolution.

Salt loss from the original Louann Salt can occur, however, by two different mechanisms, (1) subsurface salt dissolution and (2) salt dome extrusion and subaerial erosion. For example, Loocke (1978) and Seni and Jackson (1983) deduced that the majority of the salt loss on Hainesville salt dome occurred by surface extrusion. This surface dissolution and erosion would not contribute to the NaCl load in the subsurface waters. Another technique for calculating salt loss by ground-water dissolution is by calculating the volume of salt that had to be dissolved to leave the anhydrite cap rock residuum present on many East Texas domes.

2. Approach 2. Cap Rock

The volume of halite dissolved by subsurface ground water can be estimated by calculating the amount of diapir halite that had to be dissolved to account for the anhydrite and calcite cap rock that presently occurs on top and on the flanks of the diapirs. Using this approach, a minimum of 790 km^3 of salt has been dissolved (table 6). Approximately 2.5 times more salt has been dissovlved than presently occurs in solution.

Cap rocks on top and on the flanks of salt domes result from the dissolution of salt diapirs, leaving a residuum of anhydrite. Later diagenesis of anhydrite (or gypsum) by sulfate-reducing bacteria and oxidation of organics yield calcite and pyrite (Kreitler and Dutton, 1983). By knowing the total volume of cap rock and the original $CaSO_4$ percent in the diapir salt, the amount of salt that had to be dissolved can be calculated. The following assumptions were used.

(1) The Louann Salt in the East Texas Basin originally contained 98% NaCl and 2% $CaSO_4$. (This figure represents a mean from Balk, 1944; Kreitler and Muehlberger, 1981; and Dix and Jackson, 1982).

(2) That all anhydrite in the cap rocks formed by residual accumulation during dissolution of dome salt.

(3) There was no removal of cap rock by dissolution or erosion.

(4) No significant volume changes occurred in cap rock during diagenesis from pure anhydrite to the present mixture of anhydrite, calcite, and gypsum.

Cap-rock volumes were calculated for 15 shallow domes in the East Texas Basin (table 6) using gravity models (Exploration Techniques, 1979) and geophysical logs. The total cap-rock volume is approximately 16 km^3. If the original diapir salt contained 2% $CaSO_4$, then 774 km^3 of halite have been dissolved. This estimate is considered a minimum because the cap rock on the dome flanks (which is also a dissolution residuum) was not accounted for.

Approach 2 also indicates that all NaCl presently in solution can be accounted for by salt dome dissolution.

Table 6

Salt Domes	Cap Rock Volume (km^3)
BETHEL	1.2
BOGGY CREEK	3.4
BROOKS	1.4
BRUSHY CREEK	0.1
BULLARD	0.2
BUTLER	0.0*
EAST TYLER	1.8
GRAND SALINE	0.3
HAINESVILLE	0.6
KEECHI	2.1
MOUNT SYLVAN	0.5
PALESTINE	0.1
OAKWOOD	2.4
STEEN	1.0
WHITEHOUSE	0.7
	15.8 km^3 ≈ 774 km^3 halite

* True cap-rock material is absent. "Fake caprock" over Butler Dome consists of calcite cemented sandstone.

Timing of Salt Dissolution

Evidence presented in the previous section of this report suggests that the dissolved NaCl in the saline aquifers of the East Texas Basin is the result of salt dome dissolution. This is an important conclusion in the context of the suitability of salt domes for nuclear waste isolation because it indicates that there has been extensive salt loss over the geologic history of the domes. The next critical question is a question of timing. Is dome dissolution presently occurring and, if not, when did it occur? Interpretation of available data suggests that large-scale dome dissolution by deep basin waters is not presently occurring and much of the dissolution occurred early in the history of the basin. This conclusion is based on three different lines of investigation: (1) salinity (NaCl) distribution around salt domes in the Woodbine Formation, (2) Cl^{36} age dating and (3) timing of rim syncline and cap-rock formation.

Salinity of Woodbine Waters Around Salt Domes, East Texas Basin

Water salinities were calculated for the Woodbine Formation in local cross sections across salt domes (fig. 10) and in regional cross sections through the East Texas Basin (figs. 11-18) to determine if there were consistently higher salinities around the domes. The Woodbine was chosen because its relatively high transmissivity and shallow depth would presumably cause the highest dissolution rates of the saline aquifers. No consistent pattern of increased salinity was found near the domes. High salinities were evident near seven domes--Bethel, Brushy Creek, Bullard, Grand Saline, Hainesville, La Rue, and Palestine, but not seven others--Boggy Creek, Butler, Keechi, Steen, Whitehouse, Oakwood, and Mt. Sylvan. Often salinities increased away from the dome. Areas where no domes are present also exhibit high, erratic salinities (fig. 11-18). Variability in calculated salinity may stem from errors in method. Figure 20 indicates errors of approximately $\pm$20,000 ppm.

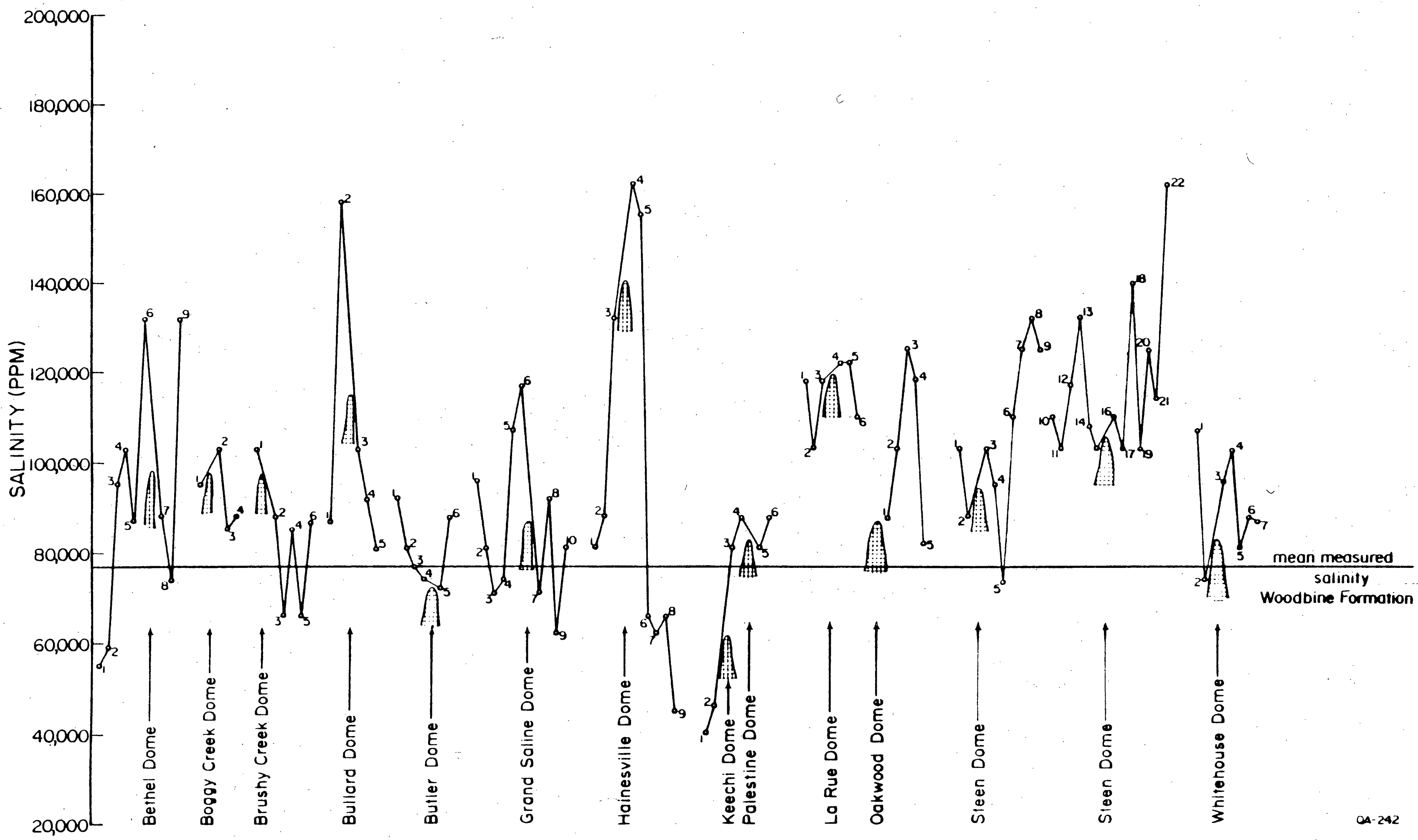

Figure 10. Composite cross section showing distribution of salinity in Woodbine Formation across 14 salt domes. Location of cross sections in Figure 19.

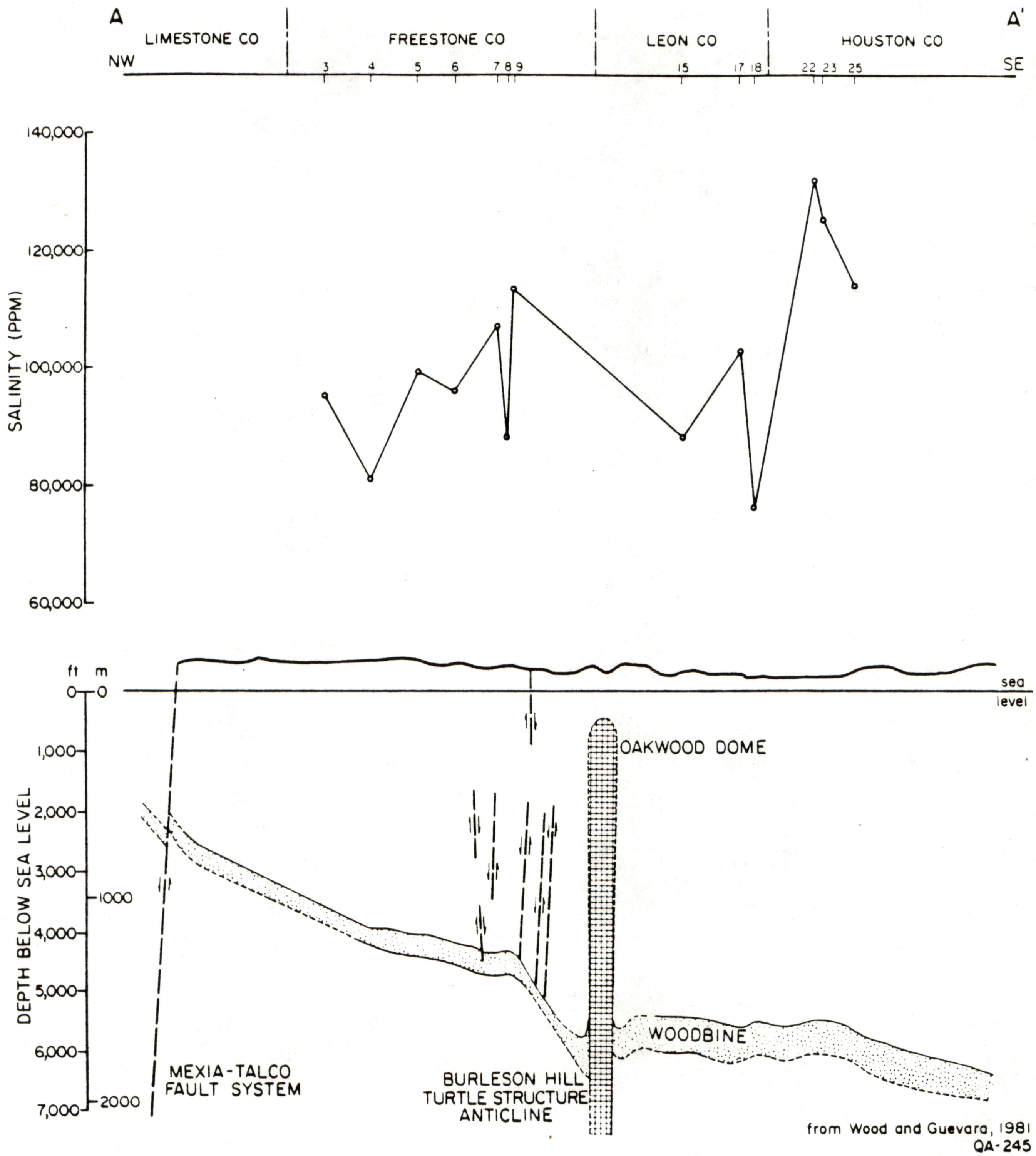

Figure 11. Salinity distribution in Woodbine Formation along cross section AA'. Location of line AA' on Figure 19.

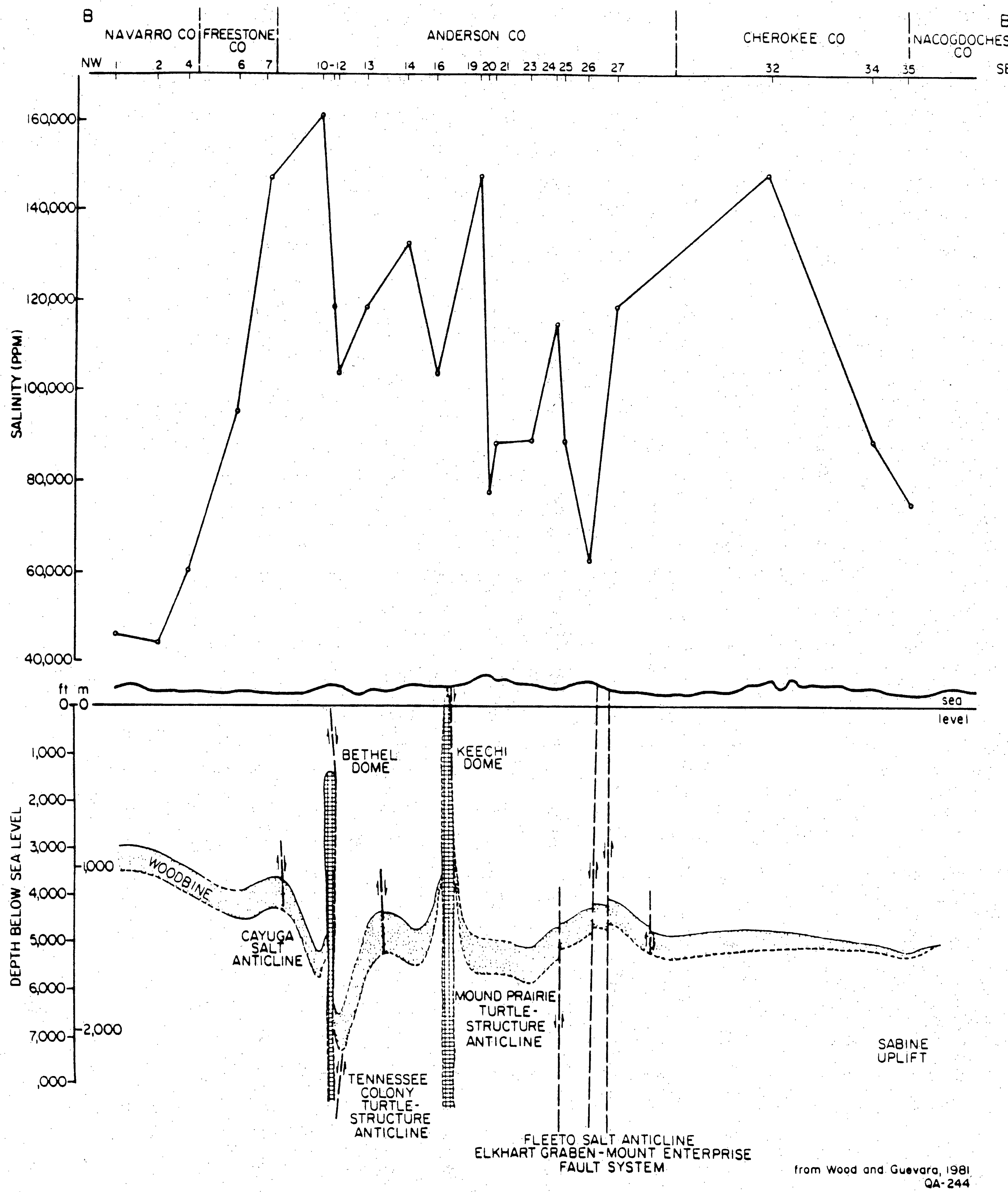

Figure 12. Salinity distribution in Woodbine Formation along cross section BB'. Location of line BB' on Figure 19.

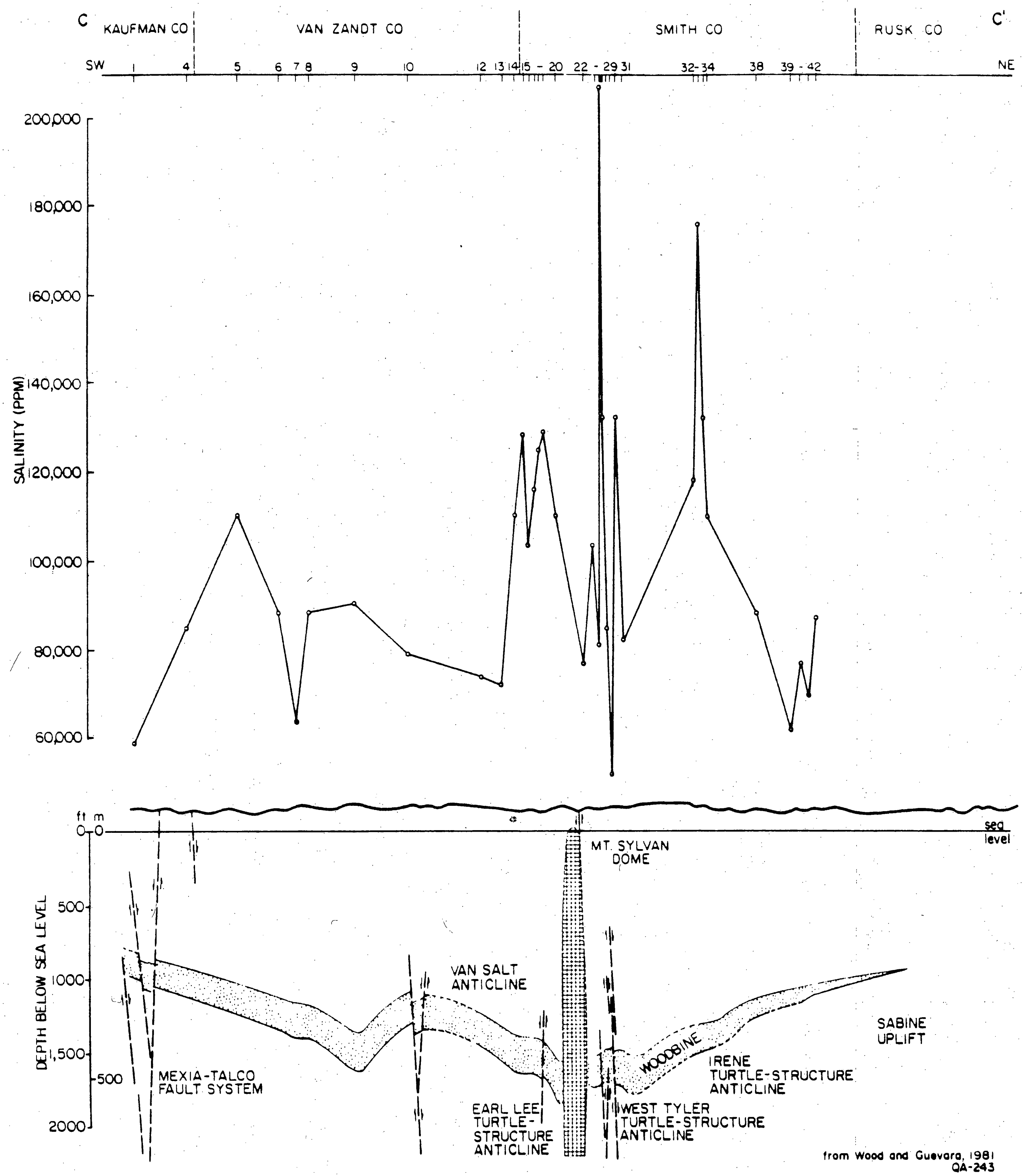

Figure 13. Salinity distribution in Woodbine Formation along cross section CC'. Location of line CC' on Figure 19.

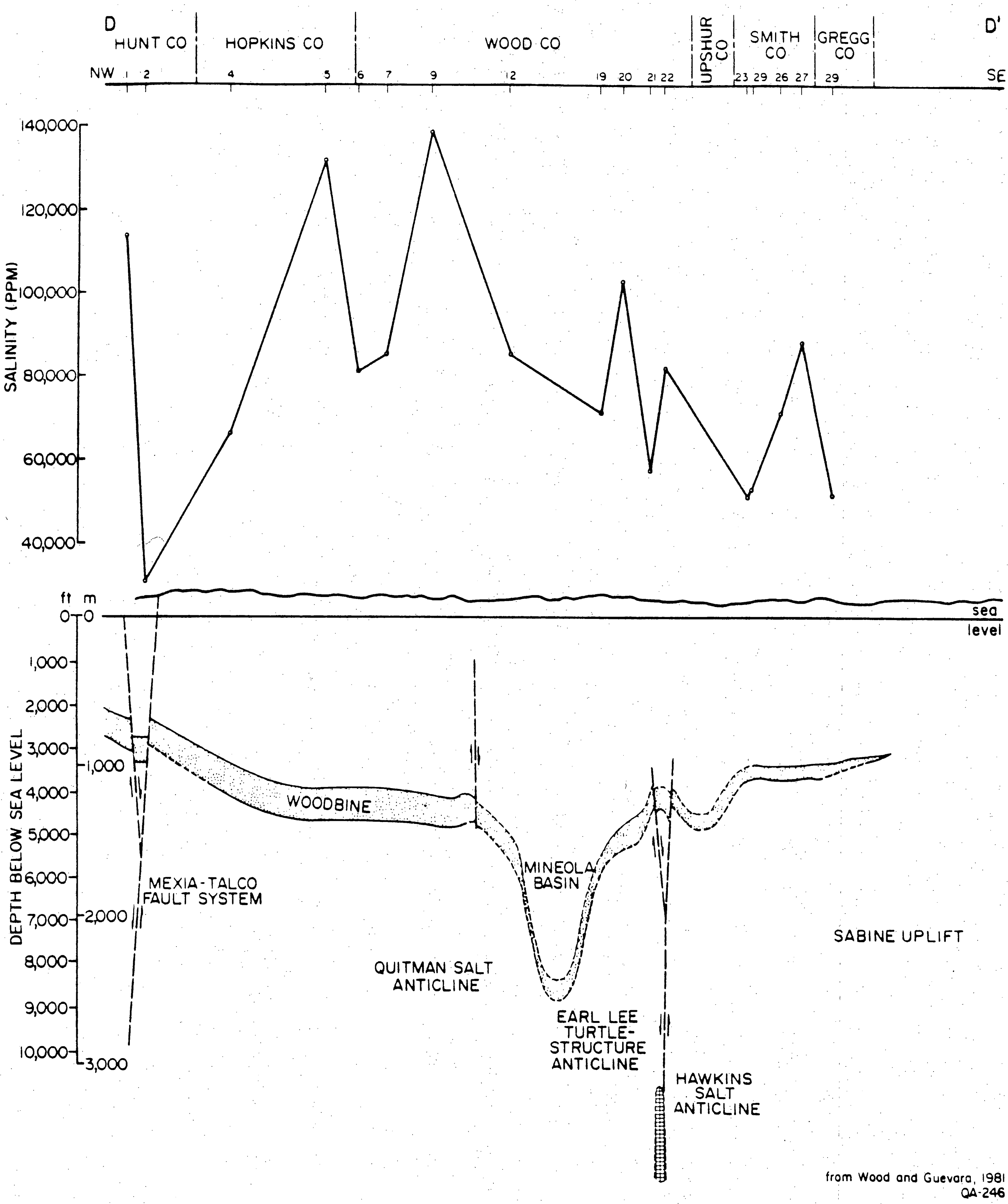

Figure 14. Salinity distribution in Woodbine Formation along cross section DD'. Location of line DD' on Figure 19.

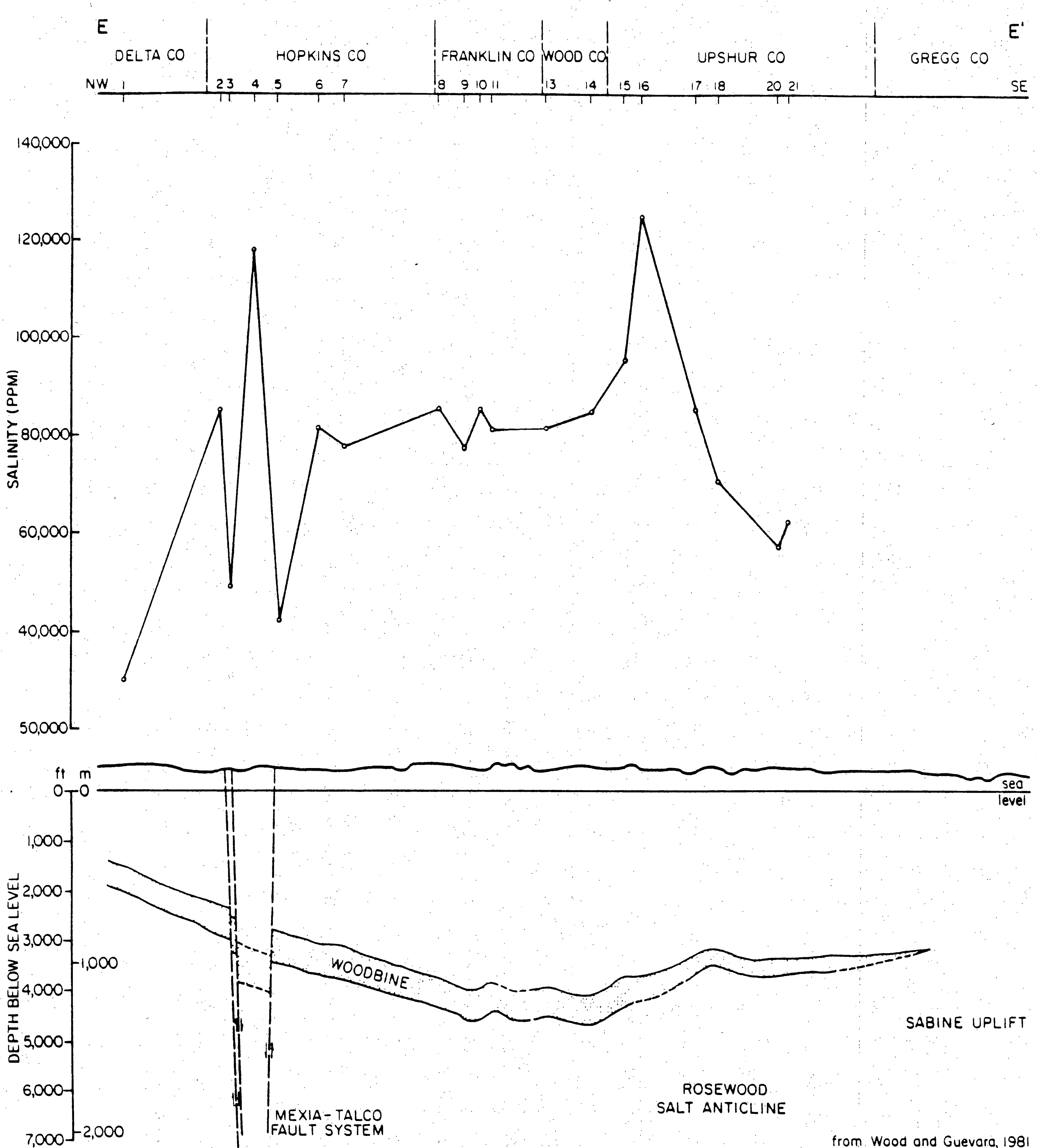

Figure 15. Salinity distribution along cross section EE'. Location of EE' on Figure 19.

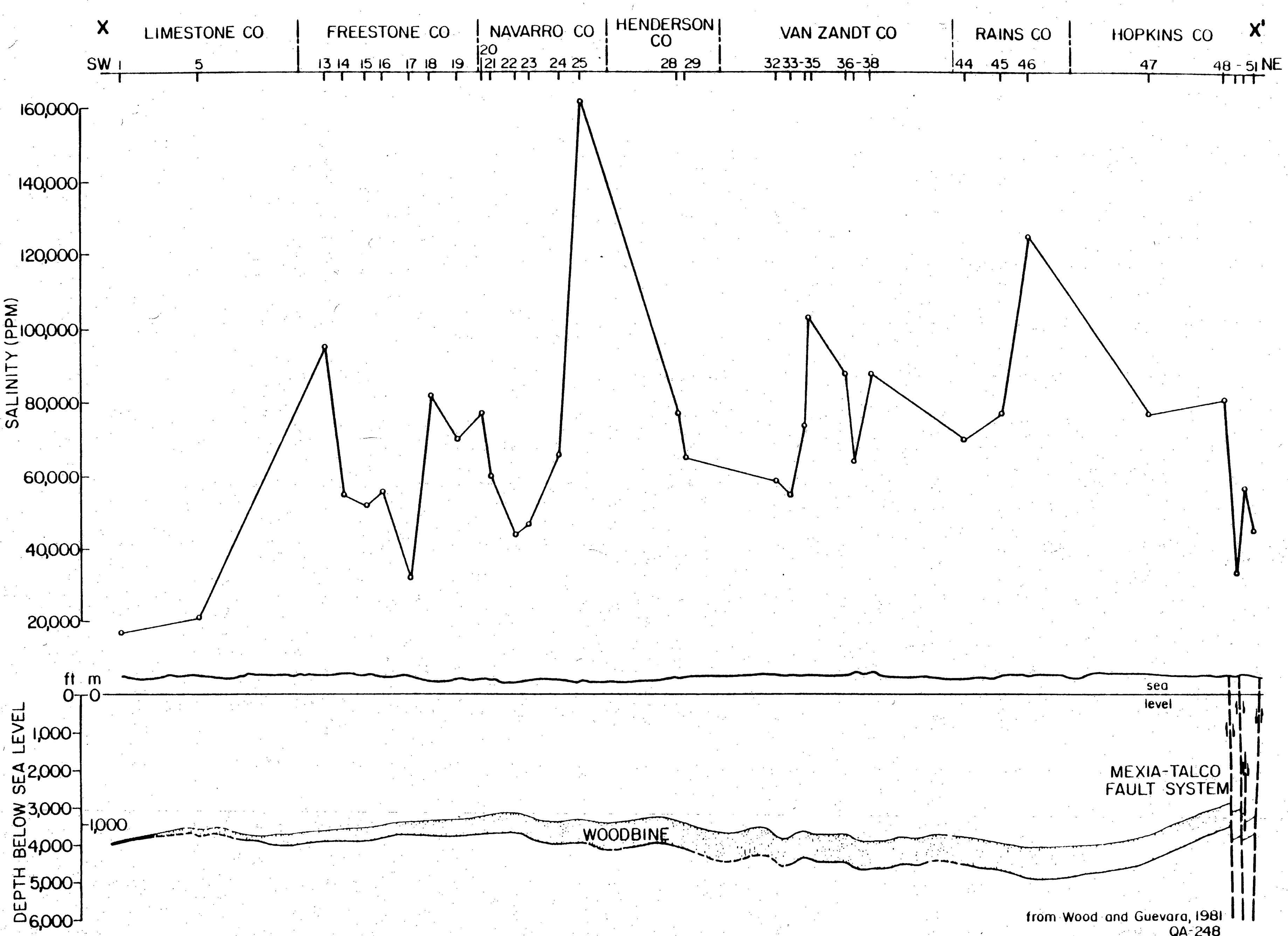

Figure 16. Salinity distribution in Woodbine Formation along cross section XX'. Location of line XX' on Figure 19.

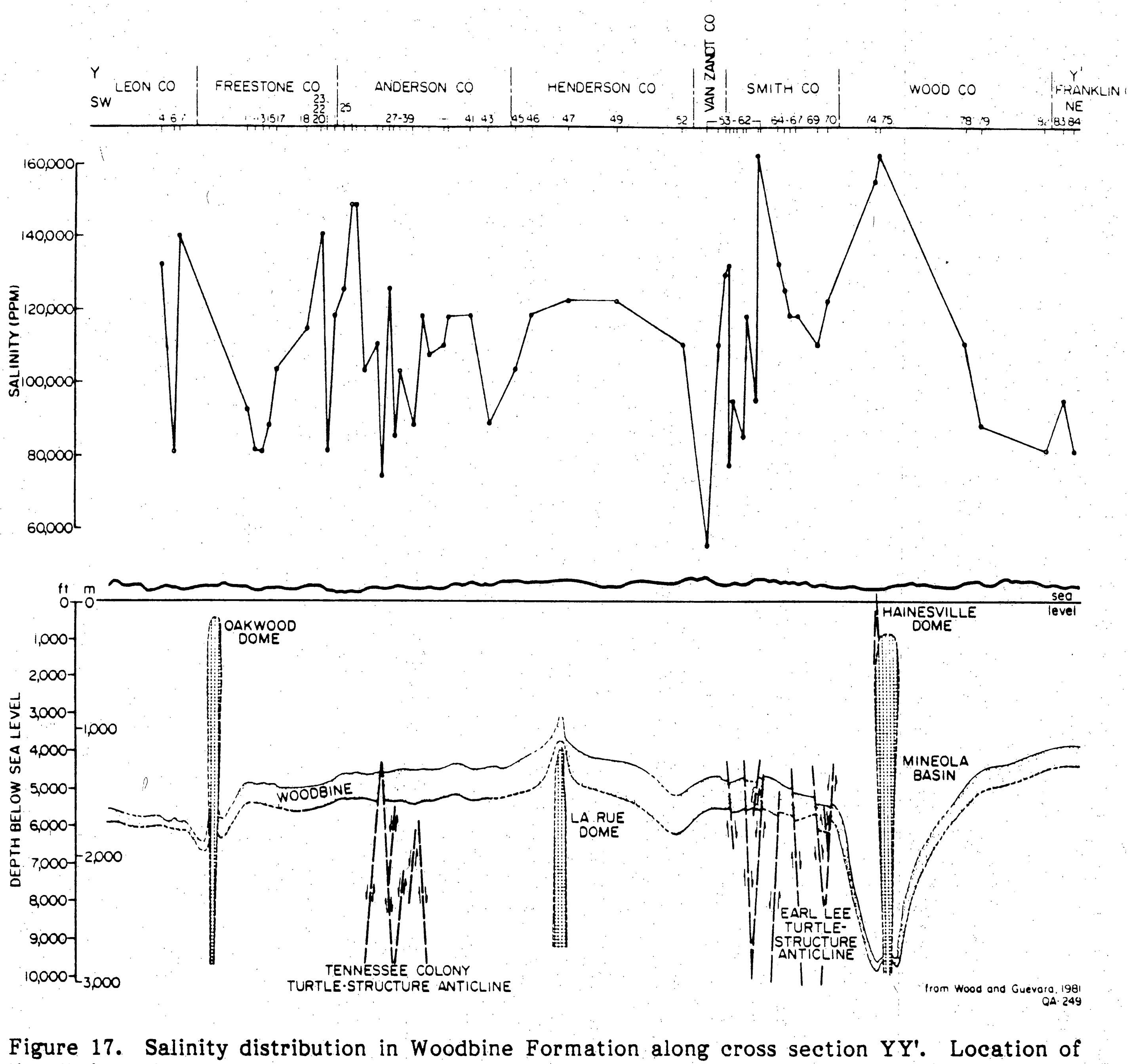

Figure 17. Salinity distribution in Woodbine Formation along cross section YY'. Location of line YY' on Figure 19.

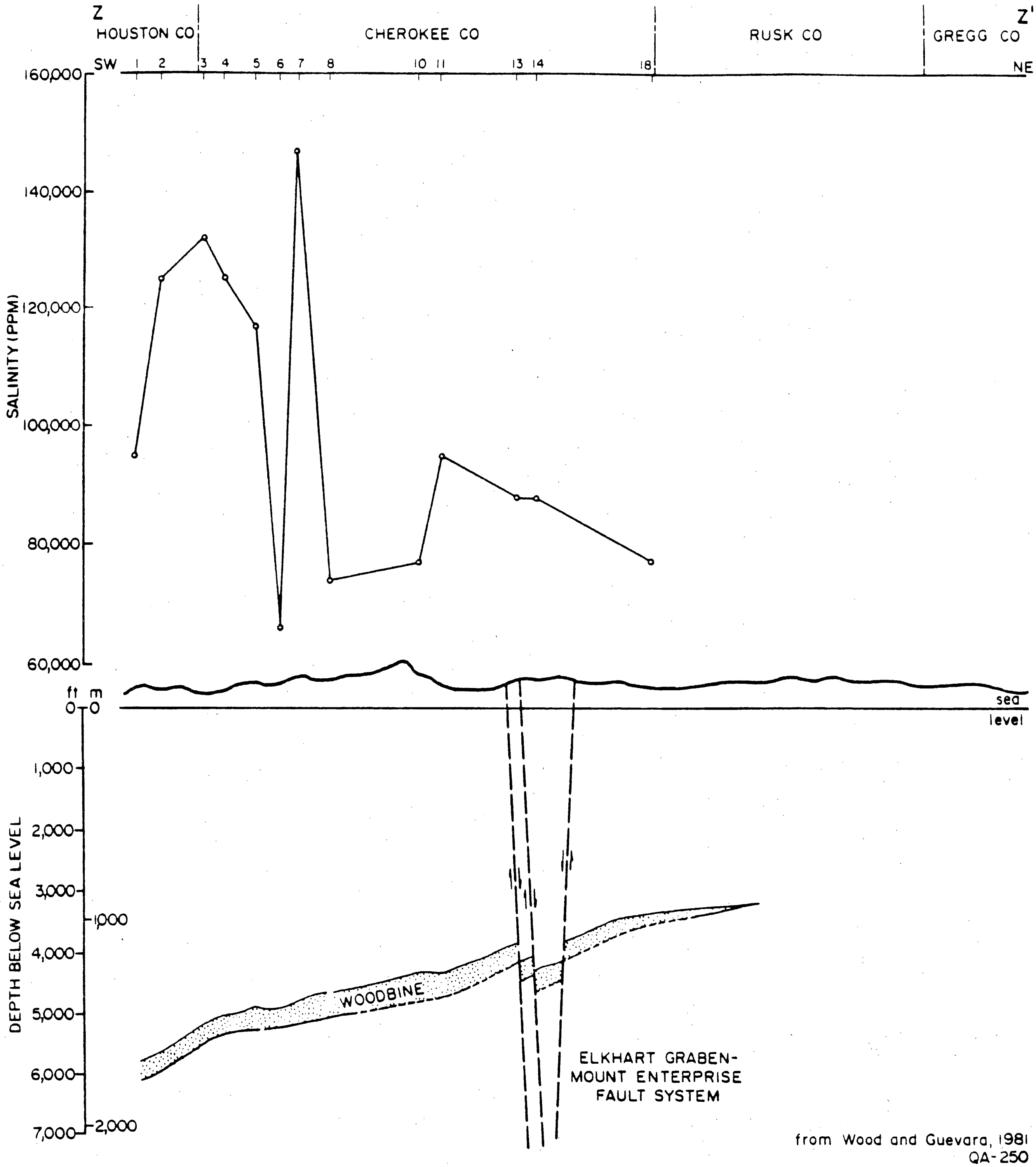

Figure 18. Salinity distribution in Woodbine Formation along cross section ZZ'. Location of line ZZ' on Figure 19.

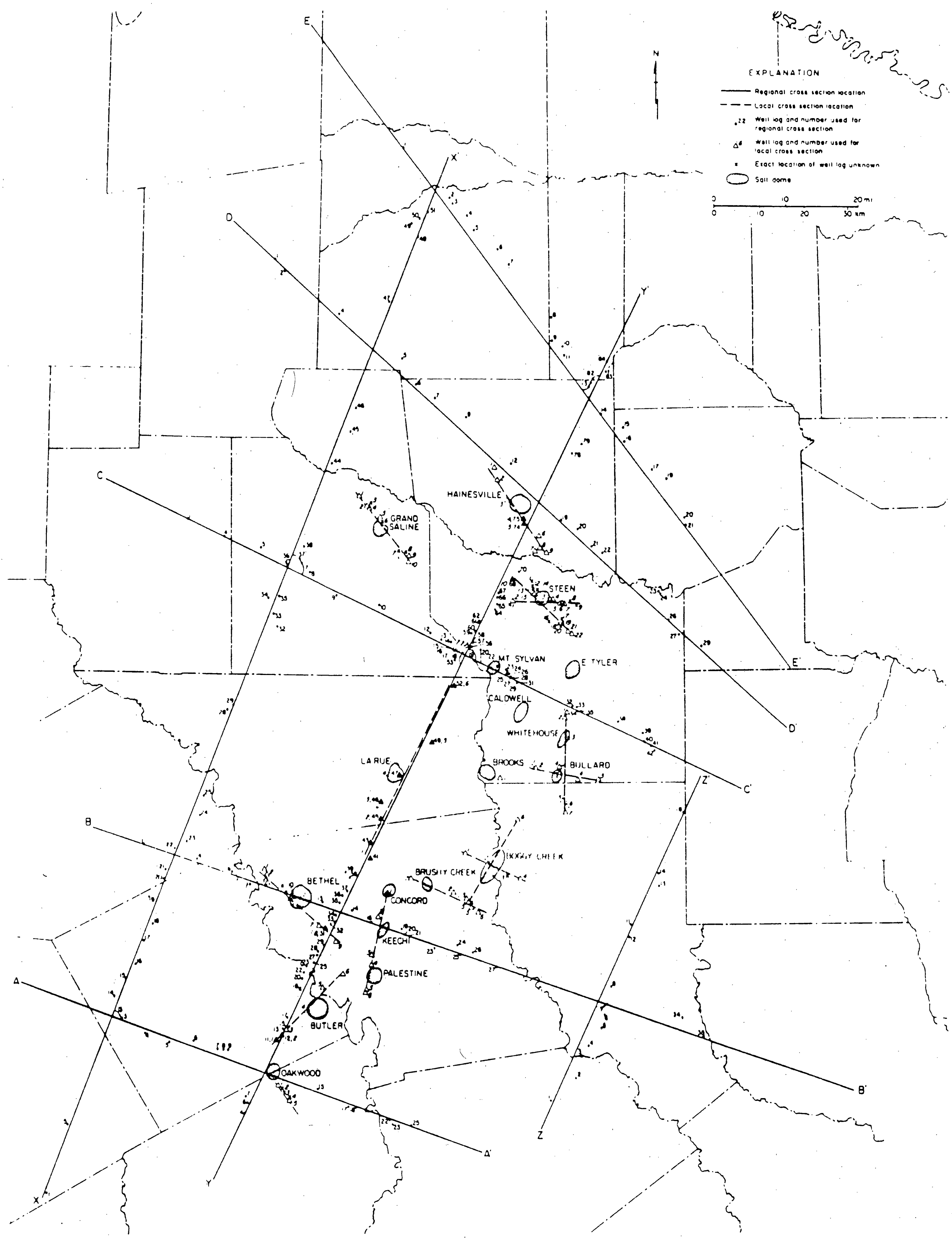

Figure 19. Index map of local (Figure 10) and regional (Figures 11-18) Woodbine salinity cross sections. Regional cross sections are from Wood and Guevara (1981).

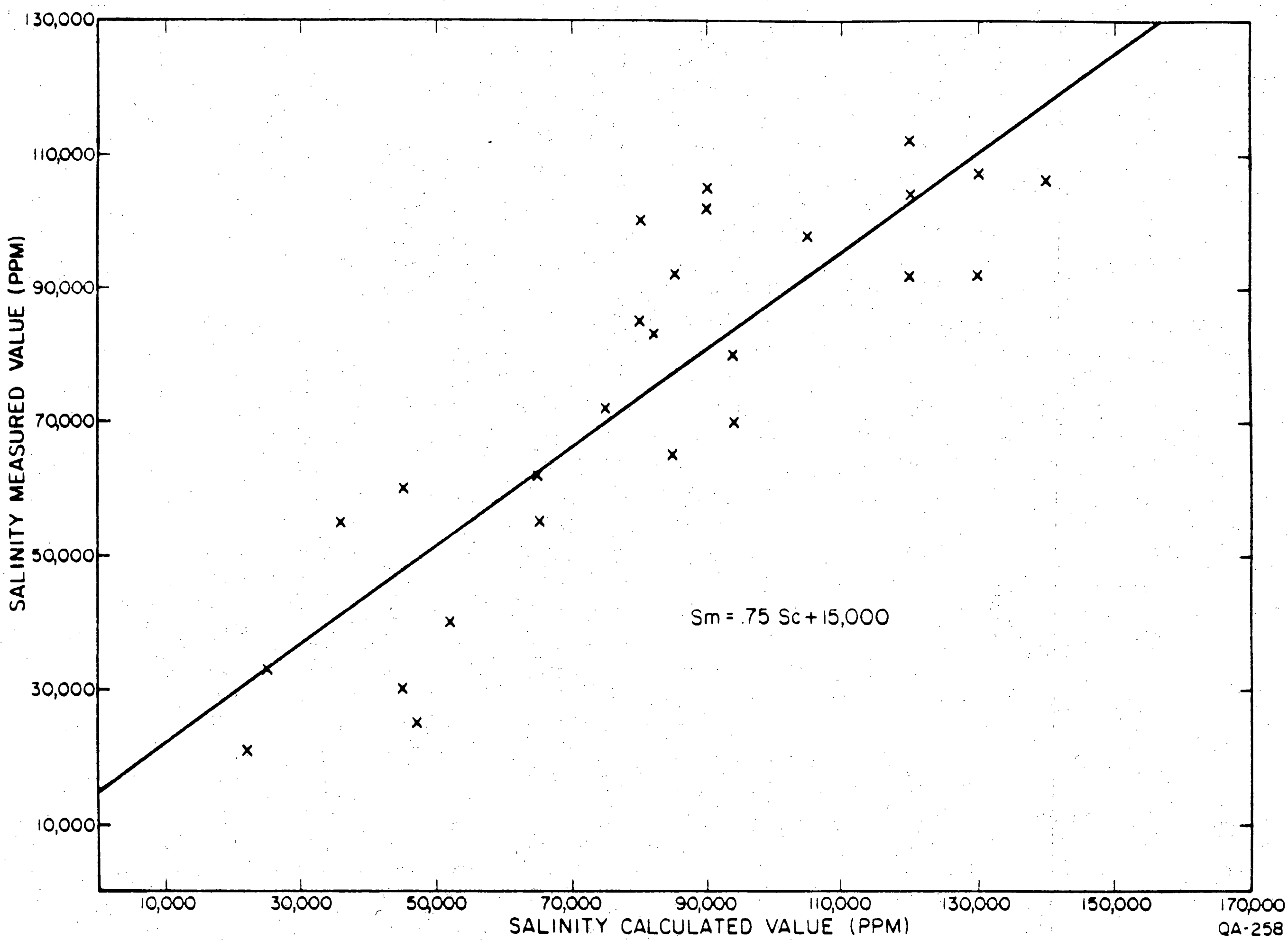

Figure 20. Measured salinity versus calculated salinity.

Technique for Calculating Water Salinity of Woodbine Formation

Water salinities for the Woodbine Formation along the cross sections (figs. 10-18) were calculated using spontaneous potential logs based on Dresser Atlas (1975, p. 3-4). Twenty-eight chemical analyses of Woodbine Formation waters were then compared to the calculated salinity values from the geophysical logs to correct the calculated values to "true" salinity values. Figure 20 shows measured and calculated salinities and a linear regression line of best fit. The correlation coefficient is .88. The corrected values were used in the cross sections (figs. 10-18).

Chlorine-36 Age Dating of Salt Dome Dissolution in the East Texas Basin

Based on ^{36}Cl age dating techniques, the chloride in two brine samples from the East Texas Basin resulted from salt dome dissolution more than approximately 1 million years ago.

Chlorine-36 (^{36}Cl) is a radioactive isotope of chlorine with a half-life of 3.01×10^5 years (Davis and Bentley, 1982). Because of its long half-life, it offers a promising potential for absolute dating of old waters. Measurement of chlorine-36 was made by Harold Bentley (Hydrogeochem, Inc.) on a tandem Van de Graff accelerator at the University of Rochester Nuclear Structure Laboratory, Rochester, New York. Analyses are given as the ratio of ^{36}Cl nuclei to the total number of chlorine nuclei $\times 10^{-15}$.

Chlorine-36 has two sources in a ground-water system, (1) an atmospheric and soil surface source and a subsurface production by natural subsurface neutron flux (Bentley, 1978). Because of the interaction of these two sources of ^{36}Cl, the ^{36}Cl dating technique has both advantages and disadvantages for dating saline waters in deep sedimentary basins. If atmospheric chloride is the only source of chloride in aquifers, the maximum age a water can be dated at is 1,000,000 years old (Davis and Bentley, 1982). As the activity of ^{36}Cl of groundwater chloride declines because of radioactive decay, there is also an increase in ^{36}Cl by subsurface neutron bombardment. The two sources reach equal concentrations in the age range of 800,000 to 1.2 million years old (fig. 21). Waters with low $^{36}Cl/Cl$ ratios can only be assigned ages of 1 million

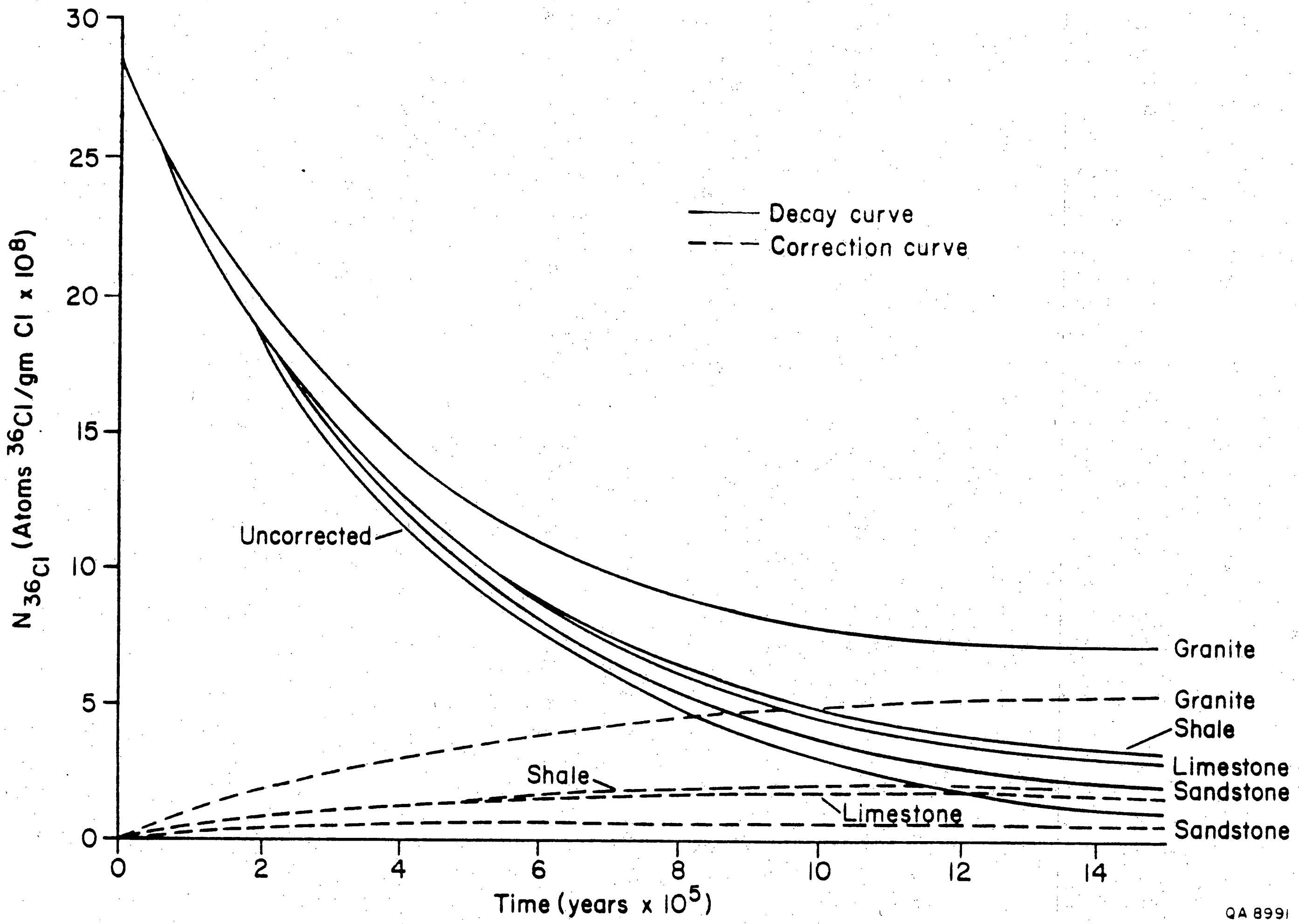

Figure 21. Decay curve of representative ^{36}Cl ground-water samples from different aquifers. The curves rising with time represent the subsurface contribution to ^{36}Cl as a function of aquifer type. The decay curves assume an initial concentration of 2.8 x 10^9 atoms ^{36}Cl/gm Cl (atmospheric component) and 1 x 10^8 atoms ^{36}Cl/gm Cl (soil surface component) (from Bentley, 1978).

years or greater. ^{36}Cl dating of saline waters is further complicated because the atmospheric chloride is swamped by dead chloride from a nonatmospheric source making absolute dating of the water even more tenuous.

Because of the buildup of ^{36}Cl by subsurface neutron flux and the massive addition of dome salt by salt dissolution, the ages of the waters in the saline aquifers of the East Texas Basin cannot be determined. However, minimum ages of dome dissolution can be estimated. Louann salt (i.e., dome salt) should have no ^{36}Cl because of its Jurassic age. There also should be no buildup of ^{36}Cl in halite by subsurface neutron bombardment, because the dome shields itself from neutron bombardment (Davis and Bentley, 1982). Two halite samples, one from the Kleer Mine, Grand Saline salt dome, East Texas Basin and the other from Permian Clear Fork Formation, Palo Duro Basin, West Texas, have ^{36}Cl/gm Cl ratios of 0 $\pm$ 2 and 1 $\pm$ 2, respectively. In contrast, two brine water samples from the Pettet Formation flanking the Bethel salt dome and from the Woodbine Formation flanking the Boggy Creek salt dome have ^{36}Cl/gm Cl ratios of 22 and 6, respectively (table 17); these values are considered to be in the range expected for a secular equilibrium caused by neutron bombardment (Bentley, personal communication, 1982). Based on Table 7 and Figure 21 the salt dome dissolution that resulted in these brines occurred at least one million years ago.

In contrast two samples were analyzed for ^{36}Cl from a shallow fresh-water Carrizo aquifer flanking the Oakwood Dome. The ^{36}Cl was measured to determine if the Cl in the shallow low TDS ground water was from dome dissolution. The ^{36}Cl values were 230 $^{36}Cl/Cl$ and 280 $^{36}Cl/Cl$, typical of young waters with an atmospheric source and not of Jurassic halite. No salt dome dissolution was evident from these specific wells sampled for this study.

Geologic Evidence for Early Dissolution

Salinity typically increases with depth in many sedimentary basins. This is true for the Michigan, Illinois, Alberta (Graf and others, 1966), Palo Duro (Bassett and Bentley, 1983), and San Juan Basins (Berry, 1968) as well as the East Texas Basin (fig. 22). The cause for the continual increase is as enigmatic as is the original source of chloride. The following

Table 7. ^{36}Cl in Halite and Water Samples

Sample Name	Location	Cl (mg/L)	$^{36}Cl/Cl$ ($\times 10^{15}$)
halite	Clear Fork Formation Palo Duro Basin, West Texas	--	1 ± 2
halite	Kleer Mine, Grand Saline Salt Dome, East Texas Basin	--	0 ± 2
Bethel	Pettit Formation Bethel Dome	154,000	22
Boggy Creek	Woodbine Formation Boggy Creek Dome	65,000	6
OK-102	Carrizo Formation Oakwood Dome	39	230
TOH-5	Carrizo Formation Oakwood Dome	130	280

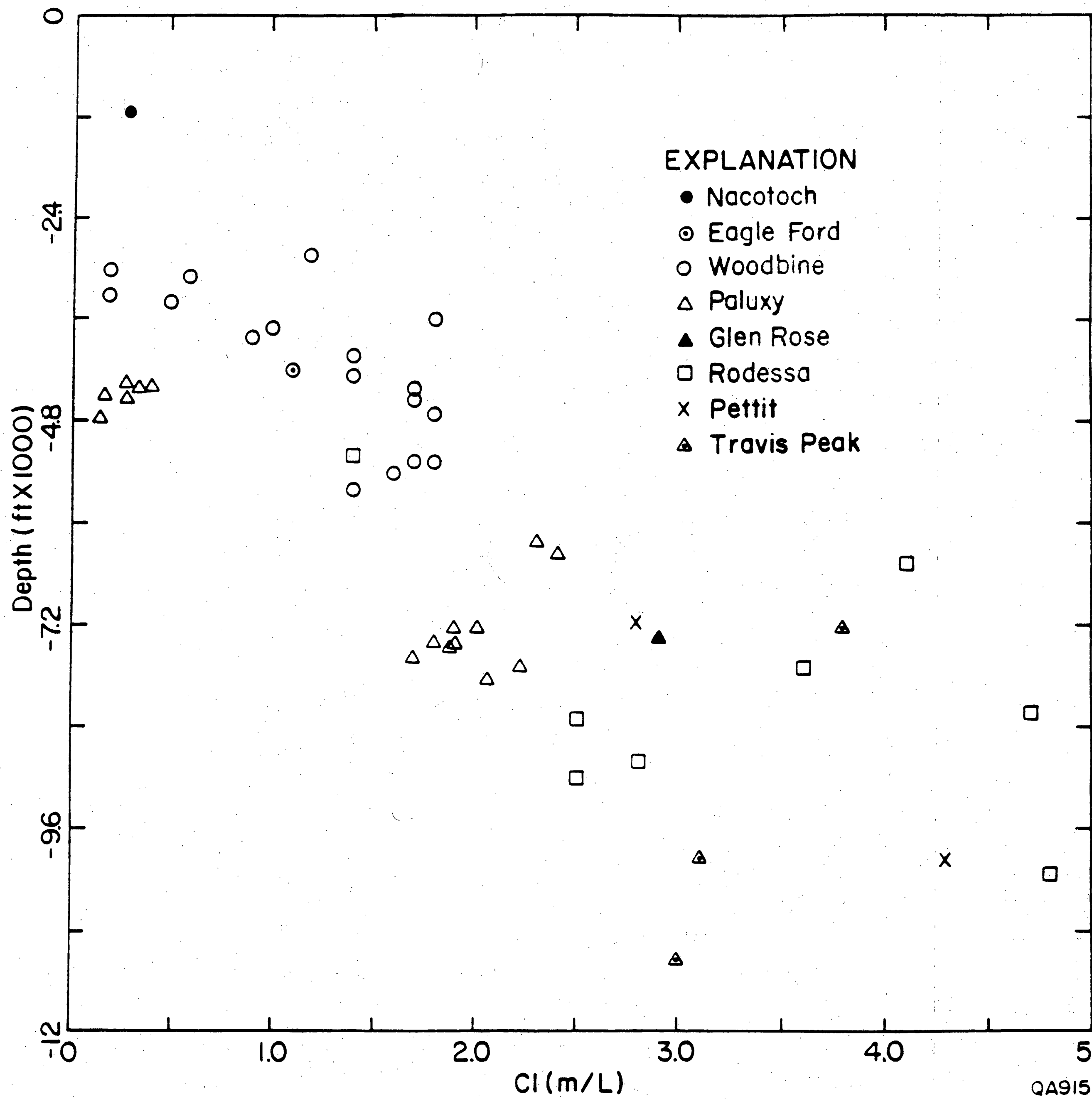

Figure 22. Cl (m/L) vs. depth, note increase in Cl with depth. Chemical analyses in Table 1.

hypotheses have been offered as mechanisms to explain this phenomenon. (1) Mixing of shallow, lower salinity waters with a deeper saline source (Carpenter, 1978; Land and Prezbindowski, 1981), (2) As water moves deeper it increases salinity by dissolving evaporites or other Cl sources, (3) If there is a general upward flow component, salinities in the deep basin are increased by ultra-filtration through shale membranes (Graf and others, 1965; Hitchon and Freedman, 1969).

The hypothesis that best explains the increased salinity with depth in the East Texas Basin is that most of the dissolution of salt in the basin occurred early in the history of the basin and those Jurasic or Cretaceous waters are still present in the formations. Jurassic formations contain Jurassic and Cretaceous waters and Cretaceous formations contain Cretaceous waters. If we accept the previous argument that the NaCl in solution in the East Texas Basin results from dome dissolution, we may be able to determine when in the history of the basin the NaCl was added to the ground water by understanding when the domes were dissolved.

Kreitler and Dutton (1983) concluded that the formation of the 600 ft thick cap rock on Oakwood Dome in the East Texas Basin occurred during Late Jurassic and Early Cretaceous time. They argued that the evidence for large-scale salt dissolution was evident in the rim synclines surrounding a dome. At Oakwood Dome the only significant rim synclines are in Upper Jurassic and Lower Cretaceous formations; therefore, major dome dissolution and subsequent initial cap rock should have formed in this time period.

At Oakwood Dome 50 km^3 of salt was dissolved to form the cap rock. The dissolution of 50 km^3 of salt represents a major geologic event. The Oakwood salt stock contains approximately 5 km^3 of halite. Ten diapir volumes of halite had to pass through Oakwood dome to be able to accumulate the present volume of caprock. This volume of lost salt should be evident in the salt withdrawal basins surrounding a dome. In Cretaceous (Glen Rose and later) and Tertiary times only 13 km^3 of salt withdrawal from rim synclines occurred. Therefore a majority of the dome dissolution probably occurred pre-Glen Rose time (table 8a,b).

Table 8a. Volume of salt dissolved from Oakwood dome to form its cap rock

Cap-rock thickness (anhydrite and calcite)	140 m
Cap-rock radius	1,500 m
Cap-rock volume	9.9×10^8 m^3
Anhydrite content of Oakwood salt dome	2%
Amount of salt dissolved	50 km^3 (11.7 $miles^3$)

Table 8b. Timing and volumes of rim synclines surrounding Oakwood dome. Volume of rim syncline is considered as equivalent to the volume of salt that flowed into the dome and was lost by dissolution.

Stratigraphic Interval	Rim Syncline Volume (km^3)
Top Cotton Valley to Top of Travis Peak[1]	significant
Top James to Top Glen Rose[2]	no closure
Paluxy[2]	no closure
Top Kiamichi to Top Buda[2]	9.7
Woodbine[2]	no closure
Base Austin Chalk to Top Pecan Gap[2]	3.5
Top Pecan Gap to Top Midway[2]	no closure

[1]from seismic data

[2]from electric log data

A similar approach is applicable for the other domes in the East Texas Basin. The occurrence of a rim syncline (peripheral sink) in a formation indicates that there was salt flow either 1) intrusion of the diapir into overlying formations, 2) flow of salt within the diapir and salt loss by extrusion out of the diapir crest, or 3) flow of salt into the dome and salt loss by dissolution of the diapir by ground water. Conversely, if there are no rim synclines, then there was no major salt loss--either by dome dissolution or dome extrusion. Seni and Jackson (in press) determined that most East Texas salt domes grew fastest during Early Cretaceous (fig. 23). Their conclusions are based on the presence and rate of sediment accumulation in rim synclines. Therefore, most dome dissolution also occurred during that time. In contrast to most of the domes, Hainesville and Bethel salt domes did most of their growing in late Cretaceous. The dissolved NaCl in the Woodbine and younger formations may result from the dissolution of these domes in this later time period. Based on this line of reasoning much of the salt dome dissolution and addition of NaCl to the ground waters may have occurred early in the history of the basin. The waters in the deeper formations therefore are also very old (Jurassic and Cretaceous) and may be static. This hypothesis of greater growth and greater diapir dissolution early in the infilling of the basin explains the relationship of increasing salinity with depth that is observed in the East Texas Basin (fig. 22).

The trend of enrichment of $\delta^{18}O$ with increasing salinity (fig. 9) may be circumstantial. The $\delta^{18}O$ enrichment of the waters is more logically explained by increased burial and greater temperatures. These waters that have become enriched in ^{18}O were also emplaced in an earlier time where greater amounts of dome dissolution were occurring. This would explain a correlation of enrichment of $\delta^{18}O$ with increased salinities.

WATER CHEMISTRY

Introduction--Summary

The waters in the saline deep basin aquifers appear to have a meteoric continental origin. They were recharged predominantly during Cretaceous times. The dissolved NaCl in the

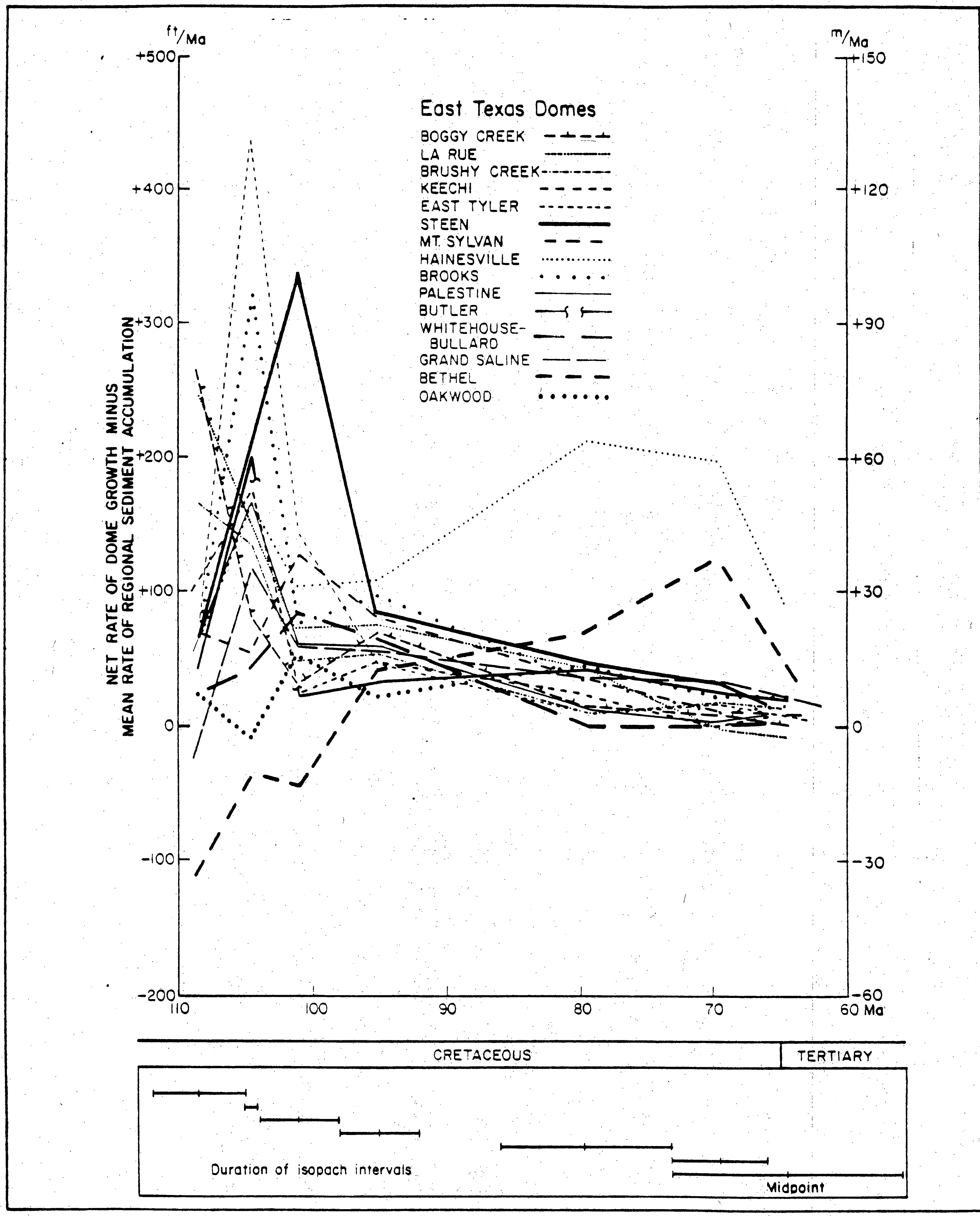

Figure 23. Net rate of dome growth for 16 East Texas domes (calculated by rate of sediment accumulation in peripheral sinks minus mean rate of sediment accumulation) from 112 to 56 ma. Most domes grew fastest during the Early Cretaceous (from Jackson and Seni, in press).

aquifers is predominantly from salt dome solution. The presence of calcium, magnesium, potassium, strontium, and bromide in the basinal waters appears to result primarily from the interaction of the NaCl waters with the rock matrix. The high calcium concentrations may result from albitization of plagioclase. The potassium may result from either albitization or dissolution of potassic feldspars. High magnesium concentrations result from dedolomitization. The bromide may result from Br depletion of halite.

Based on the water chemistry there appear to be two major aquifer systems. The Woodbine and shallower Cretaceous formations are dominated by Na-Cl type waters. Glen Rose and deeper formations are dominated by Na-Ca-Cl type waters. The Na-Ca-Cl type waters have evolved from Na-Cl waters.

Chemical Analysis of Deep-Basin Brines

New Data

Fifty water samples were collected and analyzed for HCO_3, SO_4, F, Cl, Br, I, H_2S, Na, K, Mg, Ca, Sr, Ba, Fe, B, SiO_2, Al, Ti, Cu, Mn, Zn, Pb, Li (table 1). These samples were collected and analyzed to verify the trends observed in the data base containing the 813 analyses (Appendix A) and to collect data on species not analyzed in the earlier data set. The earlier data set only includes analyses for Na, Ca, Mg, Cl, SO_4, pH, and alkalinity.

Sample Collection and Methods of Analysis

Samples were collected as close to the well head as possible. For Woodbine samples the oil-water ratio was sufficiently high to allow sample collection at the well head for all but two samples. Deeper samples were generally collected from a separator or storage tank since water production was low. Oil wells were sampled in preference to gas wells to avoid condensate water contamination from produced gas, but, generally, even gas wells yielded reliable formation water samples.

Samples were initially filtered through a funnel filled with pyrex glass wool to remove oil and large particulate matter. The water was then filtered through a 0.45 micron filter using nitrogen pressure to minimize atmospheric contamination. At each sampling site the following samples were collected in sequence from one gallon of sample water: (1) 125 ml preserved with 5 ml CdAc for H_2S analysis; (2) one liter, unacidified, for individually analyzed ions; (3) one liter, unacidified, for storage at the Mineral Studies Lab; (4) 500 ml, unacidified, for isotopic analysis; (5) 250 ml, acidified with 10 ml 6N HCl for ICP analysis of cations; and (6) 25 ml, diluted with 100 ml distilled water, for SiO_2 analysis.

All chemical analyses were performed by Mineral Studies Lab, Bureau of Economic Geology, University of Texas at Austin. Bicarbonate analyses were done in the laboratory rather than at the well head or on pressurized samples collected downhole and their concentration should only be considered approximate.

Deleted Data

Twelve analyses have not been included in the data base of brine water chemistry because the analyses (except CH.T.P.) indicated abnormally low concentrations of Na, Cl, Ca, Mg, Br, I, Sr, and B (table 2). Sample (CH.T.P.) had a hydrogen and oxygen composition that was unrealistic in that it plotted above the meteoric water line (table 2). Eleven of these twelve samples were not collected at the well head but from storage tanks or separators where water from another source may have been mixed with the formation water (table 2a).

Previously Published Data

Eight hundred thirteen previously published chemical analyses were collected from Hawkins and others (1964) and University of Oklahoma (1980) and are listed in Appendix A. Most samples were collected before 1964. One-hundred-eighteen analyses had cation/anion balances greater than $\pm$ 5% and were therefore considered inaccurate and therefore excluded. Bicarbonate and pH analyses should also be considered as approximate because the alkalinity and pH measurements were probably made in the laboratory (and not in the field) at an unknown time after collection.

Comparison of New Analyses to Previously Published Analyses

A comparison of the chemical composition of the recently collected waters (table 1) to chemical composition of previously published analyses (Appendix A) for the same field and similar depths shows that the analyses are similar (table 9). Two conclusions can be drawn from this observation: (1) the old analyses are correct and (2) secondary recovery operations (such as water flooding) have not altered the water chemistry of the recently collected samples.

Geochemical Trends

Several geochemical trends are evident from both the recently collected samples and from the previously published analyses. The trends observed on individual plots are similar for both data sets; therefore, only those plots with the recent data are shown in this section. A few identical plots using the older, larger data set are included to show the agreement.

The following scattergram plots of the water samples collected for this study also include 20 samples from the older data base from the Paluxy Formation. Only two wells in the Paluxy were sampled for this study. The water chemistry in the Paluxy appears critical in understanding the geochemical evolution of water types between the shallower saline Nacatoch, Eagle Ford, and Woodbine Formations and the deeper Glen Rose and Travis Peak Formations. Twenty Paluxy analyses from the older data set are included in some of the scattergrams (figs. 24, 26, 28, 33, 36, 39, 40) to provide a more complete data base.

Each scattergram includes data for the formations studied. The geochemical trends are not as evident if the data are plotted solely by formation. The different sampled formations are indicated by different symbols so that ionic concentrations for each formation are identified.

In the scattergrams concentrations (either as moles (or millimoles) per liter or milligrams/liter) are used instead of activities because of the problem of calculating correct activity coefficients for varying ionic strengths (up to 250,000 ppm).

Table 9. Comparison of previously published analyses to chemical analyses from this study.

Sample No.	Formation	Depth	Sample Type	Temp.	pH	Na	K	Ca	Mg	HCO_3	SO_4	Cl	NO_3	F
Quitman	Eagle Ford	old 4,250				31,415		1,474	205	137	21	51,287		
		new 4,210				23,800		1,030	203	187	< 4	40,400		
Boggy Creek	Woodbine	old 3,634				37,615		3,451	582	329	184	65,499		
		new 3,600				37,900		3,250	465	160	120	65,500		
Neches	Woodbine	old 4,742				35,582		3,520	586	274	180	62,520		
		new 4,704				35,700		3,200	545	150	90	62,100		
Cayuga	Woodbine	old 4,049				29,833		1,620	350	348	118	49,600		
		new 4,030				29,600		1,200	210	160	120	48,500		
Long Lake	Woodbine	old 5,250				36,432		2,806	474	376	119	62,232		
		new 5,272				36,400		2,400	280	170	110	62,200		
Powell	Woodbine	old 3,000				3,964		62	26	1,393	---	5,462		
		new 3,000				4,400		74.5	27	350	60	6,500		
Van	Woodbine	old 2,912				27,491		825	368	536	11	44,600		
		new 2,900				25,100		1,160	290	120	60	43,100		
Slocum-NW	Woodbine	old 5,686				32,910		3,000	430	260	190	57,000		
		new 5,400				32,500		2,700	460	98	73	58,100		
Hawkins	Woodbine	old 4,650				35,668		2,850	530	406	206	61,200		
		new 4,531				35,200		2,300	290	170	250	59,500		
Mexia	Woodbine	old 3,065				11,818		561	179	290	4	19,573		
		new 3,100				12,270		570	142	263	< 6	20,300		
Richland	Woodbine	old 2,985				5,654		124	37	683	0	8,652		
		new 3,300				5,285		94	29	350	< 6	8,280		
Quitman	Paluxy	old 6,211				39,627		9,731	1,388	96	460	82,009		
		new 6,230				39,000		9,540	936	54	389	81,300		

Na^+ versus Cl^- (figs. 24 and 25)

Na^+ increases directly with Cl for all samples analyzed. Based on the slope of the line, there are two subsets of data. Up to Cl concentrations of 2 m/l, the slope of Na/Cl is ≃ 1. These data included Nacatoch, Eagle Ford and Woodbine Formations. Above a Cl concentration of 2 m/l, the slope drops to 0.6. These data include Paluxy, Glen Rose, Pettet and Travis Peak Formations.

Ca^{++} versus Cl^- (figs. 26 and 27)

Ca^{++} concentrations remain low up to Cl^- concentrations of approximately 2 m/l Cl, then Ca concentration increases up to 0.8 m/l in figure 26--to 1.1 m/l in Figure 27. Different trends for Ca versus Cl occur in the same formations as for Na versus Cl. High Ca concentrations begin in the Paluxy Formation.

(Na^+ + 2 Ca^{++}) versus Cl^- (fig. 28)

A scattergram of (Na^+ + 2Ca^{++}) versus Cl^- shows a slope of 1. Two Ca are added to the Na to determine whether the 0.6 slope observed for Na/Cl plot (figs. 24 and 25) was caused by an exchange of Na for Ca. The Ca concentrations are multiplied by 2 to maintain charge balance. If Ca is exchanging for Na, then 2 Na will be lost from the brine. The addition of Ca and depletion of Na relative to Cl appear to be related to the same geochemical reaction.

K^+ versus Cl^- (fig. 29)

The scattergram of K versus Cl shows two different trends. For Cl concentrations less than 2 m/l, Cl increases independently of K. For Cl concentrations greater than 2 m/l, K concentrations increase significantly. This is a similar pattern as observed for Ca versus Cl.

Br^- versus Cl^- (fig. 30)

The scattergram of Br versus Cl shows two different trends. For Cl concentrations less than 2 m/l Cl and in Nacatoch, Eagle Ford or Woodbine Formations Cl increases independently of Br. For Cl concentrations greater than 2 m/l, Br increases proportionally with Cl at a slope

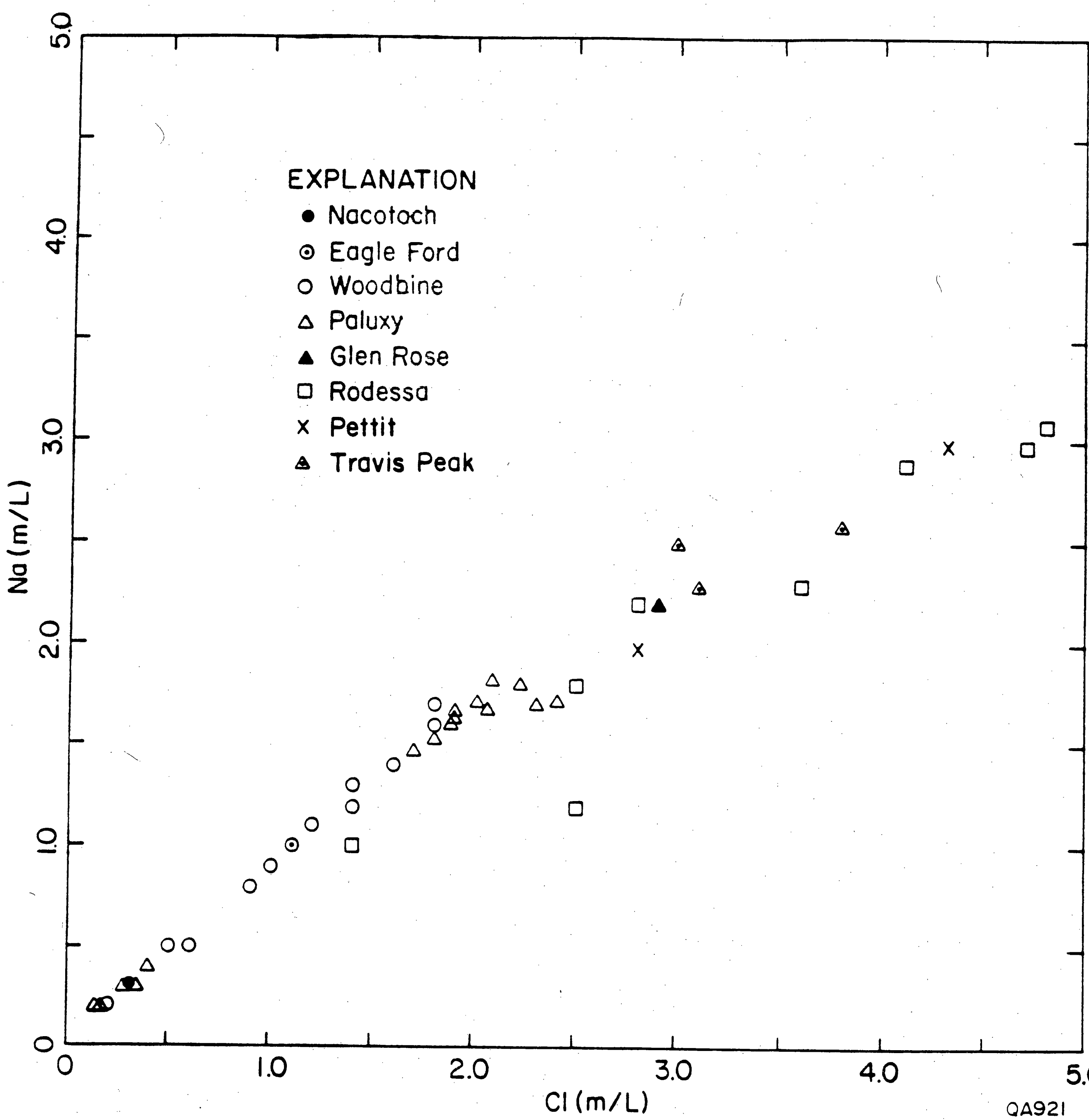

Figure 24. Sodium concentrations (m/L) versus chloride (m/L). Data from Table 1 (new data) plus additional Paluxy data from Appendix A.

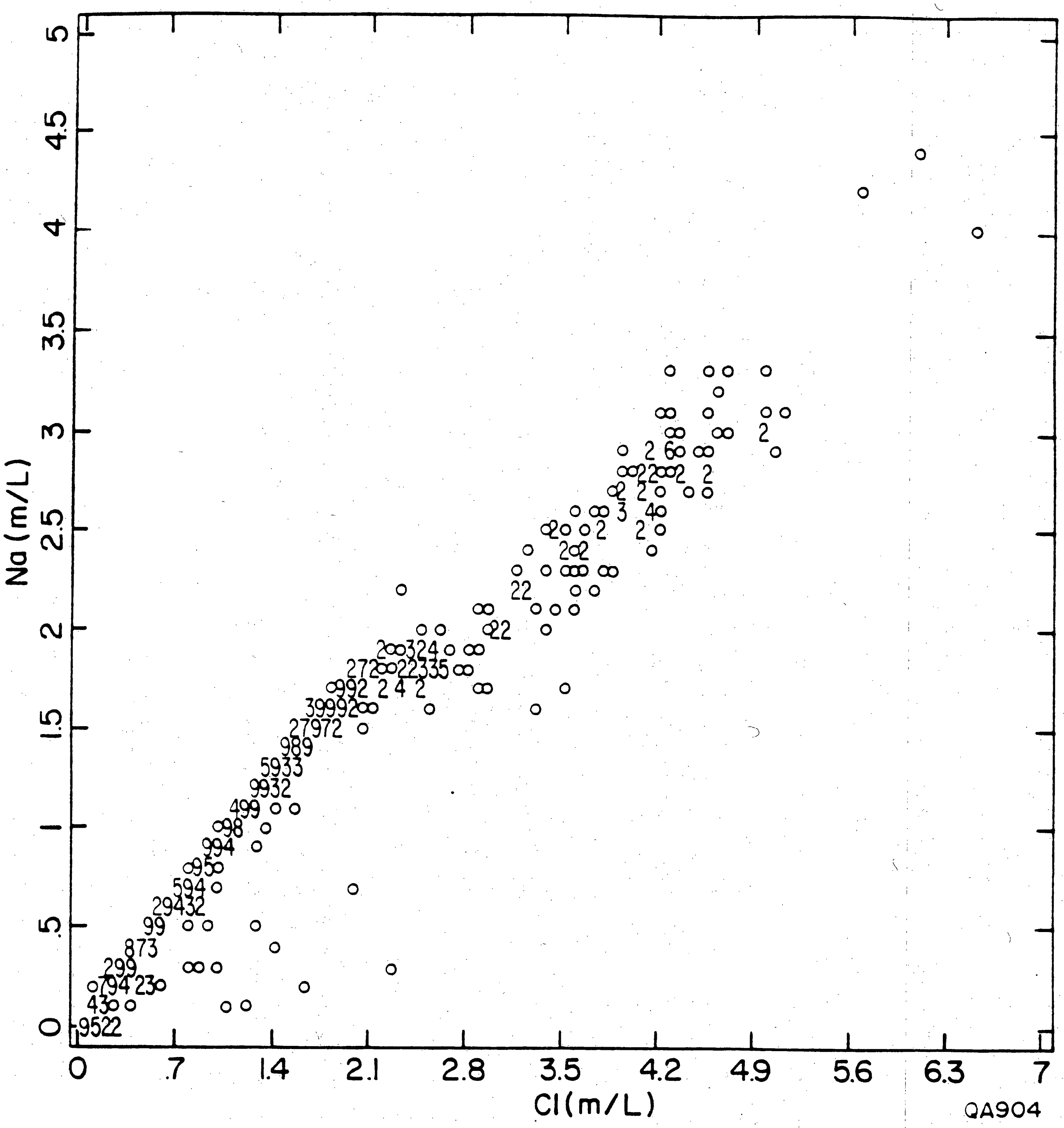

Figure 25. Sodium concentrations (m/L) versus chloride (m/L). Data from Appendix A (previously published data).

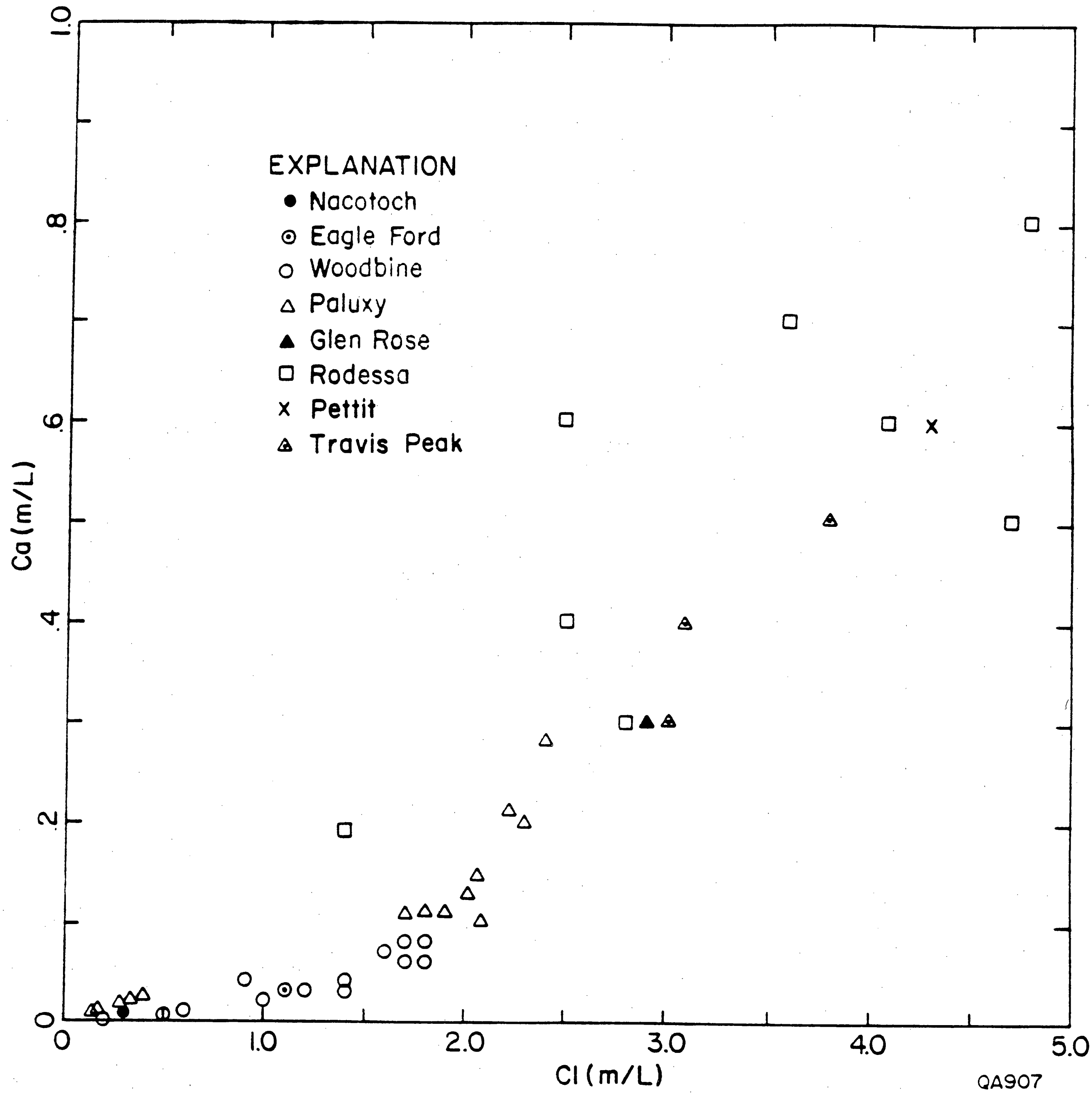

Figure 26. Calcium concentrations (m/L) versus chloride (m/L). Data from Table 1 (new data) plus additional Paluxy data from Appendix A.

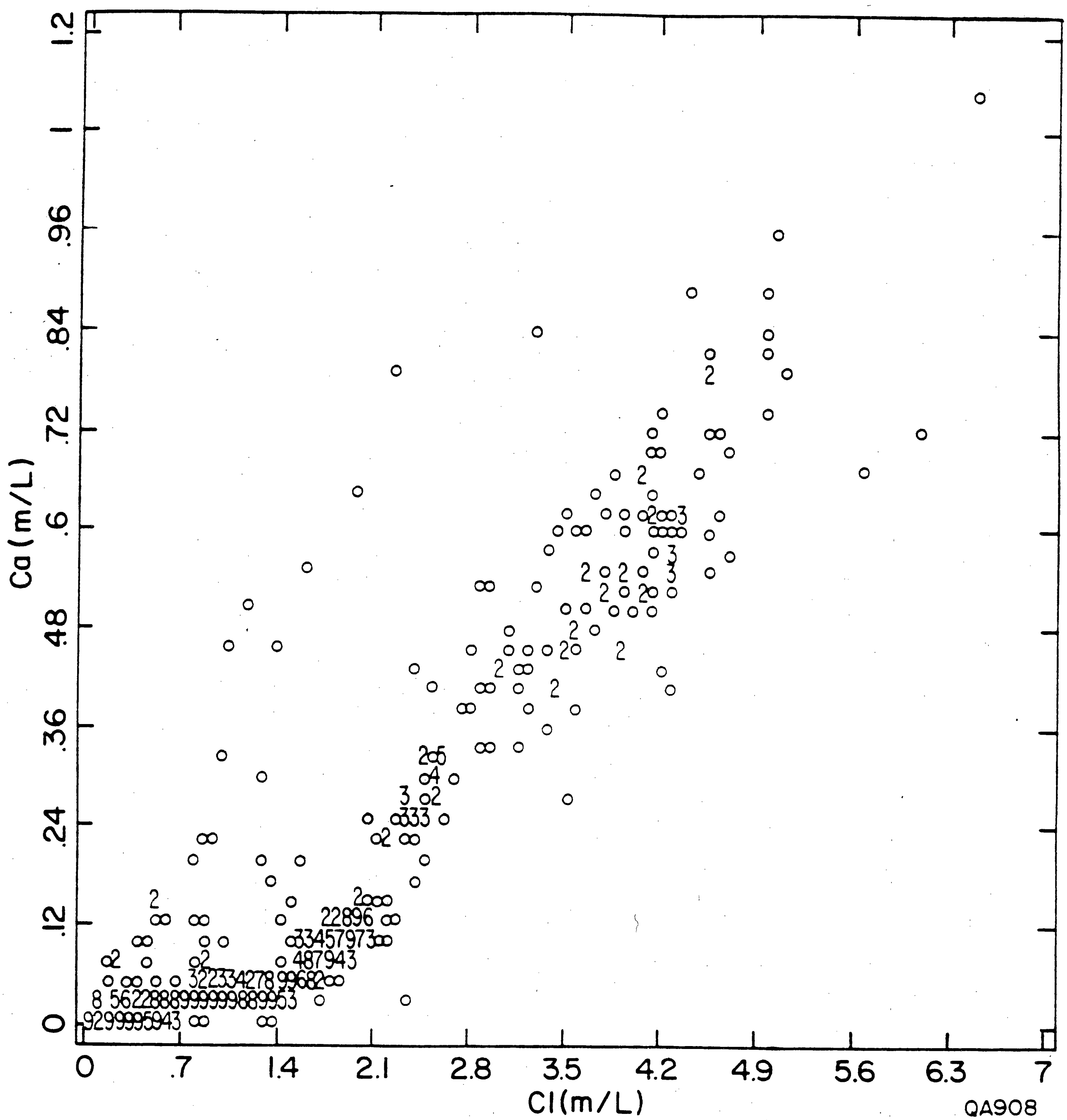

Figure 27. Calcium concentrations (m/L) versus chloride (m/L). Data from Appendix A.

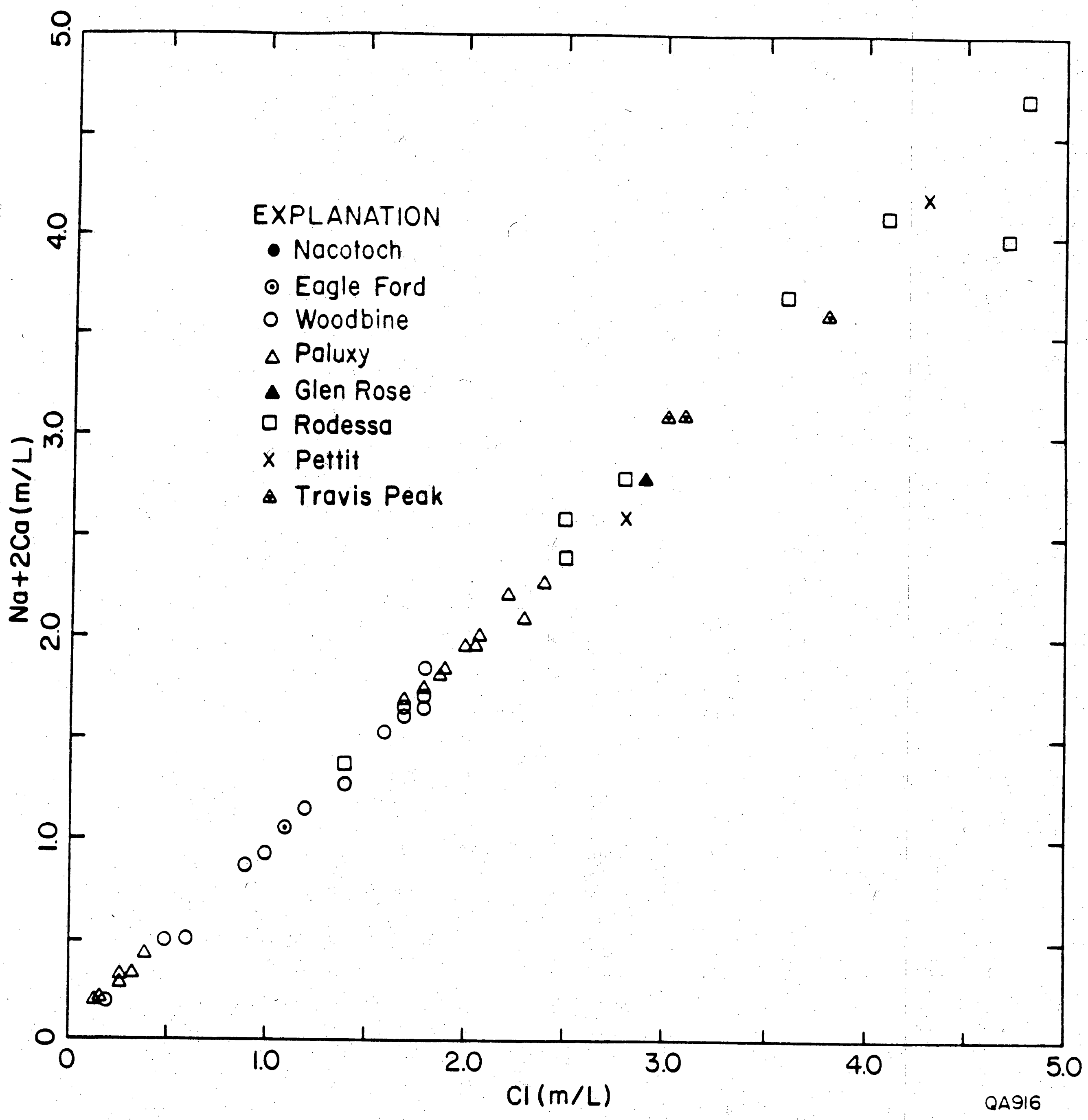

Figure 28. (Na^{+} + 2 Ca^{++}) concentrations (m/L) versus chloride (m/L). Data from Table 1 plus additional Paluxy data from Appendix A.

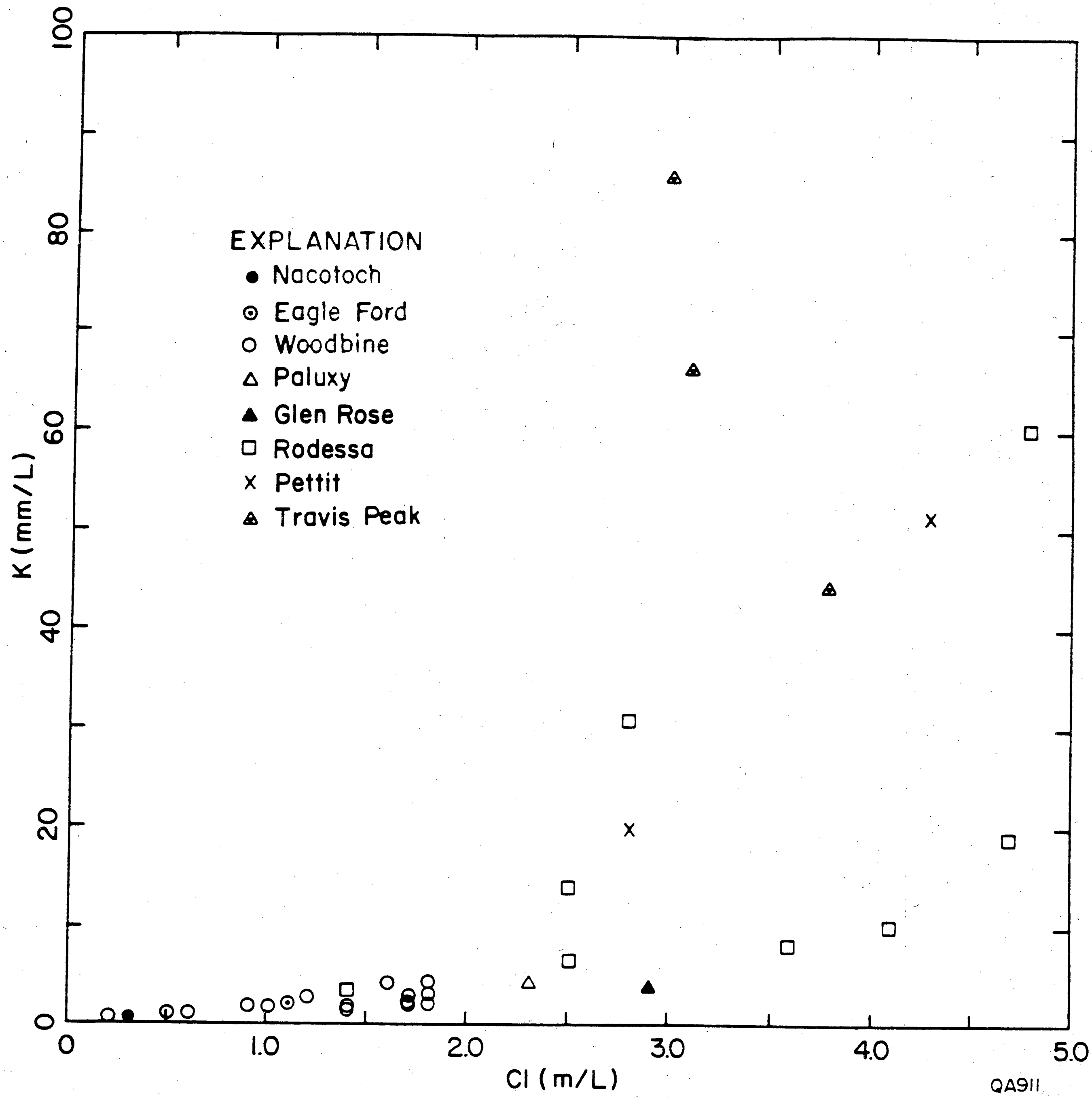

Figure 29. Potassium concentrations (mm/L) versus chloride (m/L). Data from Table 1.

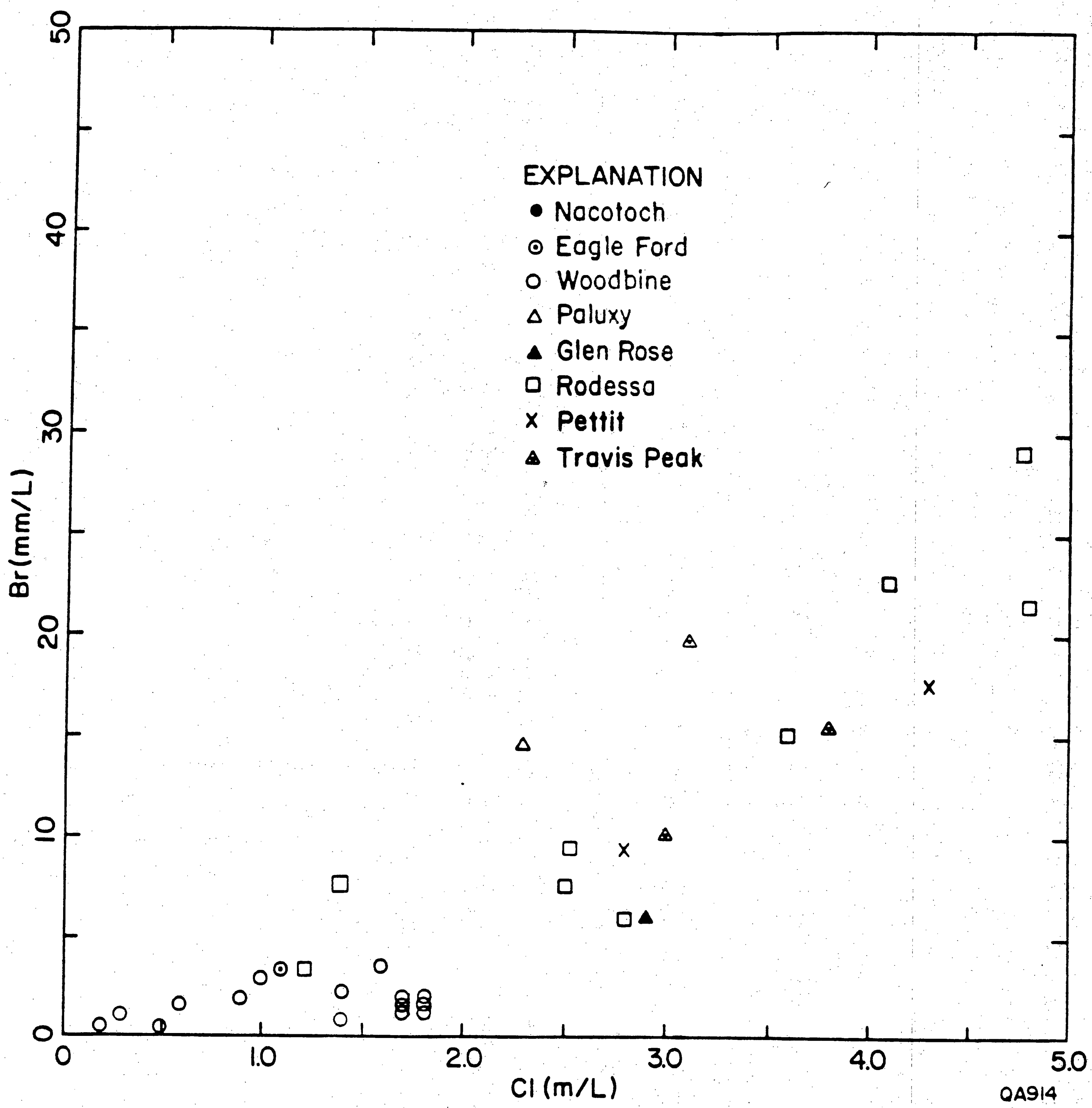

Figure 30. Bromide concentrations (mm/L) versus chloride (m/L). Data from Table 1.

of .006. The Br concentration increases at approximately the chlorinity value where Ca and K also increase significantly.

Sr^{++} versus Cl^{-} (fig. 31)

The scattergram of Sr versus Cl shows a continual increase of Sr with greater Cl concentrations. In contrast to the scattergrams of Ca versus Cl, K versus Cl, and Br versus Cl (figs. 26, 29, 30), Sr is increasing proportionately to Cl in the shallower formations.

Mg^{++} versus Ca^{++} (fig. 32)

The scattergram of Mg versus Ca shows a continual increase of Mg with increasing Ca concentrations. The slope of calcium versus magnesium for the Woodbine, Nacatoch, and Eagle Ford Formations appears greater than for Paluxy, Glen Rose, Rodessa, Pettet, and Travis Peak Formations.

Br^{-} versus I^{-} (fig. 33)

The scattergram of Br versus I shows no correlation between species. Br concentrations increase independent of I concentrations.

Li^{+} versus Cl^{-} (fig. 34)

For Cl concentrations less than approximately 50,000, Cl increases independent of Li. For Cl concentrations greater than 50,000, Li concentrations increase significantly. The Li concentrations increase at approximately the chlorinity value where Ca, K, and Br increase significantly.

Cl^{-} versus Depth (fig. 22)

The scattergram of Cl versus Depth shows a continual increase of Cl with increasing depth. There is a greater scatter of data for the deeper formations (Paluxy, Glen Rose, Pettet, and Travis Peak).

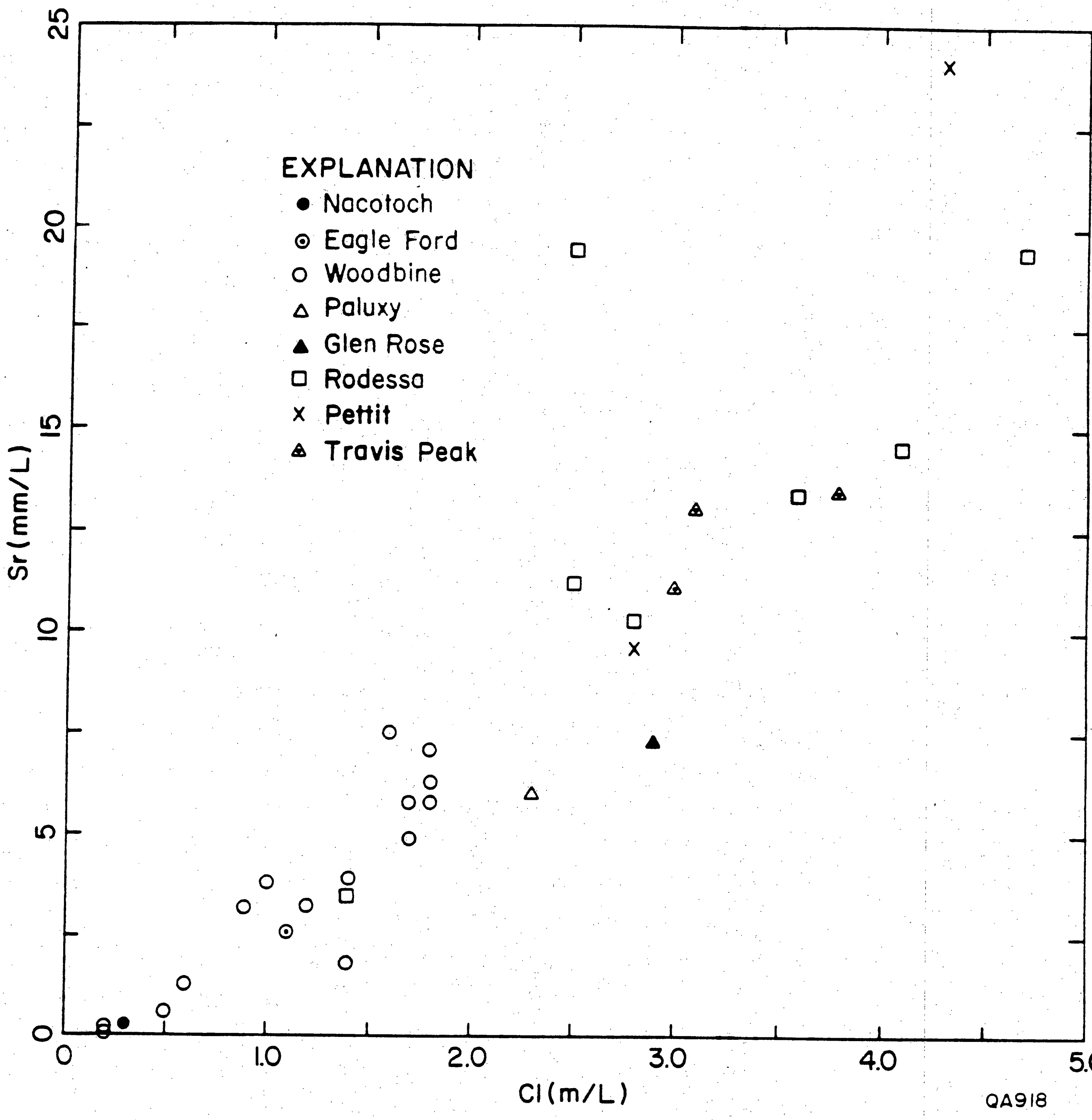

Figure 31. Strontium concentrations (mm/L) versus chloride concentrations (m/L). Data from Table 1.

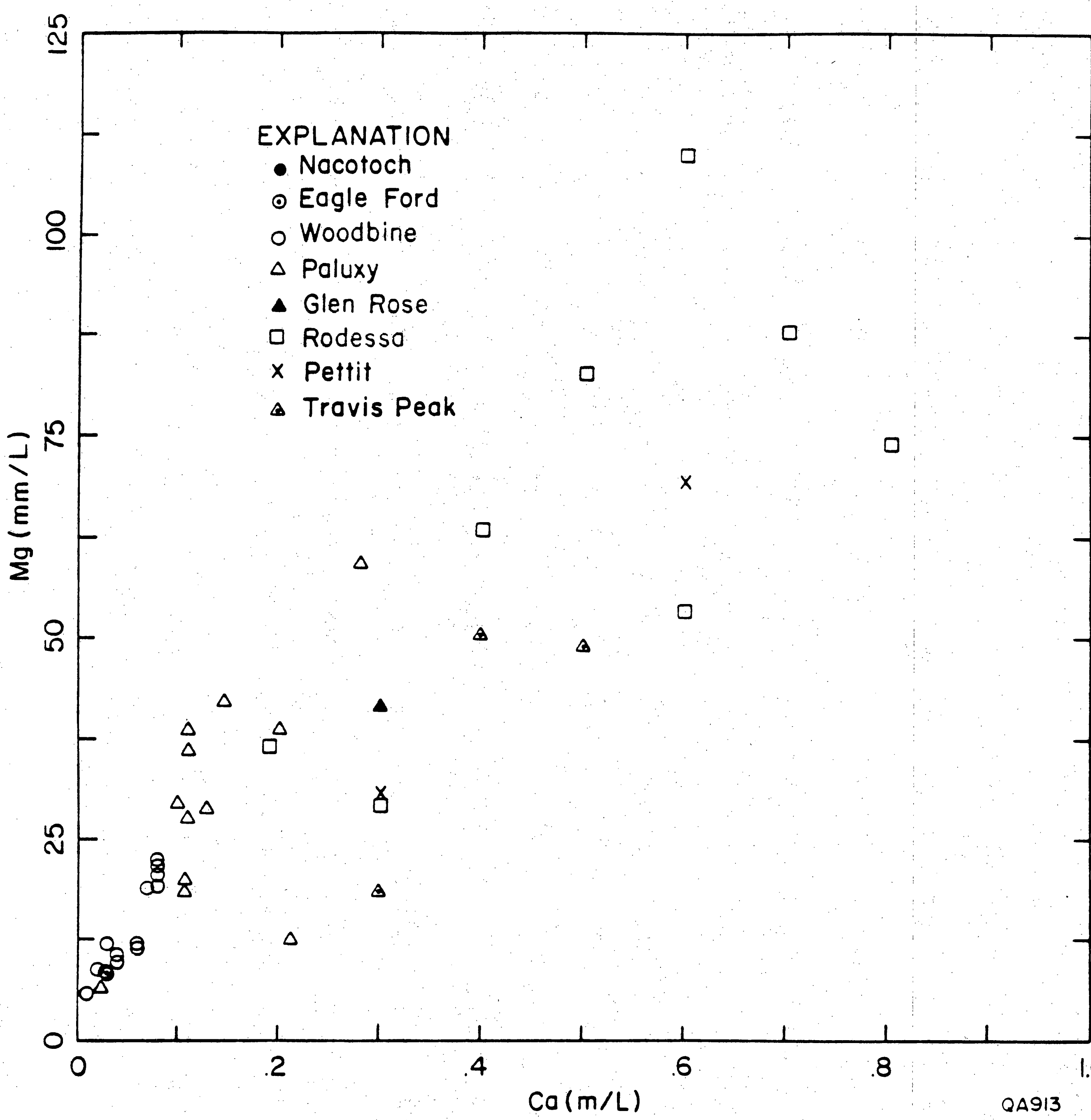

Figure 32. Magnesium concentrations (mm/L) versus calcium (m/L). Data from Table 1 plus additional Paluxy data from Appendix A.

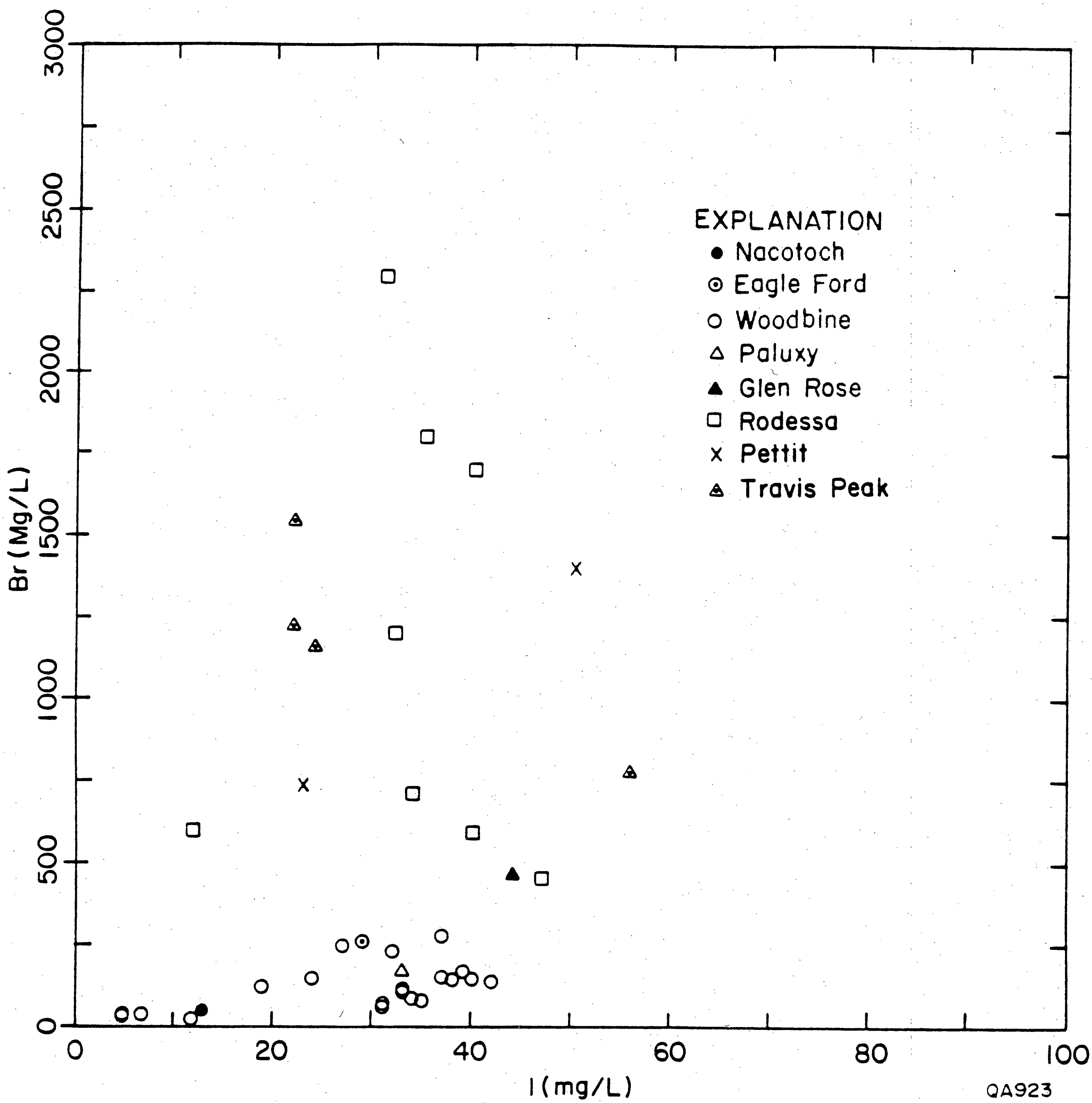

Figure 33. Bromide concentrations (mg/L) versus iodide concentrations (mg/L). Data from Table 1.

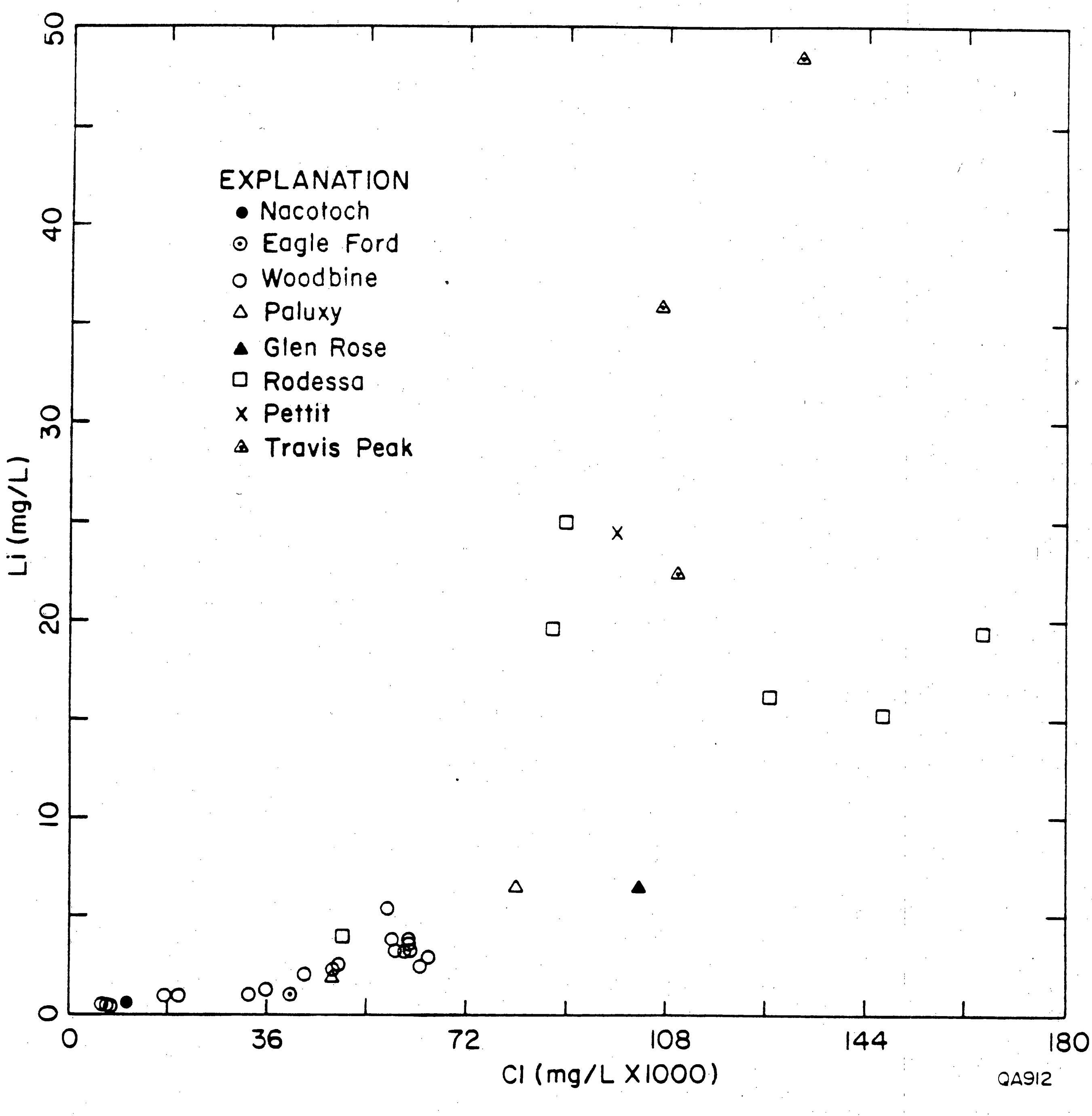

Figure 34. Lithium concentrations (mg/L) versus chloride concentrations (mg/L x 1000). Data from Table 1.

Ca^{++} versus Depth (figs. 35 and 36)

The scattergram of Ca versus Depth shows two different trends. For samples shallower than 6,000 ft, Ca concentration stays relatively low. In contrast to the shallow sampling depths, the Ca concentrations for the deeper sample are significantly higher and show a wide scatter. This change in trends at approximately 6,000 ft is also coincident with the 0.2 molar Cl concentrations observed to be important on the Ca versus Cl (fig. 26), K versus Cl (fig. 29), and Br versus Cl (fig. 30) graphs.

Br^{-} versus Depth (fig. 37)

The scattergram of Br^{-} versus Depth shows two different geochemical trends which are similar to the trends observed for Ca versus Depth. At shallow depths Br concentrations are low and consistent. At depths greater than 6,000 ft, Br concentrations are greater and have a wider scatter.

Discussion of Water Chemistry

The ionic solutes in the deep-basin brines result initially from the dissolution of salt domes by meteoric ground water. The previous discussion on the hydrogren and oxygen isotopic composition of the waters indicates that all waters sampled are of a meteoric origin. The mass balance calculations of original Louann Salt versus the amount of remaining domal salt indicate that dome dissolution through the geological history of the basin can easily accommodate for all the Na and Cl presently in solution. Additional geochemical reactions between the water and the rock matrix result in the addition or loss of ionic species in the water.

If dome dissolution appears to be the only important reaction affecting the Na concentrations in the basin, then the Na/Cl molar ratio should be approximately 1. This appears to be true for the shallower formations, Woodbine, Eagle Ford, and Nacatoch (figs. 24, 25). The concentrations of Ca, K, and Br conversely are small indicating minimal water-rock interactions (figs. 26, 29, and 30).

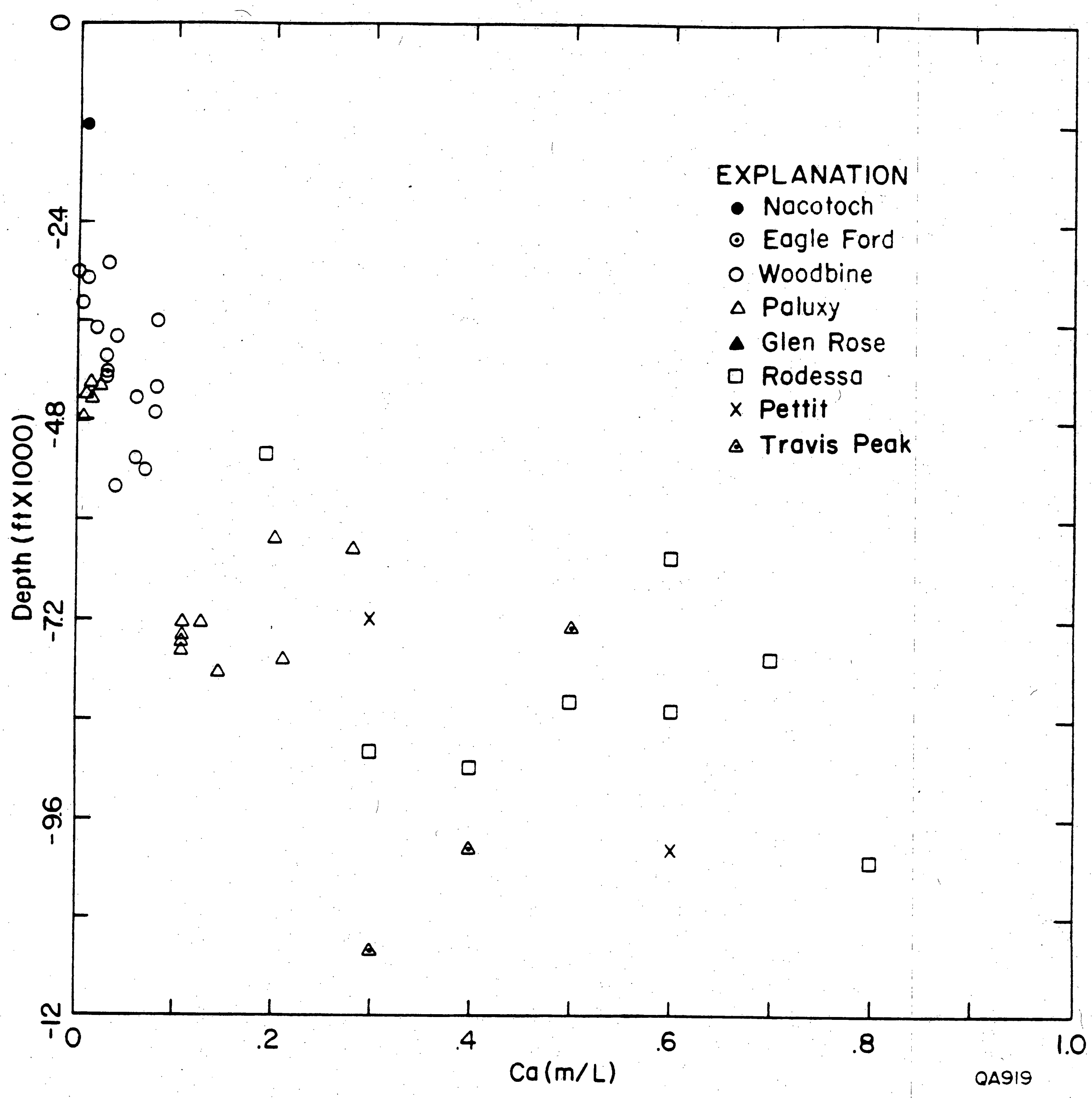

Figure 35. Calcium concentrations (m/L) versus depth. Data from Table 1 plus additional Paluxy data from Appendix A.

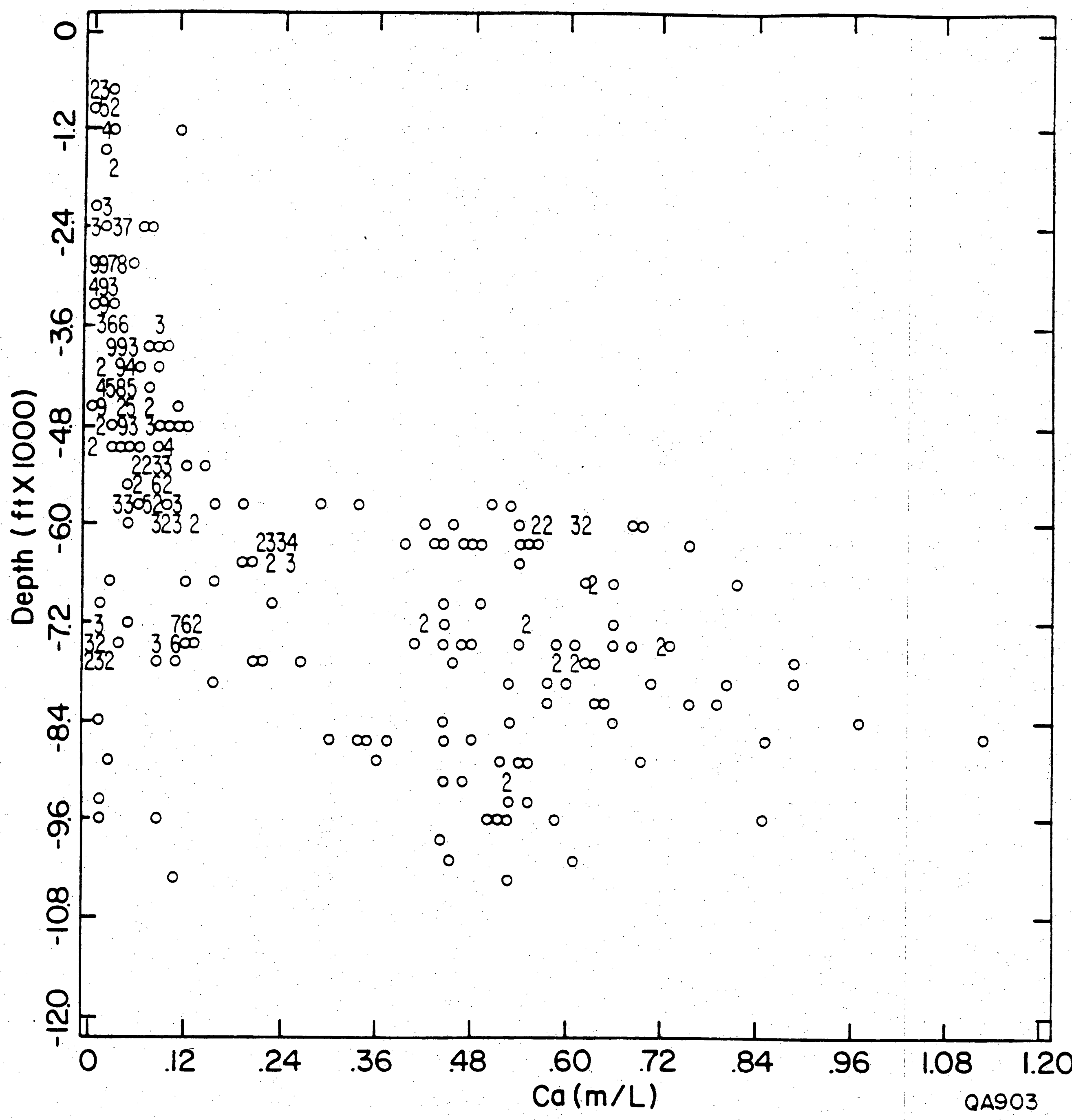

Figure 36. Calcium concentrations (m/L) versus depth. Data from Appendix A.

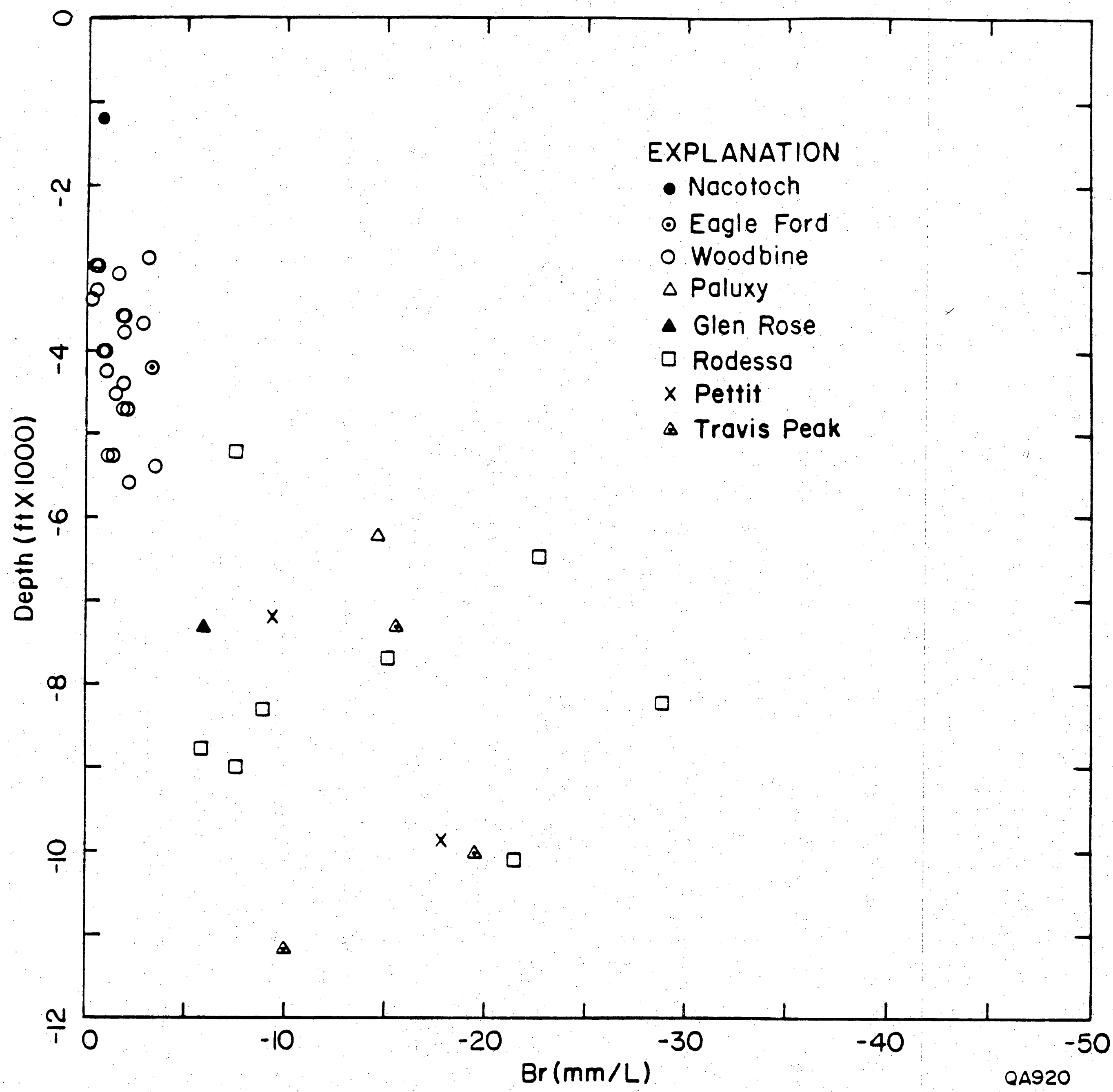

Figure 37. Bromide concentration (m/L) versus depth. Data from Table 1.

The chemical composition of waters in the deeper formations, in contrast, indicates several geochemical reactions have occurred or are presently occurring. The slope of Na to Cl for the deep brines is approximately 0.7 (figs. 24 and 25). Either halite dissolution was not the mechanism contributing to the Na-Cl load or Na has been lost from the brines. The first hypothesis is not considered realistic since a lower concentration brine from which the deeper waters have appeared to evolve, have approximately a 1:1 Na-Cl ratio. Secondly, the waters are continental meteoric in origin and not marine.

The increase in calcium (figs. 26, 27) and loss of Na (figs. 24, 25) are attributed to albitization. In this reaction sodium in solution is exchanged for calcium in the plagioclase. Land and Prezbindowski (1982) defined the equation (1) as follows.

Equation (1) plagioclase + halite + water = Na-Ca-Cl brine + albite

By adding the calcium (2 Ca, for charge balance purposes) to the Na concentrations, there is a close 1:1 molar ratio betwen Na + Ca/Cl (fig. 28). This 1:1 slope argues that there has been an exchange process that has caused the depletion of Na and the increase of Ca. This 1:1 slope also argues against the solution of anhydrite and subsequent reduction of the sulfate. If sulfate reduction was a dominant reaction, then the Na:Cl molar ratio should remain constant at 1 and not decrease to the observed 0.7 value. The lack of H_2S in the deep-basin brines (table 1) may also argue against sulfate reduction. Wescott (1983) observed that the most common secondary porosity in the Schuler Sandstone (the major sandstone directly beneath the Travis Peak) resulted from feldspar dissolution. Many of the feldspars had been albitized (Dunay, 1981). Garbarini (1979) also observed extensive albitization in the Hosston (Travis Peak) in Mississippi.

Potassium concentrations also increase significantly in the deeper formations. This increase in K could be attributed to either the dissolution of K-feldspars or the alteration of K-feldspars to albite (equation 2), a similar reaction to the albitization of plagioclase.

Equation (2) K-feldspar + halite + water = Na-K-Cl brine + albite

In Dunay's study of the Cotton Valley, minimal dissolution of K-feldspar was observed.

The mechanism which initiates the albitization of potassic and calcic feldspars may be the ionic strength of the brine and/or temperature. The sharp increase in both Ca and K starts at 2 molar Cl solutions. The approximate temperature is 70°C (based on a depth of 6,000 ft and an average geothermal gradient of 1.6°F (.9°C)/100 ft for the region. This temperature is lower than the 120°C suggested by Boles (1979) and Milliken and others (1981) for the albitization threshold temperature. Though the sharp increase in concentrations occurs at 2 molar solution and 70°C, the albitization reaction may be occurring at shallower depths and in less concentrated solutions. Plots of Na/Cl versus depth (fig. 38) and Na/Cl versus Cl (fig. 39) show that the shift of the Na/Cl ratio toward lower values starts in the shallower aquifers with the lower TDS values. This shift may also result from exchange reactions other than albitization such as cation exchange on clays.

Magnesium concentrations increase linearly with calcium (fig. 32). The Mg probably results from dedolomitization. With the increase in calcium in solution from the albitization reaction, the waters become undersaturated with respect to dolomite and dolomite solution should occur until equilibrium is reestablished, by the following equation.

Equation (3) $Ca + CaMg(CO_3)_2 = Mg + 2CaCO_3$

These waters are considered to be in equilibrium concurrently with calcite and dolomite, as evidenced by the relationship between the Ca/Mg ratio and temperature (fig. 40). With an increase in temperature, the calcite/dolomite equilibrium shifts toward dolomite, that is, dolomite becomes more stable (Land and Prezbindowski, 1981; Stoessel and Moore, 1983; Land, 1981). This shift in equilibrium should be observed in the Ca/Mg ratio with increasing temperatures. A linear increase in the ratio with increasing temperature is observed (fig. 40). Molar concentrations of calcium and magnesium are used in Figure 40 instead of the activity values, based on the arguments of Land and Prezbindowski (1981) that the ratio of concentrations is comparable to the activity ratios. The Ca/Mg ratio follows the calcite/dolomite equilibrium curve of Stoessel and Moore (1983) based on Robie et al. (1979) indicating that the waters are in equilibrium with calcite and dolomite.

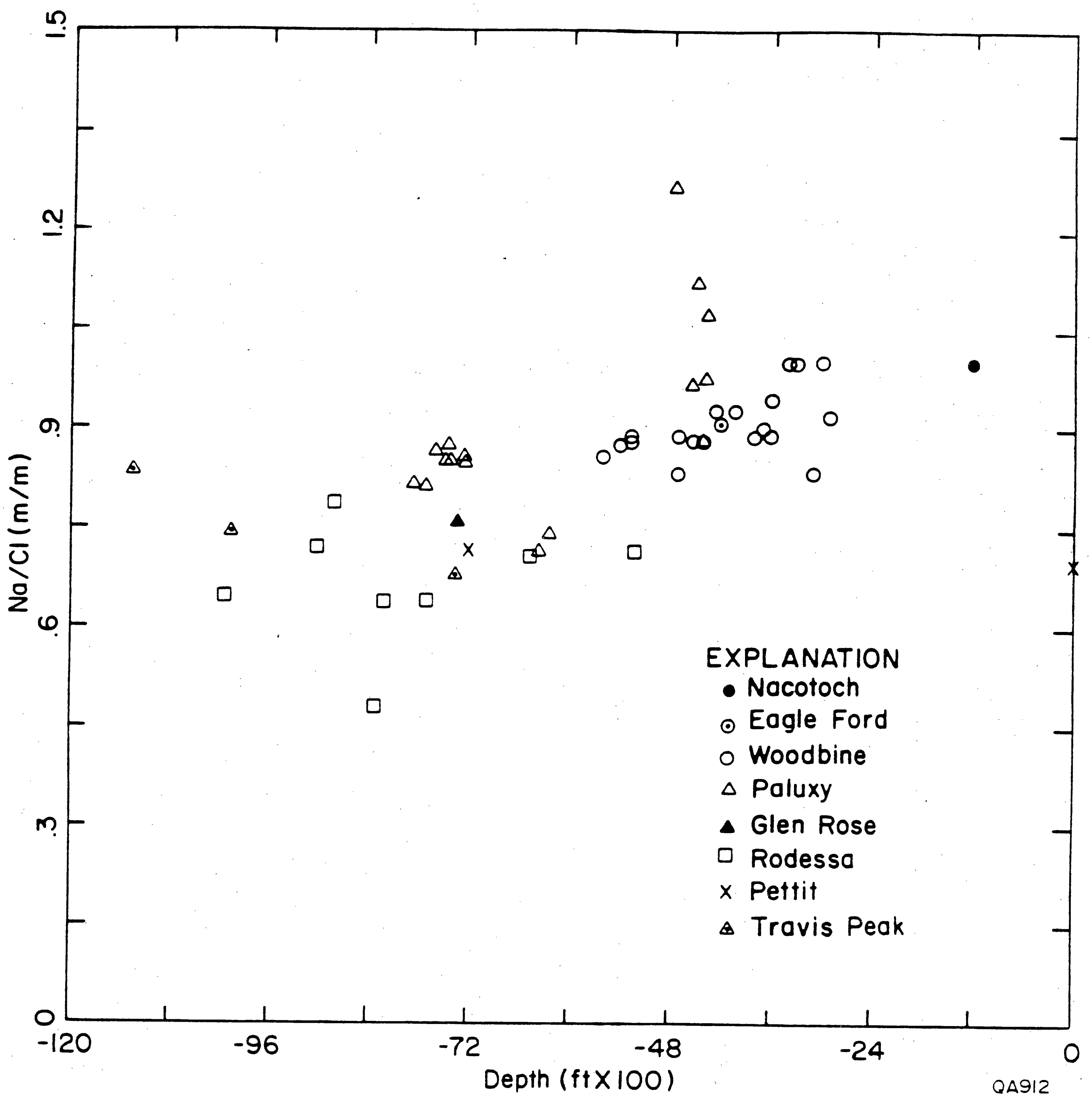

Figure 38. Na/Cl molar ratio versus depth. Data from Table 1 plus additional Paluxy data from Appendix A.

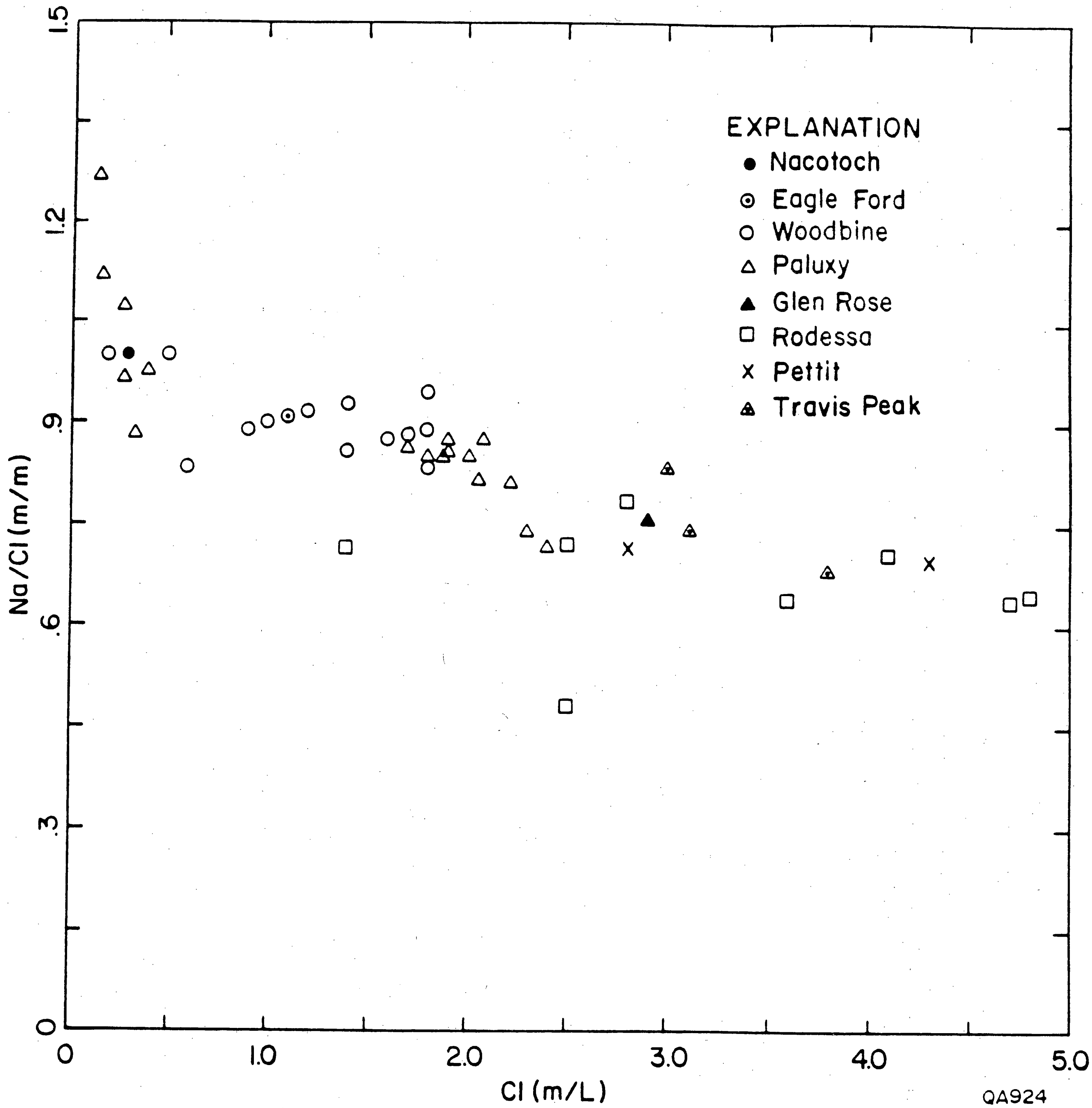

Figure 39. Na/Cl molar ratio versus chloride concentrations (m/L). Data from Table 1 plus additional Paluxy data from Appendix A.

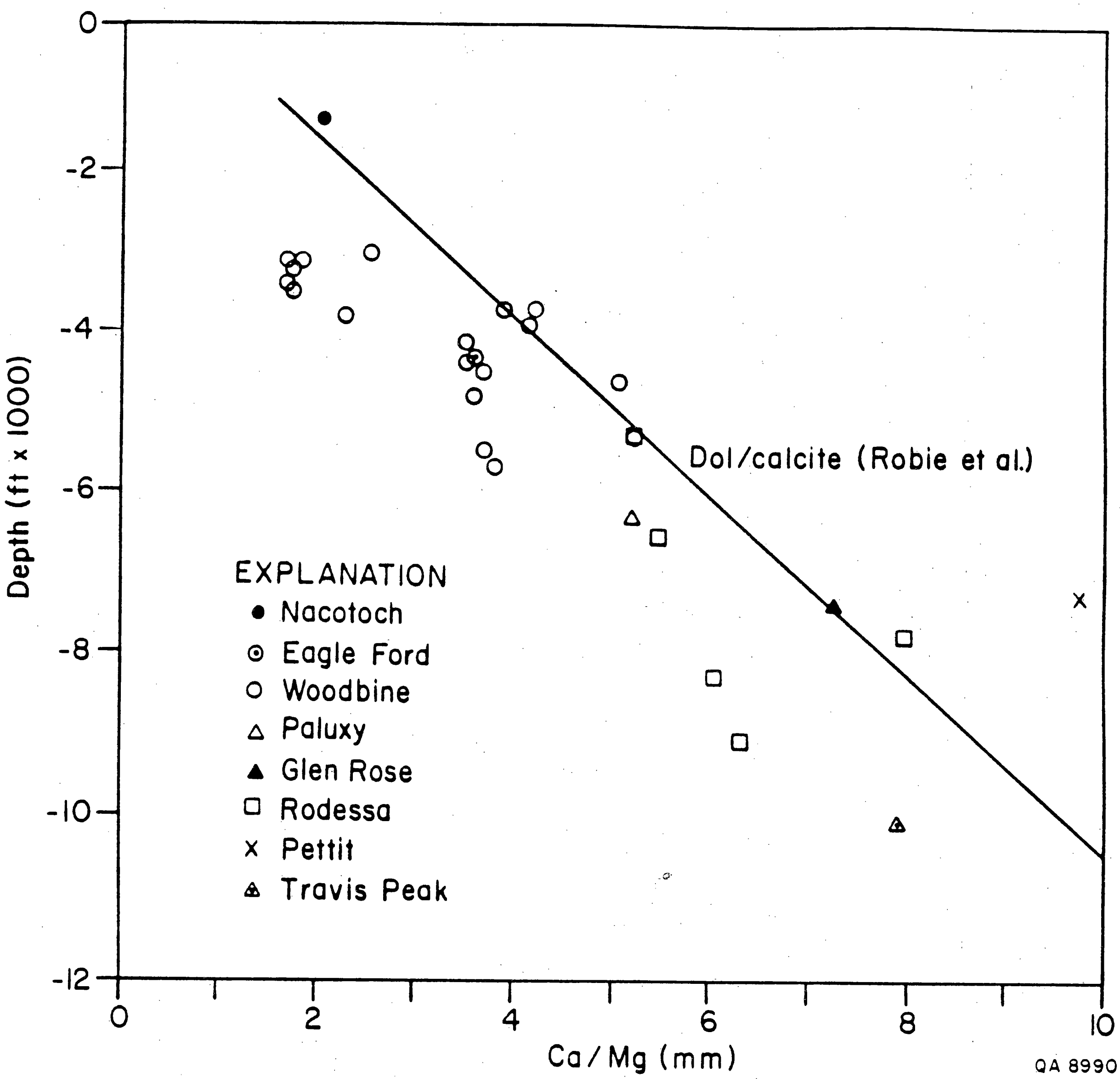

Figure 40. Ca/Mg molar ratio versus depth (Temperature). Data follows calcite/dolomite equilibrium line calculated by Stoessel and Moore (1983) from data of Robie et al (1978). Data from Table 1.

The Br composition of the deep basinal saline waters (figs. 30, 37) also appears to subdivide into two groups: low Br concentrations for Nacatoch, Eagle Ford and Woodbine Formations and significantly higher concentrations for the deeper units. The source of Br in saline deep-basinal water has been enigmatic. Carpenter (1978) suggested that the bromide results from residual brine squeezed out of the Louann Salt. Land and Prezbindowski (1981) suggest that the high Br concentrations result from a solution-reprecipitation of the halite which depletes the halite in Br and conversely enriches the solution in Br. If there is total solution of halite, then the Br/Cl ratio in the water will be the same in the original salt. If there has been solution/reprecipitation, then the Br content will be greater than in the original halite. This second hypothesis is considered a reasonable explanation for the Br in the East Texas brines.

Carpenter's residual Louann brine concept is considered unacceptable for the following reason. The amount of residual brine-pocket fluid needed for the observed Br concentrations through the Glen Rose and Travis Peak Formations is too large. If the Br in solution in the deep formation came from brine pockets squeezed out of the Louann Salt during deep burial, then the volume of the bittern brine can be estimated by (1) knowing the Br in the Glen Rose and Travis Peak Formations and by estimating the Br content in a late stage evaporite fluid. The brine content in the deep formations (Glen Rose and below) is estimated at 3×10^{15} g of Br. Assuming the Br concentration in a late-stage evaporation brine is 5,000 mg/l based on approximate Br content during K-salt precipitation (Carpenter, 1978), then the estimated volume of the residual brines is 600 km^3. This 600 km^3 constitutes 10 percent of the volume of the original salt dome province or a porosity of 10 percent. The salt thickness is estimated at 1,500 m. Maintaining this 10 percent porosity during the accumulation of 1,500 m of halite is considered unrealistic.

The solution-reprecipitation mechanism is preferred for the following reasons. The Br concentration of the halite from Oakwood salt dome (East Texas) averages 45 ppm, which is slightly depleted from 65 to 75 ppm Br expected for "first cycle" halite (Holser, 1979). Dix and

Jackson (1981) interpret this depletion as the result of solution and reprecipitation. The Br in the original Louannn Salt may have been much higher. Kreitler and Muehlberger (1981) noted that Grand Saline salt dome had undergone very little dissolution and the geochemistry of these salts might approximate the chemical composition of the original Louann Salt. In Grand Saline, Br concentrations ranged from 100 to 300. If the bromide in the halite at Grand Saline represents original Br concentrations of the Louann Salt, then the halite in Oakwood Dome, and possibly the halite in other domes have undergone a significant depletion of bromide.

Kumar and Hoda (1978) observed Br concentrations in brine pools and brine springs in the Weeks Island and Belle Island salt domes mines that ranged from 1,100 to 13,500 mg/l with a mean of 6,200. Chloride concentrations ranged from 194,000 to 276,000 mg/l. These waters should represent brines that have equilibrated with the mineralogy of the salt stock and may therefore be analogous to formation waters that have equilibrated with the salt stock on its exterior. Their data indicate that high Br concentrations can result from basinal water reacting with a salt dome. Kumar and Hoda's (1978) Br/Cl molar ratio of .09 is higher than Br/Cl molar ratio (.007) observed in the Glen Rose and Travis Peak brines from this study. East Texas deep-basin brines, however, would be the product of both halite dissolution as well as equilibrating with a Br-enriched halite and therefore have Br/Cl ratios lower than observed in pools and springs observed in the mines.

Carpenter and Trout (1978) suggested that Br and I in saline ground water may result from the decomposition of organic material. Figure 33 shows no correlation between Br and I. If iodine is coming from organic decomposition (a reasonable idea), then the Br is not.

The deep-basinal brines also are high in Sr. There are at least two possible sources for the Sr in solution. (1) Disseminated anhydrite in salt dome halite has a strontium content of approximately 1,500 mg/kg (Kreitler and Dutton, 1983). The dissolution of salt dome halite should result in the dissolution of some anhydrite and release of strontium. (2) Albitization of plagioclase may release Sr as well as Ca. Smith (1975) measured Sr concentrations in feldspars up to 5,000 ppm.

A plot of Sr versus Cl (fig. 31) shows a continual increase of Sr with Cl which is in contrast to the Ca versus Cl, K versus Cl and Br versus Cl plots (figs. 26, 29, and 30). This indicates that a geochemical reaction envisioned for brines albitizing Sr-bearing plagioclase in the Paluxy, Glen Rose and Travis Peak is not the sole cause of Sr in solution.

The chemical composition of the saline waters in the Glen Rose (Pettet and Rodessa are part of Glen Rose) and Travis Peak is significantly different than the chemical composition of the waters in the Nacatoch, Eagle Ford and Woodbine Formations. Chemical composition of waters in the Paluxy appears transitional between these deeper and shallower formations. Figures 35, 36, and 37 show an abrupt increase in Ca and Br concentrations at a depth of approximately 6,000 feet. This depth is the general depth of the Paluxy and top of Glen Rose. This depth is also coincident with 2 molar Cl concentration (figure 26) which appears to be an important concentration for initiating albitization and other rock-water reactions.

This break in chemical composition at ≃ 6,000 feet also coincides with the fluid pressure/depth relationships. Shallower than 6,000 ft, the basin pressures are hydrostatic to subhydrostatic. Below 6,000 ft, the pore fluid pressures are slightly overpressured. (A more detailed discussion of basin pressure is in a later section.)

The Na-Ca-Cl waters initially were Na-Cl waters. The addition of Ca, Mg, Sr, and other trace elements had to have occurred after the addition of 2 moles of NaCl. If these waters started as a Na-Ca-Cl water, they should trend to a 0,0 position rather than the 2 mole position (fig. 26).

The transition of a Na-Cl water to a Na-Ca-Cl water implies but does not prove hydrologic continuity between the Na-Cl waters and the Na-Ca-Cl waters. Kreitler and others (1978) in a study of Gulf Coast aquifers and Fogg and Kreitler (1982) in a study of the Carrizo-Wilcox aquifer in East Texas used the continual change in water chemistry as a tool for identifying flow paths. This probably is not a continuous flow system from the shallow saline aquifers to the deeper aquifers in the East Texas basin. The fact that the Na-Ca-Cl waters evolved from a Na-Cl water only indicates that the deeper waters and the shallower saline waters are following the same geochemical evolution and the deeper waters have evolved significantly further.

The chemical composition of the Paluxy waters appears transitional between the shallower Na-Cl waters and the deeper Na-Ca-Cl waters (figs. 24 and 26). This may result from two processes. (1) The Paluxy waters may be in the appropriate temperature and salinity environment such that a Na-Ca-Cl water results, or (2) the chemical composition of these waters may result from the mixing of the two different water types. Leakage may be occurring from the slightly overpressured Glen Rose into the Paluxy.

This subdivision of chemical composition into Na-Cl waters and Na-Ca-Cl waters appears to be independent of lithology within each major group. The Na-Ca-Cl waters occur in both sandstones (Travis Peak) and limestones (Glen Rose Group). The change in chemical compositions may be related to three factors. (1) The two molar NaCl concentration may be a threshold value to cause major rock water reactions; (2) The temperatures at 6,000 feet may be sufficient to initiate the rock-water reactions; (3) The waters in the deeper formations may be much older and have thus permitted greater rock-water interaction.

The interpretation of rock/water geochemical reactions is based only on the chemical analysis of the waters. Minimal petrographic analyses of the different formations are available. This represents a major limitation of the study. If reactions such as albitization of feldspars or dedolomitization have occurred, then they should be evident in the rock record.

Water Chemistry Proximal to Salt Structures

The previous discussion identified the major chemical composition trends in the saline aquifers. Study of the water chemistry from oil and gas fields close to salt domes might indicate anomalous hydrologic or geochemical processes because of the presence of the dome. Anomalous chemical composition might indicate ongoing dome dissolution or leakage from deeper or shallower formations.

Sixteen water samples of the 38 samples listed in table 1 are near or overlying salt domes or salt pillows (table 10). Seven of these 16 samples were collected from formations that either laterally abutted a salt structure or were less than 1,000 ft overlying a salt structure. There are only a few producing oil fields on the flanks of the salt domes; therefore, samples from dome flanks are very limited. Most of the oil associated with salt structures are fields overlying salt anticlines. The salt anticlines often are very deep and the fields overlying them are shallow in comparison.

Neither the total 16 samples associated with salt structures nor the 7 samples in closer continuity with the salt dome show consistently anomalous water chemistry in comparison to the general trends observed for all the water chemistry analyses (fig. 41 and 42). The salt domes are presently not affecting the chemical composition of the brines. The conclusion is in agreement with the electric log SP interpretation of the Woodbine.

HYDRAULIC POTENTIAL DISTRIBUTION, EAST TEXAS BASIN

Introduction--Summary

The hydraulic potential distribution of the saline aquifers in the East Texas Basin has been evaluated by analysis of drill-stem test data. Based on these data, there appear to be two major hydrologic systems: the Upper Cretaceous aquifers and the Lower Cretaceous-Upper Jurassic Formations. The Lower Cretaceous-Upper Jurassic system may be a closed hydrologic system with some leakage into the overlying Paluxy Formation. In the upper aquifer system the Woodbine Formation has been depressurized because of extensive hydrocarbon production. It is doubtful whether fluid pressures in the Woodbine would return to natural levels in the near future.

Methods of Analysis

Approximately 300 drill-stem pressure measurements were obtained from the files of Petroleum Information Corporation and scout cards (Appendix B). Final shut-in pressures have

Table 10. Water Samples from Fields Near Salt Domes and Salt Pillows

Sample	Depth (ft)	Depth to top of salt (ft)
VAN N	1,200	12,000
V. W	2,900	"
VAN GR	7,230	"
VAN R	5,220	"
B.C.1	3,600	3,000
B.C.2	3,600	"
N.W.1	4,704	"
N.W.2	4,704	"
H.W.	9,776	< 1,000
C.W.	4,404	5,000
CAY.W1	4,030	16,000
CAY.W2	4,030	"
CAY.R	7,460	"
CAY.P	7,550	"
NWSW	5,400	10,000
HAW.W	4,531	12,000
HAW.R	8,300	"
B.D.ROD	10,100	< 1,000
B.D.PET	10,300	"
OP.R	8,630	14,000
OP.P	8,900	"
OP.TP	10,000	"
G.S.R.	8,200	0

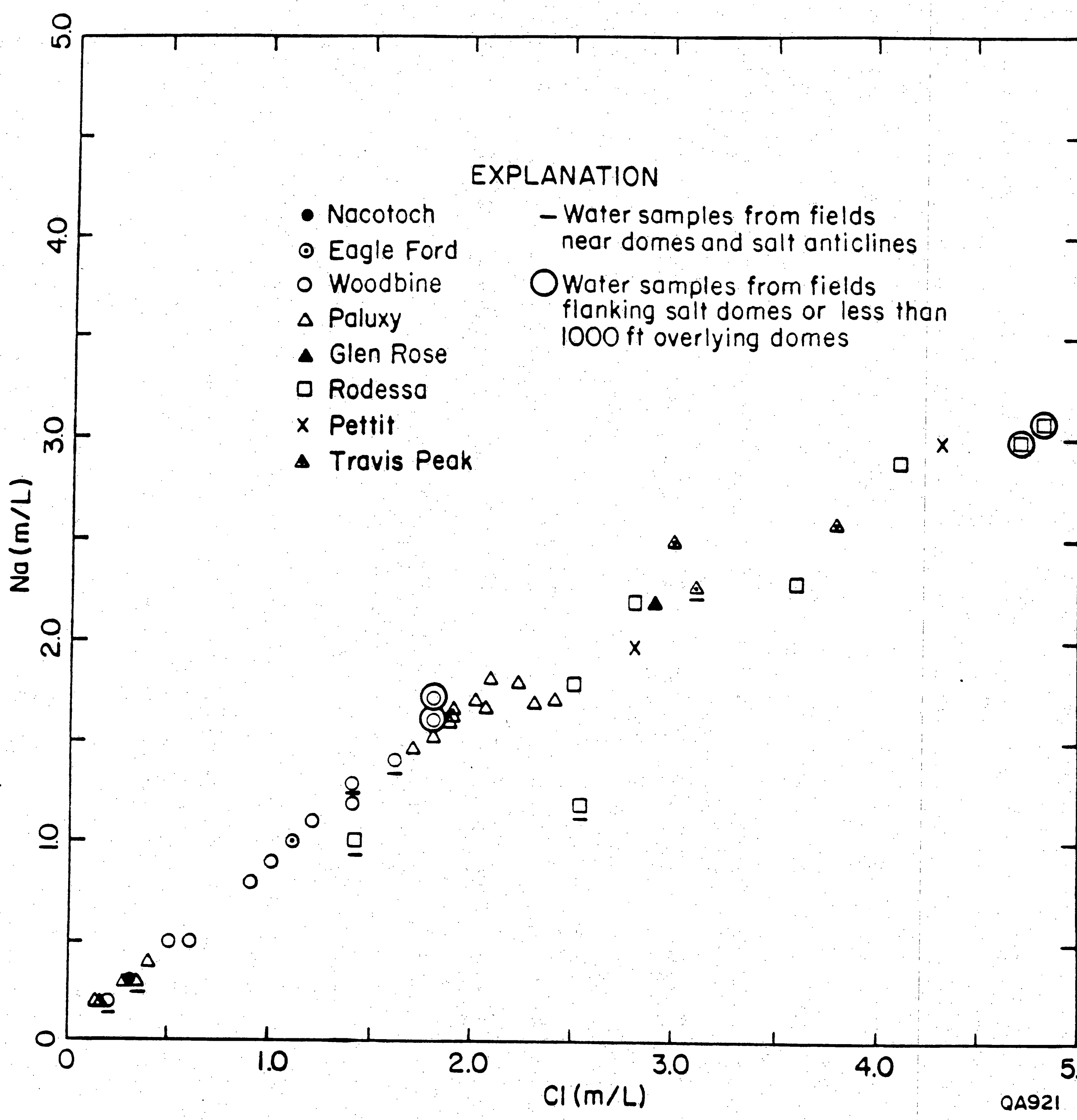

Figure 41. Effect of proximity to salt structures on water chemisty: Ca versus Cl. Data from Table 1.

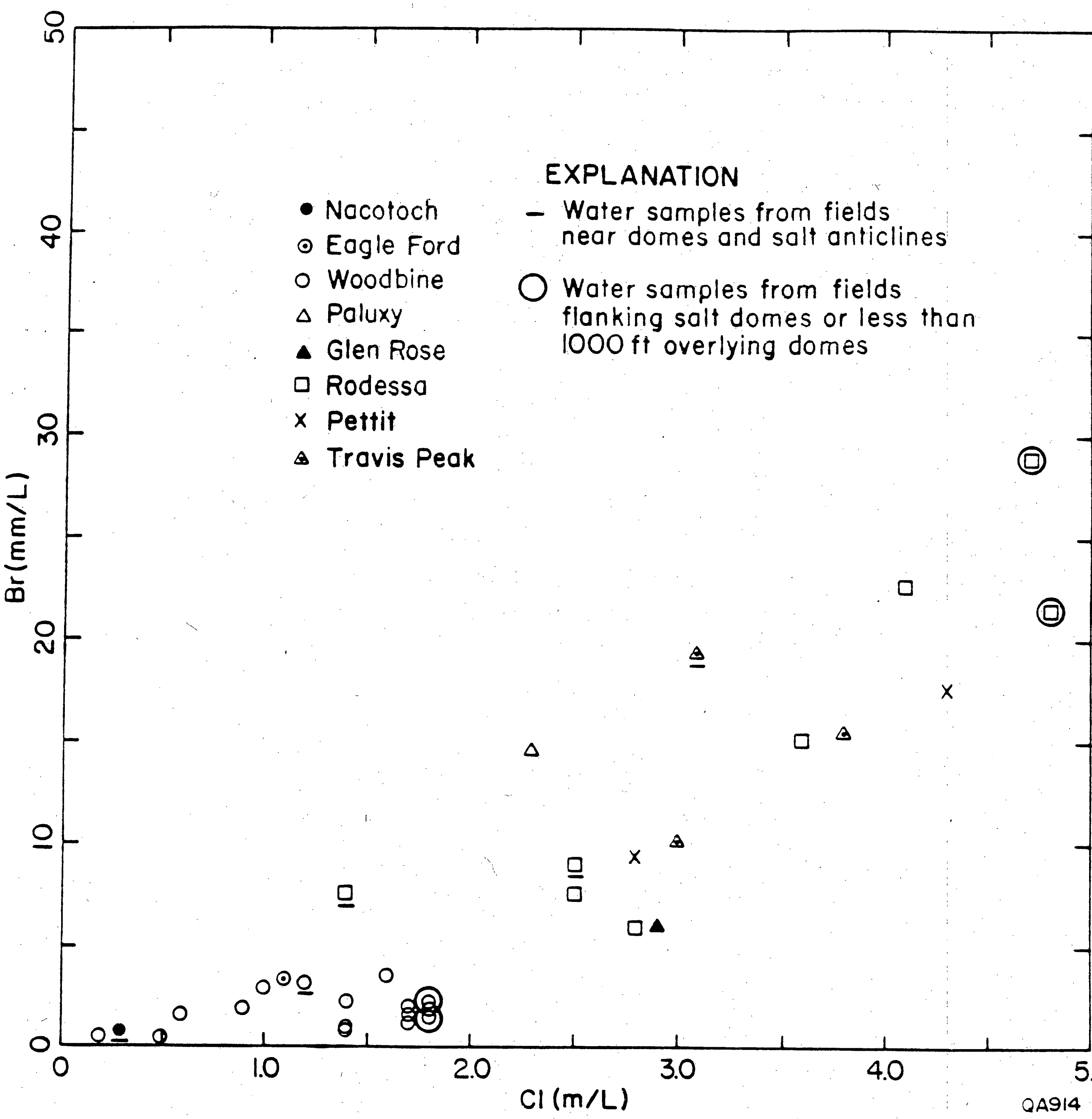

Figure 42. Effect of proximity to salt structures on water chemistry. Br versus Cl. Data from Table 1.

been plotted against depth (fig. 43). The quality of drill-stem test data is always suspect because of the normal difficulties in obtaining good tests. Optimally the test data should include the trace of the test, including an initial shut-in pressure (ISIP) and a final shut-in pressure (FSIP) (Bredehoeft, 1964). Too often, however, only the FSIP is recorded. This is true for the East Texas data. Only 11 out of 300 have both FSIP and ISIP. Fifty-five percent of these tests had FSIP within 10% of the ISIP. No traces of the actual test were available. Without this additional information the accuracy of the FSIP cannot be evaluated. Considering these constraints, it is recognized that the following discussion is based on a less than satisfactory data base.

Results and Discussion

Two pressure-depth regimes are observed in the East Texas Basin. The Woodbine and shallower formations approach hydrostatic or are subhydrostatic (fig. 43). The lower pressures are the result of hydrocarbon production (Bell and Shepherd, 1951). In contrast, the deeper formations (Glen Rose, Travis Peak, Cotton Valley, Sligo, Buckner, and Smackover) are slightly overpressured (fig. 43) (gradient ≈ .6 psi/ft). Several tests in these deeper zones indicate underpressured conditions that probably have resulted from hydrocarbon production or represent faulty test data.

These two different pressure/depth regimes represent two major aquifer systems: (1) the hydrostatic Upper Cretaceous sandstones and limestones and (2) the slightly overpressured Lower Cretaceous and Upper Jurassic sandstone and limestone formations. The Upper Cretaceous hydrostatic system has better porosity, better permeability and is well interconnected through the basin, in comparison to the deeper formations. Average porosities for Woodbine and Paluxy are 25% and 12%, respectively (table 4). Hydrocarbon production from the Woodbine Formation in the East Texas Field has caused pressure declines in the Woodbine across the entire basin (Bell and Shepherd, 1951; fig. 44).

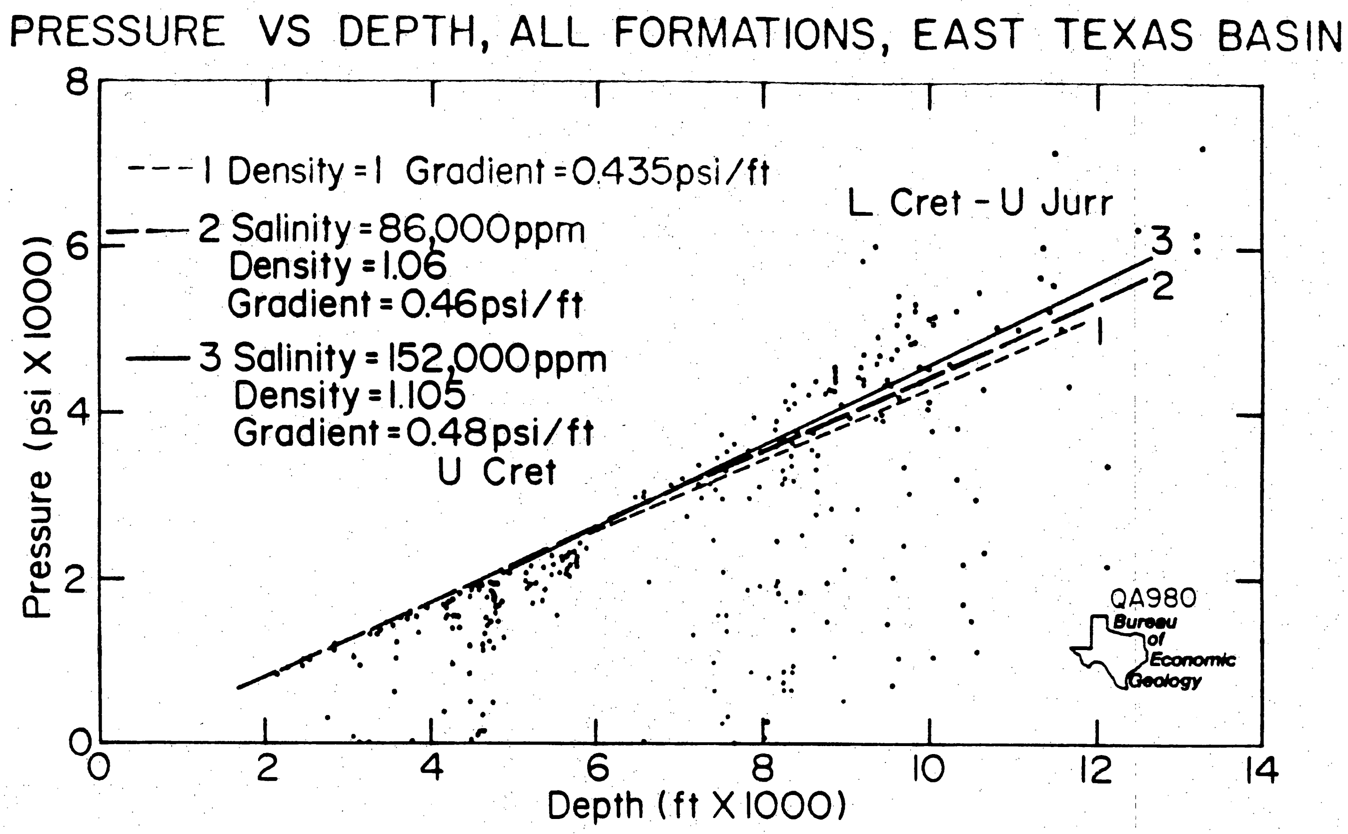

Figure 43. Pressure (psi) versus depth for saline aquifers, East Texas Basin. Data from Appendix B.

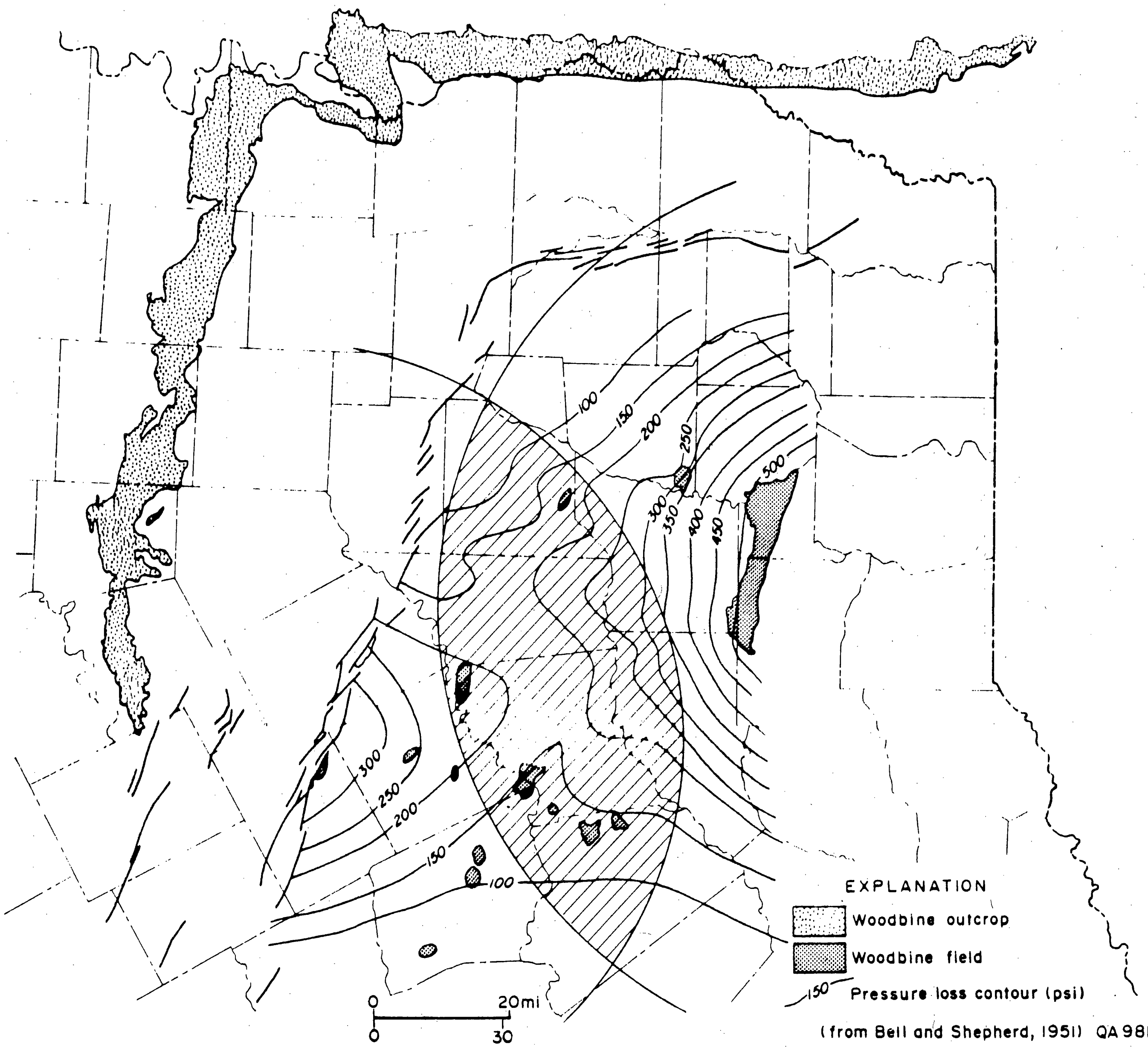

Figure 44. Estimated pressure declines in the Woodbine formation from oil production in East Texas field and the Mexia fold along the Mexia-Talco fault system (from Bell and Shepherd, 1951).

Presumed reasons for such widespread pressure declines are (1) highly permeable, laterally continuous sands; (2) low coefficient of specific storage, approximately 6×10^{-6} m^{-1} based on values of compressibility for Woodbine core samples (Hall, 1953); (3) lack of lateral recharge owing to barrier boundaries caused by the Mexia-Talco fault zone along the west and north. The Mount Enterprise - Elkhart Graben fault zone along the south, and stratigraphic pinch-out of the Woodbine sand along the east basin margin; and (4) lack of vertical recharge owing to deep burial beneath low-permeability aquitard/aquiclude strata of the Midway and Navarro. The high permeability and low specific storage coefficients give a low diffusivity coefficient (Freeze and Cherry, 1979) which would allow pressure declines to spread a greater distance in a relatively short period of time.

With final depletion and abandonment of oil and gas production in the Woodbine it is doubtful whether fluid pressures would rapidly return to their preproduction levels. A downward vertical hydraulic gradient should remain between overlying fresh-water aquifers and the Woodbine for a long, but undetermined time.

The Lower Cretaceous-Upper Jurassic hydrostratigraphic system has lower porosities, probably lower pemeabilities and less interconnectedness. Average porosities in Glen Rose and Travis Peak are 8.5% and 7.0%, respectively. The overpressuring may result from continued compaction and a minimal leakage of waters into overlying formations. Overpressuring in deep Cretaceous carbonates (Sligo) has been observed in other localities of the Gulf of Mexico (Land and Prezbindowski, 1981). Its origin probably cannot be attributed to shale compaction or shale diagenesis as is the mechanism for the overpressured Tertiary section in the Gulf of Mexico, but may be related to continued compaction and recrystallization of carbonates and sandstones. The process is not understood. This lower hydrostratigraphic system may be a relatively closed system. If this system is an active hydrodynamic system, fluid pressures should have equilibrated to hydrostatic conditions. This interpretation is in agreement with the observation that there is a significantly different water chemistry between deep Lower Cretaceous formations and the Upper Cretaceous formations.

The Paluxy sandstone may be a mixing zone for the Upper Cretaceous hydrologic system and the deeper saline system. The Paluxy Formation was expected to have similar hydrology and geochemistry as the younger Woodbine Formation, because of its similar depositional character (terrigenous sandstone with reasonable interconnectedness) and its similar stratigraphic position (i.e., above the thick Glen Rose carbonates). The depth of the Paluxy pressure data (Appendix B) is where the pressure/depth slope starts rising above brine hydrostatic (fig. 43). The chemical composition of the Paluxy water is variable. Some of the waters are NaCl water, similar to Woodbine, whereas others are Na-Ca-Cl waters and appear intermediary between the chemical composition of Woodbine waters and Travis Peak or Glen Rose waters. The chemistry and hydrology suggest that waters from the Glen Rose and Travis Peak Formations are leaking into the Paluxy.

The data base is inadequate to construct potentiometric surfaces for any of the formations. Bell and Shepherd's (1950) surface is outdated since it was constructed in 1950 and there has been extensive production since then. Without potentiometric surfaces for individual formations or the major aquifer groupings, and without a better understanding of the hydrology, prediction of flow directions or flow velocities is not possible at this time.

GENERAL HYDRODYNAMICS OF THE SALINE AQUIFERS, EAST TEXAS BASIN

Introduction

A conclusion of the water chemistry and the pressure-depth discussions of this paper is that the basin has been relatively stagnant over long geologic time. This lack of an active hydrodynamic system is probably controlled by the general hydrologic conditions of the basin. No major tectonic event has uplifted and tilted the basin to establish effective recharge and dicharge zones or steep hydraulic gradients across the basin to facilitate flushing. The East Texas Basin is still largely below sea level. Sedimentary basins such as the Palo Duro, the San

Juan, the Paradox, and the Alberta Basins have all been uplifted by postdepositional tectonic events which have permitted continued flushing of earlier formation waters.

Recharge to the East Texas Basin

Recharge to the saline formations in the East Texas Basin could be expected where these formations (e.g., Woodbine, Paluxy, Travis Peak (Hosston)) crop out. All the aquifers, however, crop out to the west of both the Balcones and the Mexia-Talco Fault Zones. These faults probably limit the recharge into the basin (Plummer and Sargent, 1931; Parker, 1969; Macpherson, 1982). The hydraulic gradient is either low or reversed, neither situation conducive for basin flushing. The hydraulic heads in the Glen Rose and deeper formations are significantly above land surface because of the slight overpressuring. Ground-water flow from outcrop downdip into the deep basin is not expected because of these high pressures in the saline formation. The Mexia-Talco fault system exhibits greater throw with depth because the faults were active through a broad range of time (Jackson, 1982). Because of the increased displacement with depth, the faults may function as more efficient impermeable barriers at greater depths. The Travis Peak and Glen Rose Formations may be more hydrologically isolated than the shallower Woodbine.

Discharge from the East Texas Basin

A deep basin must have discharge zones as well as recharge zones for fluid movement to occur. The deep saline formations of the East Texas Basin do not have obvious regional discharge zones. There are no outcrops of Woodbine, Paluxy, Glen Rose or Travis Peak Formations on the eastern or southern sides of the basin, where discharge might occur. The only available avenues for discharge may be along faults or dome flanks located in topographically low areas (Fogg and Kreitler, 1982). The depressuring of the Woodbine formation by oil production has reduced or eliminated the discharge from the Woodbine into shallower aquifers.

False Cap Rock at Butler Dome, An Example of Deep-Basin Discharge

Deep-basin ground-water discharge may have occurred along the flanks or associated radial faults of Butler Dome, Freestone County, East Texas. A calcite-cemented sandstone identified as "false cap rock" is being quarried from the flanks of Butler Dome. This false cap rock appears to have resulted from the oxidation of hydrocarbons in hot saline waters being discharged up the dome flanks. Saline springs were present over the dome before the depressuring of the Woodbine Formation occurred (DeGolyer, 1919; and Powers, 1920). The springs no longer exist.

Rocks exposed in the East Texas Stone Company's Blue Mountain Quarry on the NNE side of Butler Dome comprise the Eocene-Claiborne Carrizo and Reklaw Formations (fig. 45). Claiborne sediments dip away from the dome's center at a maximum of 25°NE, and are unconformably overlain by Quaternary terrace deposits. The Quaternary deposits reveal no evidence of warping due to dome uplift. A normal fault strikes N10° - 30°E, lateral to the western quarry wall, and dips 70°SE (fig. 46). Claiborne sediments are displaced about 1.5 m. In the quarry on the downthrown side of the fault, Carrizo sandstone is cemented with $CaCO_3$. Typically the Carrizo sandstone in the East Texas Basin is friable. This bell-ringing hard, calcite-cemented Carrizo represents an anomalous case. Sands on the upthrown side of the fault to the west are not cemented with $CaCO_3$. Large ellipsoid calcitic, pyritic concretions are scattered randomly through outcrop (fig. 47). Along the fault plane calcite has precipitated as fracture-filled veins (fig. 48). The fault appears to have been the primary path for fluid movement. At the eastern quarry wall, the calcareous sandstone gradually grades into an uncemented friable sand with only a few patches of $CaCO_3$ cemented sandstone. Some of the sand lenses within the shales and mudstone of the Reklaw Formation are also cemented with $CaCO_3$, but none of the Quaternary sands and gravels have $CaCO_3$ cement. This observation suggests that precipitation of the $CaCO_3$ cement occurred before Quaternary time or that the deeper discharging fluids could not rise any closer to land surface.

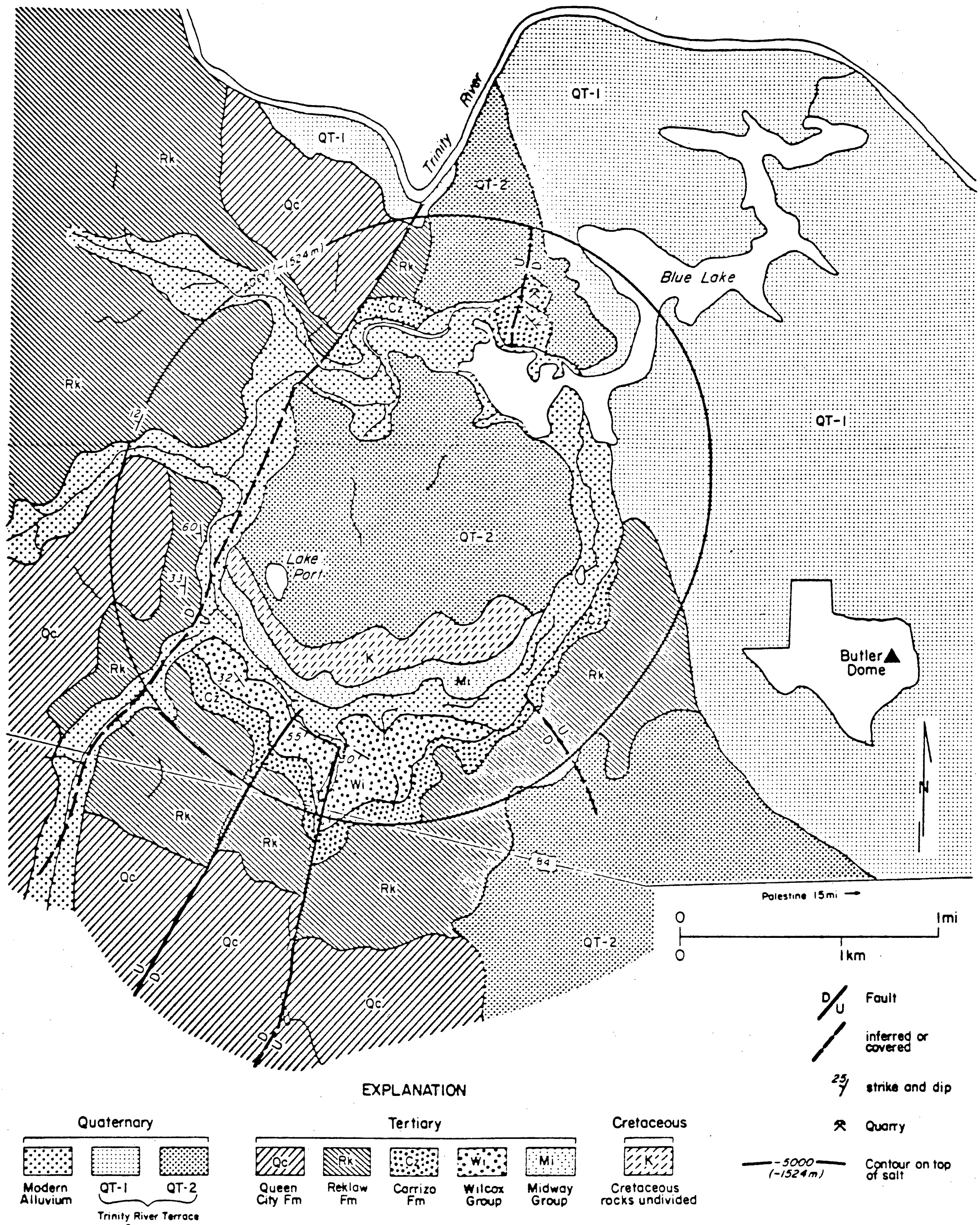

Figure 45. Geologic map of Butler dome, East Texas (modified from Barnes, 1967).

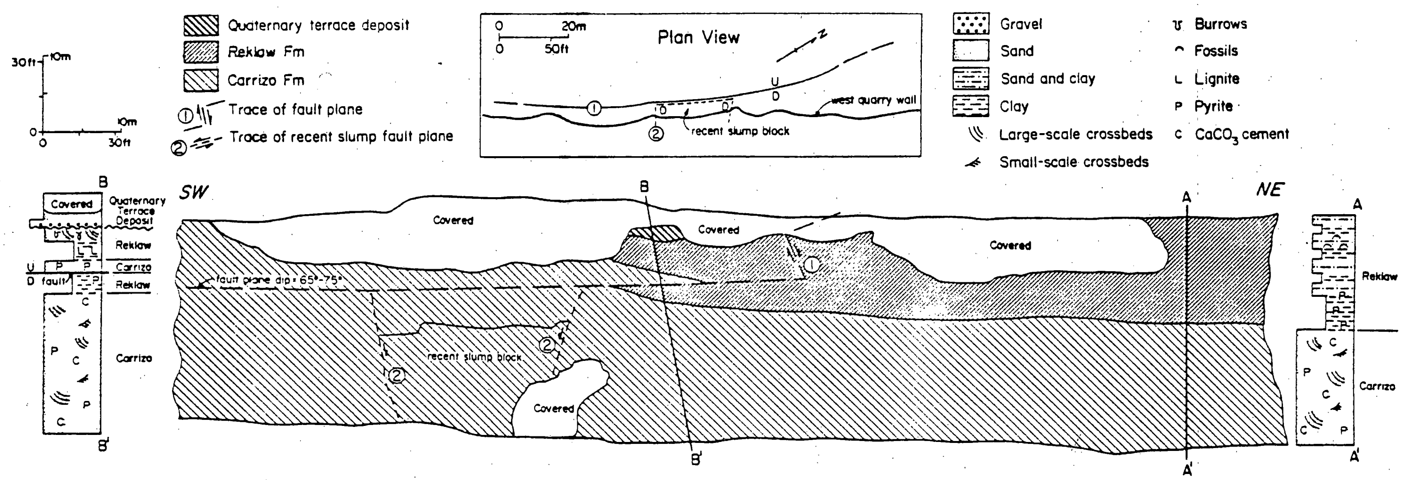

Figure 46. Cross section and map view of fault in Blue Mountain quarry on flank of Butler dome.

Petrographic analyses of these calcareous sandstone samples indicate that the quartz sand grains are cemented with some pyrite and more commonly sparry to prismatic calcite. Little of the original sandstone porosity exists and the cement is commonly poikilotopic (fig. 49). Replacement of the clastic grains by calcite and pyrite is common.

The calcite cement appears to result from oxidation of hydrocarbons by the reaction:

$$CaSO_4 + CH_4 \rightleftarrows H_2S + CaCO_3 + H_2O$$

The $\delta^{13}C$ values of the cements range from -20 to -32 (table 11 and fig. 50), indicative of a hydrocarbon source for the carbon (Feely and Kulp, 1957; Kreitler and Dutton, 1983). The $\delta^{18}O$ values of calcite cements ranged from -8.2 to -9.4%, which is considered to be indicative of calcite precipitation from a hot water. Kreitler and Dutton (1983) observed $\delta^{18}O$ values for Oakwood Dome cap rock in the range of -9 to -11°/oo. Similar depleted $\delta^{18}O$ values (-8.6 to -10°/oo) were measured for the calite cap rock at Vacherie Dome (Smith and Kolb, 1981). In contrast, the calcite concretions on the uncemented northern side of the fault ranged from -3.4 to -4.1°/oo, which is considered to be indicative of calcite precipitation from shallow ground water.

Both DeGolyer (1919) and Powers (1920) observed brine and sulfurous springs over the dome and attributed them to waters rising from great depths. The springs were used intermittently for salt since the Civil War. The springs could not be found in 1980, and it is assumed that depressuring of the Woodbine has stopped spring flow. The combined evidence of saline springs and the presence of the false cap rock at the dome indicate that faults surrounding the dome have functioned as recently as the early 1900's as conduits for deep-basin discharge.

Palestine salt dome, 5 miles to the north of Butler dome, may also have false cap rock associated with its outcrops of Carrizo sandstone which surround the dome and are highly cemented. Petrographic analysis identified a poikilotopic calcite cement similar to the cementation observed at Butler dome.

Table 11. Isotopic composition of calcite-cemented Carrizo Sandstone, Butler Salt Dome.

Calcite-cemented Carrizo sandstone from southern side of fault.

Sample No.	$\delta^{13}C\%$	$\delta^{18}O\%$
1	-29.2	-8.4
2	-22.1	-8.2
3	-28.8	-8.5
4	-25.8	-8.2
5	-26.6	-8.0
6	-30.5	-8.7
7	-24.9	-8.9
8	-31.5	-8.5
9	-32.2	-8.5
10	-25.4	-9.4
11	-21.9	-8.9
12	-27.2	-8.8
13	-25.6	-8.3
14	-31.1	-8.6
15	-20.1	-8.7
16	-23.6	-8.3

Calcite-cemented concretion from northern side of fault.

Sample No.	$\delta^{13}C\%$	$\delta^{18}O\%$
C1	-23.4	-3.4
C2	-24.7	-3.5
C3	-19.1	-4.1
C4	-19.0	-4.1

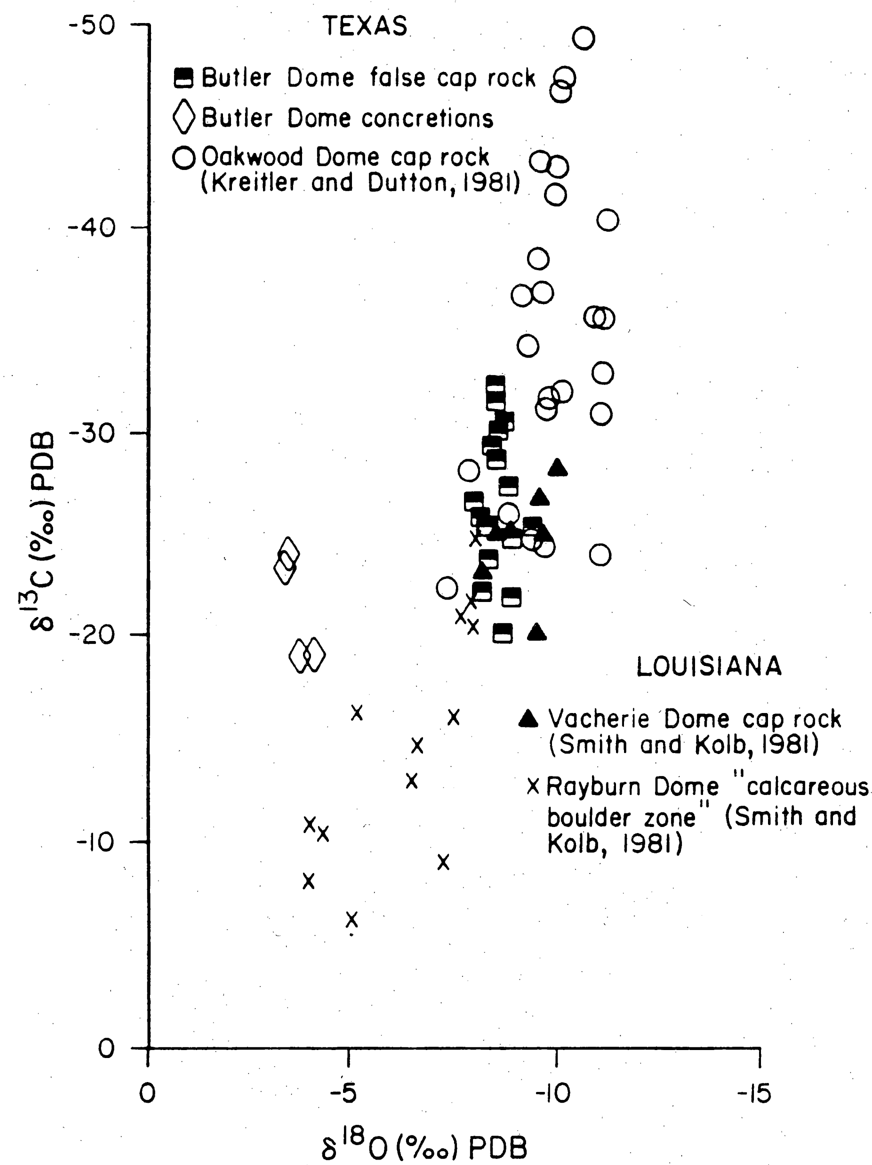

Figure 50. Oxygen ($\delta^{18}O$) and carbon ($\delta^{13}C$) isotopic composition of calcite cements from cemented Carrizo sandstones and calcite concretions from Blue Mountain Quarry (Butler Dome) and other calcites associated with salt domes. Data in Table 11. Location of samples from cemented Carrizo sandstone shown in Figure 51.

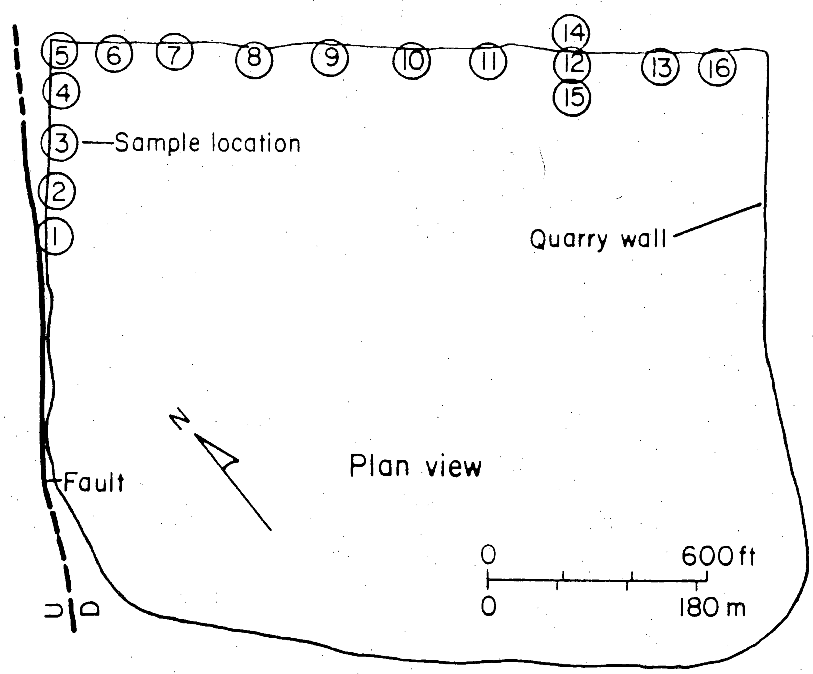

Figure 51. Location of cemented Carrizo Sandstone sampled in Blue Mountain Quarry for carbon and oxygen isotopic analyses.

These are the only domes in the East Texas Basin where false cap rocks have been observed. It is interesting to note that they are located in a low of the Carrizo-Wilcox potentiometric surface. The incision of the Trinity River into the Carrizo has caused this depression in the potentiometric surface (Fogg and Kreitler, 1982). Areas of low hydraulic head in the shallow aquifers could be regional discharge points for the saline aquifers. Only in such areas would the potentials in the shallow fresh-water aquifers be low enough for deep basinal discharge.

SUMMARY--WASTE ISOLATION IMPLICATIONS

Ground waters in the deep aquifers (Nacatoch to Travis Peak) range in salinity from 20,000 to over 200,000 mg/l. Based on their isotopic compositions, they were originally recharged as continental meteoric waters. Recharge probably occurred predominantly during Cretaceous time; therefore, the waters are very old. The Mexia-Talco fault system on the northern and western sides of the basin probably limit recharge to the basin. Because the basin has not been uplifted and eroded, there are no major discharge zones. The flanks of domes and radial faults associated with domes may function as localized discharge points. Both the water chemistry and the hydraulic pressures for the aquifers indicate two major aquifer systems: (1) the upper Cretaceous aquifers (Woodbine and shallower) which are hydrostatic and (2) the deep lower Cretaceous and deeper formations (Glen Rose, Travis Peak, and older units), which are slightly overpressured.

The source of sodium and chloride in the saline waters is considered to be from salt dome dissolution. Mass-balance equations indicate there has been extensive dissolution of the domes and the amount of dissolution is greater than presently exists in the formations. Most of the dissolution probably occurred during the Cretaceous. The timing of major dissolution has been estimated by determining when salt withdrawal basins surrounding the domes were formed. Chlorine-36 analyses suggest that dome solution is not presently occurring. Salinity cross sections across individual domes do not indicate that ongoing solution is an important process.

The major chemical reactions in the saline aquifers are dome dissolution, albitization, and dedolomitization. Albitization and dedolomitization are important only in the deeper formations. The high Na concentrations in the deeper aquifers system results in the alteration of plagioclase to albite and the release of Ca into solution. The increase in Ca concentrations causes a shift in the calcite/dolomite equilibrium. Dolomite should dissolve resulting in the observed increase in Mg. These conclusions on the dominant chemical reactions are based on the analysis of the water chemistry. Petrographic and geochemical studies of the mineral assemblages are needed to confirm these observations.

The critical factors in the utilization of salt domes for disposal of high-level nuclear waste is whether the wastes could leak from a candidate dome and where they would migrate. Salt domes under investigation in the East Texas, Louisiana, and Mississippi basins are in contact with both fresh and saline aquifers. The potential for dome dissolution and radionuclide migration needs to be considered for both systems. The saline aquifers need to be studied because a potential repository would be located at a depth adjacent to saline rather than freshwater formations. This study has addressed the problems of dome dissolution in the saline aquifers and the general hydrologic characteristics of the saline formations. The following conclusions are applicable to the problem of waste isolation in salt domes.

(1) Salt domes in the East Texas Basin have extensively dissolved. The NaCl in the saline aquifers is primarily from this process. Major dissolution, however, probably occurred in the Cretaceous time. There is little evidence for ongoing salt dome dissolution in the saline aquifers.

(2) If there was a release to a saline aquifer, waste migration would either be along the dome flanks or laterally away from the dome. If there is a permeability conduit along the dome flanks, then contaminants could migrate to the fresh-water aquifers. The migration of saline fluids to the surface is dependent on two factors: (a) Is the hydraulic head in saline aquifer high enough to cause flow at the surface or into shallow aquifers? A potential repository in a salt dome would probably be located at a depth adjacent to the hydrostatic-subhydrostatic aquifer

system. The present depressuring of the Woodbine Formation would probably prevent flow to the surface. (b) Is the hydraulic head in the shallow fresh-water aquifers depressed in the domal area? Upward fluid migration is dependent on the potential in the shallow aquifers as well as the potential in the saline systems. Potentiometric levels in the shallow East Texas aquifers are controlled primarily by topography. The lower the elevation of land surface, the lower will be the level of the potentiometric surface. Salt domes located in regionally topographically low areas (e.g., river valleys) probably have a greater chance for fluid flow up their dome flanks than salt domes located in areas with higher topography. If contaminants migrated laterally into the deep-basin aquifers, they probably would not reach the biosphere. The deep-basinal fluids appear relatively stagnant. The waters are probably very old, and there are no major discharge points from the basin. There is, however, no way to predict flow paths or travel times because there are insufficient data to construct potentiometric maps. Calculation of performance assessment scenarios should use the worst-case scenario of leakage along the flanks of the candidate dome. From this perspective then, a critical unknown is the direction and potential for vertical flow between the Woodbine and shallow Tertiary aquifers, and, in turn, whether cessation of oil and gas production from the Woodbine will reverse the vertical hydraulic gradient from downward to upward within the life of a nuclear waste repository.

(3) The observations and conclusions in this paper are based on information obtained for the East Texas Basin. It is expected that the research approach and general conclusions would be similar for the North Louisiana and Mississippi Basin. Detailed investigations would be needed to confirm the applicability of East Texas Basin results to other basins.

REFERENCES

Agagu, O. K., Guevara, E. H., and Wood, D. H., 1980, Stratigraphic framework and depositional sequences of the East Texas Basin, in Kreitler, C. W., and others, Geology and geohydrology of the East Texas Basin--A report on the progress of nuclear waste isolation feasibility studies: The University of Texas at Austin, Bureau of Economic Geology Geological Circular 80-12, p. 4-10.

Balk, R., 1949, Structure of Grand Saline salt dome, Van Zandt County, Texas: AAPG Bull., v. 33, no. 11, p. 1791-1829.

Barnes, V. E., project director, 1967, Palestine Sheet, University of Texas at Austin, Bureau of Economic Geology Geologic Atlas of Texas, scale 1:250,000.

Bassett, R. L., and Bentley, M. E., 1983, Deep brine aquifers in the Palo Duro Basin: Regional flow and geochemical constraints: The University of Texas at Austin, Bureau of Economic Geology Report of Investigations No. 130, 59 p.

Bell, J. S., and Shepherd, J. M., 1951, Pressure behavior in the Woodbine sand: Petroleum Transactions, AIME, v. 192, p. 19-28.

Bentley, H. W., 1978, Some comments on the use of chlorine-36 for dating very old ground water, in Davis, S. N., (ed.), Report on Workshop on Dating Old Ground Water: (Y/OWI/Sub-78/55412), p. 102-111.

Berry, F. A. F., 1958, Hydrodynamics and geochemistry of the Jurassic and Cretaceous systems in the San Juan Basin, northwestern New Mexico and southwestern Colorado: Stanford University, Ph.D. Thesis, 192 p.

Bishop, W. F., 1968, Petrology of Upper Smackover limestone in north Haynesville field, Claiborne Parish, Louisiana: American Association of Petroleum Geologists Bulletin, v. 52, no. 1, p. 92-128.

Boles, J. R., 1979, Active albitization of plagioclase in Gulf Coast Tertiary Sandstones: Geol. Soc. Am., Abstr. Progr., p. 391.

Bredehoeft, J. D., 1964, The drill stem test: the petroleum industry's deep-well pumping test: Ground Water, v. 3, no. 3, p. 31-36.

Bushaw, D. J., 1968, Environmental synthesis of the East Texas lower Cretaceous: Gulf Coast Association of Geological Societies Transactions, v. 18, p. 416-438.

Carpenter, A. B., 1978, Origin and chemical evolution of brines in sedimentary basins, in Johnson, K. S., and Russell, J. (eds.), 13th Annual Forum on Geology of Industrial Minerals: Oklahoma Geological Survey Circular 78: 60-77.

Carpenter, A. B., and Trout, M. L., 1978, Geochemistry of bromine-rich brines of the Dead Sea and southern Arkansas, in Johnson, K. S., and Russell, J. R., (eds.), 13th Industrial Minerals Forum: Oklahoma Geological Survey Circular, v. 79, p. 78-88.

Clayton, R. N., 1959, Oxygen isotope fractionation in the system calcium carbonate-water: J. Chem. Phys., v. 30, p. 1246-1250.

Clayton, R. N., 1961, Oxygen isotope fractionation between calcium carbonate and water: J. Chem. Phys., v. 34, p. 724-726.

Clayton, R. N., Friedman, I., Graf, D. L., Mayeda, T. K., Meents, W. F., and Shimp, N. F., 1966, The origin of saline formation waters, I. Isotopic composition: J. Geophys. Res., v. 71, p. 3869-3882.

Cloos, H., 1968, Experimental analysis of Gulf Coast fracture patterns: American Association of Petroleum Geologists Bulletin, v. 52, no. 3, p. 420-444.

Craig, H., 1961, Isotopic variations in meteoric waters: Science, v. 33, p. 1702-1703.

Davis, S. N., and Bentley, H. W., 1982, Dating ground water--a short review, in Currie, L. A., (ed.), Nuclear and chemical dating techniques: Interpreting the environmental record: American Chemical Society Series, no. 176, p. 187-222.

Degens, E., Hunt, J. M., Reuter, J. H., Reed, W. E., 1964, Data on the distribution of amino acids and oxygen isotopes in petroleum brine waters of various geologic ages: Sedimentology, v. 3, p. 199-225.

DeGolyer, E., 1919, The West Point, Texas, salt dome, Freestone County: Journal of Geology, v. 27, p. 647-663.

Dix, O. R., and Jackson, M. P. A., 1981, Statistical analysis of lineaments and their relation to fracturing, faulting, and halokinesis in the East Texas Basin: The University of Texas at Austin, Bureau of Economic Geology Report of Investigations No. 110, 30 p.

Dresser Atlas, 1975, Log Interpretation Fundamentals: Dresser Atlas Division, Dresser Industries, Inc.

Dunay, M. A., 1981, Porosity and permeability reduction in the Cotton Valley sandstone, east Texas: Unpublished Master's thesis, University of Missouri-Columbia, 127 p.

Eaton, R. W., 1956, Resume on subsurface geology of northeast Texas with emphasis on salt structures: Gulf Coast Association of Geological Societies Transactions, v. 5, p. 79-84.

Exploration Techniques, Inc., 1979, Report on gravity modeling for Keechi and Oakwood Domes: Report prepared for Law Engineering Testing Co., Houston, Texas.

Feely, H. W., and Kulp, J. L., 1957, Origin of Gulf Coast salt dome sulfur deposits: American Association of Petroleum Geologists Bulletin, v. 41, no. 8, p. 1802-1853.

Fogg, G. E., and Kreitler, C. W., 1981, Ground-water hydrology around salt domes in the East Texas Basin: A practical approach to the contaminant transport problem: Bull. Assoc. Engineering Geologist, v. 18, no. 4, p. 387-411.

Fogg, G. E., and Kreitler, C. W., 1982, Ground-water hydraulics and hydrochemical facies in Eocene aquifers of the East Texas Basin: The University of Texas at Austin, Bureau of Economic Geology Report of Investigations No. 127, 75 p.

Fogg, G. E., Seni, S. J., and Kreitler, C. W., 1983, Three-dimensional ground-water modeling in depositional systems, Wilcox Group, Oakwood salt dome area, East Texas: The University of Texas at Austin, Bureau of Economic Geology, Report of Investigations No. 133, 55 p.

Graf, D. L., Friedman, I., and Meents, W. F., 1965, The origin of saline formation waters, II: Isotopic fractionation by shale micropore systems: Illinois State Geological Survey Circular 393, 32 p.

Graf, D. L., Meents, W. F., Friedman, I., and Shimp, N. F., 1966, The origin of saline formation waters, III: calcium chloride waters: Illinois State Geological Survey Circular 397, 60 p.

Granata, W. H., 1963, Cretaceous stratigraphy and structural development of the Sabine uplift area, Texas and Louisiana, in Report on selected north Louisiana and south Arkansas oil and gas fields and regional geology: Shreveport Geological Society, Reference Volume V, p. 50-95.

Hall, H. W., 1953, Compressibility of reservoir rock: Journal Petroleum Technology Transactions, v. 198, p. 310.

Hanshaw, B. B., and Coplen, T. B., 1973, Ultrafiltration by a compacted clay membrane, II, Sodium ion exclusion at various ionic strengths: Geochim. Cosmochim. Acta, v. 37, p. 2311-2327.

Hawkins, M. E., Dietzman, W. D., and Pearson, C. A., 1964, Chemical analyses and electrical resistivities of oil field brines from fluids in east Texas: U.S. Bureau of Mines, RI 6422, 20 p.

Hitchon, B., and Freedman, I., 1969, Geochemistry and origin of formation waters in western Canada sedimentary basin, I. Stable isotopes of hydrogen and oxygen: Geochimica et Cosmochimica Acta, v. 33, p. 1321-1349.

Holser, W. T., 1979, Trace elements and isotopes in evaporites, in Burns, R. G. (ed.), Marine Minerals: Mineral. Soc. Am., Short Course Notes, v. 6, p. 295-396.

Jackson, M. P. A., 1982, Fault tectonics of the East Texas Basin: The University of Texas at Austin, Bureau of Economic Geology Geological Circular 82-4, 31 p.

Jackson, M. P. A., and Harris, D. W., 1981, Seismic stratigraphy and salt mobilization along the northwestern margin of the East Texas Basin, in Kreitler, C. W., and others, Geology and geohydrology of the East Texas Basin; a report on the progress of nuclear waste isolation feasibility studies (1980): The University of Texas at Austin, Bureau of Economic Geology Geological Circular 81-7, p. 28-31.

Jackson, M. P. A., and Seni, S. J., 1983, Geometry and evolution of salt structures in a marginal rift basin of the Gulf of Mexico, East Texas, Geology, v. 11, p. 131-135.

Knauth, L. P., Kumar, M. B., and Martinez, J. D., 1980, Isotope geochemistry of water in Gulf Coast salt domes: Journal of Geophysical Research, v. 85, no. 39, p. 4863-4871.

Kreitler, C. W., 1979, Studies of the suitability of salt domes in East Texas Basin for geologic isolation of nuclear wastes: Gulf Coast Association of Geological Societies Transaction, v. 29, p. 157-163.

Kreitler, C. W., Guevara, E., Granata, G., and McKalips, D., 1977, Hydrology of Gulf Coast aquifers, Houston-Galveston area: Texas; Bureau of Economic Geology Geological Circular 77-4, 18 p.

Kreitler, C. W., Agagu, O. K., Basciano, J. M., Collins, E. W., Dix, O. R., Dutton, S. P., Fogg, G. E., Giles, A. B., Guevara, E. H., Harris, D. W., Hobday, D. K., McGowen, M. K., Pass, D., and Wood, D. H., 1980, Geology and geohydrology of the East Texas Basin, a report on the progress of nuclear waste isolation feasibility studies (1979): The University of Texas at Austin, Bureau of Economic Geology Geological Circular 80-12, 112 p.

Kreitler, C. W., Collins, E. W., Davidson, E. D., Jr., Dix, O. R., Donaldson, G. W., Dutton, S. P., Fogg, G. E., Giles, A. B., Harris, D. W., Jackson, M. P. A., Lopez, C. M., McGowen, M. K., Muehlberger, W. R., Pennington, W. D., Seni, S. J., Wood, D. H., and Wuerch, H. V., 1981, Geology and geohydrology of the East Texas Basin, a report on the progress of nuclear waste isolation feasibility studies (1980): The University of Texas at Austin, Bureau of Economic Geology Geological Circular 81-7, 207 p.

Kreitler, C. W., and Muehlberger, W. D., 1981, Geochemical analyses of salt, Grand Saline Dome, East Texas, in Kreitler, C. W., and others, Geology and geohydrology of the East Texas Basin, a report on the progress of nuclear waste isolation feasibility studies (1980): The University of Texas at Austin, Bureau of Economic Geology Geological Circular 81-7, p. 188-194.

Kreitler, Charles W., and Dutton, Shirley P., 1983, Origin and diagenesis of cap rock, Gyp Hill and Oakwood salt domes, Texas: The University of Texas at Austin, Bureau of Economic Geology Report of Investigations No. 131, 58 p.

Kumar, M. B., and Hoda, B., 1978, Hydrologic studies of Belle Isle Salt Mine and Weeks Island Salt Mine, in Martinez and others, An investigation of the utility of Gulf Coast Salt Domes for storage and disposal of radioactive waste: Volume 1, Louisiana State University Institute for Environmental Studies (EW-78-C-05-5941/53), p. 153-234.

Land, L. S., 1982, Dolomitization: AAPG Education Course Note Series #24, 20 p.

Land, L. S., and Prezbindowski, D. R., 1981, The origin and evolution of saline formation water, Lower Cretaceous carbonates, south-central Texas: Journal of Hydrology, v. 54, p. 51-74.

Loocke, J. E., 1978, Growth history of the Hainesville salt dome, Wood County, Texas: The University of Texas at Austin, Master's thesis, 95 p.

Macpherson, G. L., 1982, Low-temperature geothermal ground water in the Hosston/Cotton Valley hydrogeologic units, Falls County area, Texas: The University of Texas at Austin, unpublished master's thesis, 234 p.

Martin, R. G., 1978, Northern and eastern Gulf of Mexico continental margin stratigraphic and structural framework, in Bouma, A. H., Moore, C. T., and Coleman J. M., eds., Framework, facies, and oil trapping characteristics of the upper continental margin: AAPG, Studies in Geology No. 7, p. 21-42.

Milliken, K. L., Land, L. S., and Loucks, R. G., 1981, History of burial diagenesis determined from isotopic geochemistry, Frio Formation, Brazoria County, Texas: AAPG, v. 65, p. 1397-1413.

Nichols, P. H., Peterson, G. E., and Wercestner, C. E., 1968, Summary of subsurface geology of northeast Texas, in Beebe, B. W., and Curtis, B. F., eds., Natural Gases of North America: American Association of Petroleum Geologists Memoir 9, v. 2, p. 982-1004.

Parker, J. W., 1969, Water history of Cretaceous aquifers, East Texas Basin: Chemical Geology, v. 4, p. 111-133.

Parker, T. J., and McDowell, A. N., 1955, Model studies of salt-dome tectonics: American Association of Petroleum Geologists Bulletin, v. 39, no. 12, p. 2384-2470.

Plummer, F. B., and Sargent, E. C., 1931, Underground waters and subsurface temperatures of the Woodbine sand in northeast Texas: The University of Texas at Austin, Bureau of Economic Geology, Bulletin No. 3138, 178 p.

Powers, Sidney, 1920, The Butler Salt Dome, Freestone County, Texas: American Journal of Science, v. 199, series 4, p. 127-142.

Ramberg, H., 1981, Gravity, deformation and the Earth's crust in theory, experiments and geological application, Second Edition: London, Academic Press, 452 p.

Robie, R. A., Hemingway, B. S., and Fisher, J. R., 1979, Thermodynamic properties of minerals and related substances at 298.15°K and 1 bar (10^5 pascals) pressure and at higher temperatures: U.S. Geol. Survey Bull., no. 1452, 456 p.

Salvador, A., and Green, A. R., 1980, Opening of the Caribbean Tethys (origin and development of the Caribbean and the Gulf of Mexico), in Colloque C5: Géologie des chaînes alpines issues de la Tethys: Bureau de Recherches Géologiques et Minières, Memoire 115, p. 224-229.

Seni, S. J., and Jackson, M. P. A., in press, Sedimentary record of Cretaceous and Tertiary salt movement, East Texas Basin; times, rates, and volumes of flow, implications to nuclear waste isolation and petroleum exploration: The University of Texas at Austin, Bureau of Economic Geology Report of Investigations.

Seni, S. J., and Jackson, M. P. A., 1983, Evolution of salt structures East Texas diapir province, Part 1: sedimentary record of halokinesis: AAPG Bull., v. 67, no. 8, p. 1219-1244.

Smith, G., and Kolb, C. R., 1981, Isotopic evidence for the origin of the Rayburn's Boulder Zone of North Louisiana: Louisiana State University, Institute for Environmental Studies, File Report QR 02.4.2, 23 p.

Stoessel, R. K., and Moore, C. H., 1983, Chemical constraints and origins of four groups of Gulf Coast Reservoir Fluids: AAPG Bull., v. 67, no. 6, p. 896-906.

Thomas, W. A., 1976, Evolution of Ouachita-Appalachian continental margin: Journal of Geology, v. 84, p. 323-342.

University of Oklahoma, 1980, Computer printout on Saline waters, East Texas Basin.

Wescott, W. A., 1983, Diagenesis of Cotton Valley sandstone (Upper Jurassic), East Texas: Implications to tight gas formation pay recognition: AAPG Bull., v. 67, no. 6, p. 1002-1013.

White, D. E., 1965, Saline waters of sedimentary rocks: Am. Assoc. Pet. Geol. Mem., v. 4, p. 342-366.

Wood, D. H., and Guevara, E. H., 1981, Regional structural cross sections and general stratigraphy, East Texas Basin: The University of Texas at Austin, Bureau of Economic Geology, 21 p.

Wood, M. L., and Walper, J. L., 1974, The evolution of the interior Mesozoic basins and the Gulf of Mexico: Gulf Coast Assoc. Geol. Soc. Trans., v. 24, p. 31-41.

Appendix A. Chemical composition of saline waters, East Texas Basin, from previously published data (Hawkins and others, University of Oklahoma, 1980).

East Texas Waste Isolation

Deep Basin Hydrology

Field	County	Depth	Constituents, Mg/liter Ca	Mg	Na	Ba-Sr	HCO_3	SO_4	Cl	Sp. Gr.	Resistivity	Total Solids (mg/liter)
					NACATOCH (KGNA)							
Calvert	Robertson	2,132-2,235	340	130	11,600	17	1,186	8	18,100	1.024	.211	31,364
		2,136-2,224	300	130	10,972	20	1,043	30	17,200	1.023	.222	29,675
		2,182-2,212	200	100	8,978	21	1,659	35	13,500	1.020	.262	24,472
Combest	Navarro	682-730	340	105	6,670	3	451	42	10,900	1.016	.354	18,508
Edens	Navarro	800-858	250	70	6,836	0	290	568	10,600	1.017	.342	18,614
Lone Star (Ponta)	Cherokee	3,300	930	230	17,738	-	606	122	29,222	1.035	.135	48,848
McCrary	Wood	2,300	355	97	11,320	-	208	0	18,250	1.022	.210	30,230
Merigale-Paul	Wood	2,240-2,245	364	95	11,170	-	215	0	18,025	1.022	.201	29,869
Mildred	Navarro	795-822	300	100	6,400	3	159	43	10,600	1.016	.337	17,602
		888-946	410	30	7,300	3	253	27	11,900	1.017	.333	19,920
		930-1,010	300	100	6,900	0	149	44	11,300	1.016	.347	18,793
Pleasant Grove (Shallow)	Rusk	2,970-2,996	600	120	18,900	0	201	0	30,500	1.043	.148	50,321
		2,970-3,000	1,302	138	19,600	-	847	0	32,500	1.041	.128	54,387
		2,970-3,000	1,314	126	19,900	-	878	0	32,600	1.042	.128	54,818
Reiter	Freestone	963-967	250	100	7,295	4	287	23	11,800	1.017	.325	19,755
		976-1,027	150	70	4,286	0	287	16	6,900	1.016	.547	11,709
Reiter, N.	Navarro	712-758	150	110	6,814	4	482	19	10,800	1.017	.320	18,375
		738-744	300	120	7,373	3	390	32	12,000	1.017	.315	20,215
Rice	Navarro	594-678	160	45	11,550	3	180	32	18,100	1.024	.220	30,067
		628-648	920	220	10,640	4	448	23	18,400	1.025	.212	30,651
Van	Van Zandt	1,246	275	105	8,216	-	1,159	0	12,841	1.016	.287	22,596
Mildred	Navarro	800-1,000	406	51	3044	101	-	-	-			20,100
Rice	Navarro	1,200	511	102	6,132	204	-	-	-			30,800
		1,200	0	72	5,110	307	-	-	-			30,200
Van	Van Zandt	825	512	205	819	20	-	-	-			23,400
					WOLFE CITY (KGWC)							
Corsicana	Navarro	986-1,027	900	270	12,100	0	143	50	20,900	1.027	.190	34,363
		1,023-1,046	900	290	11,900	6	165	38	20,600	1.027	.188	33,893

Field	County	Depth	Constituents, Mg/liter Ca	Mg	Na	Ba-Sr	HCO_3	SO_4	Cl	Sp. Gr.	Resistivity	Total Solids (mg/liter)
WOLFE CITY (KGWC) continued												
		1,055-1,105	900	270	11,900	10	159	49	20,600	1.027	.192	33,878
Powell	Navarro	1,483-1,545	700	175	11,930	15	555	30	19,800	1.026	.197	33,190
		1,604-1,679	850	230	10,646	12	268	48	18,400	1.026	.197	30,442
		1,628-1,687	1,000	290	12,800	15	159	58	22,200	1.028	.179	36,507
TOKIO (KGA)												
Marion County Shallow	Marion	2,300	960	271	11,800	7	206	28	20,500	1.026	.193	33,765
		2,400	1,060	339	15,700	0	49	18	27,000	1.033	.153	44,166
SUB-CLARKSVILLE (EAGLE FORD) (KGEF)												
Alba	Wood	4,275	1,236	271	27,589	-	872	14	44,996			74,979
		4,074-4,105	42	21	4,218	42	-	-	-			80,900
		4,057-4,082	1,430	309	28,300	-	944	32	46,492			77,507
Alba	Wood	4,110-4,144	1,200	140	18,800	0	213	0	40,800	1.049	.103	61,153
		4,113-4,133	1,260	338	25,335	-	1,129	30	41,600	1.050	.100	69,692
		4,189-4,240	1,800	600	24,200	50	128	64	44,000	1.052	.103	70,792
Camp Hill	Anderson	5,106	2,304	656	31,201	-	660	331	53,494	1.063	.081	88,646
		5,192	2,320	474	32,043	-	403	67	54,613	1.064	.081	89,920
Coke	Wood	4,053-4,142	1,400	140	25,800	0	439	0	42,500	1.054	.103	70,279
		4,095-4,131	1,185	484	25,700	10	378	0	42,900	1.053	.101	70,647
Como	Hopkins	3,970-3,977	1,500	12	29,200	0	275	0	47,500	1.051	.106	78,487
		4,028-4,034	1,300	250	24,200	0	92	181	40,100	1.051	.106	66,123
Deu Pree	Wood	4,994-5,014	1,700	560	30,300	0	537	-	51,000	1.062	.087	84,097
Grapeland	Houston	5,873-5,879	1,700	760	28,400	1	85	0	48,900	1.061	.086	79,845
		5,875-5,880	1,500	200	29,600	0	18	0	48,900	1.060	.086	80,218
		5,888-5,892	1,700	740	27,700	Trace	18	0	48,800	1.063	.085	78,958
Forest Hill	Wood	4,479-4,495	1,540	340	30,147	17	1,013	19	49,600	1.057	.091	82,659
		4,350-4,400	1,283	261	28,075	-	560	41	45,980	1.055	.093	76,200

Field	County	Depth	Constituents, Mg/liter Ca	Mg	Na	Ba-Sr	HCO_3	SO_4	Cl	Sp. Gr.	Resistivity	Total Solids (mg/liter)
SUB-CLARKSVILLE (EAGLE FORD) (KGEF) continued												
McCrary	Wood	4,350-4,418	1,367	282	28,676	0	298	62	47,377			78,217
		-	1,310	254	29,317	-	643	54	47,966			79,603
		-	1,198	286	28,928	-	408	18	47,304			78,141
McCrary	Wood	4,351-4,361	1,400	200	28,000	0	73	994	45,400	1.059	.093	76,067
		4,364-4,374	1,200	230	29,000	0	653	Trace	47,200	1.059	.093	78,283
		4,371-4,381	1,150	330	27,800	3	250	0	45,700	1.057	.094	75,230
		4,400-4,415	1,243	241	27,880	-	610	51	45,514	1.054	.094	75,539
		4,408-4,411	1,129	418	30,320	-	560	16	49,626			82,068
		-	1,214	262	29,528	-	442	24	48,162			79,632
		-	1,350	275	27,436	-	589	43	48,359			80,177
		4,750-4,800	1,470	300	27,704	-	560	60	45,820	1.055	.092	75,914
		4,833-4,904	1,349	281	48,157	189	625	36	77,436			128,531
		-	82	30	6,888	-	890	Trace	10,336			18,225
Merigale-Paul	Wood	4,750-4,800	1,395	305	28,766	-	444	55	47,410	1.056	.090	78,375
		4,755-4,813	1,600	340	31,521	12	1,025	43	51,800	1.060	.087	86,329
		4,766-4,868	1,600	360	33,730	13	970	37	55,300	1.060	.087	91,997
		4,860	1,750	380	32,546	14	842	7	53,900	1.063	.085	89,425
Manziel	Wood	4,003-4,042	2,000	230	25,500	8	378	123	43,300	1.057	.093	71,531
		4,039-4,060	1,700	350	29,100	24	55	0	48,900	1.057	.090	80,105
		4,041-4,067	1,500	500	29,400	0	427	370	48,900	1.060	.090	81,097
Manziel	Wood	4,041-4,169	1,578	351	29,767	-	628	0	49,350			81,677
		4,045-4,060	1,223	346	30,575	-	379	0	50,099	1.060	.085	82,622
Midway Lake	Wood	4,476-4,550	1,700	500	27,000	18	726	-	45,700	1.057	.093	75,626
		4,513-4,563	1,800	450	26,500	84	671	-	45,000	1.057	.093	74,421
		4,534-4,550	1,800	400	28,900	8	500	-	44,300	1.058	.090	75,900
Neches	Anderson	4,584-4,640	3,087	563	33,890	-	254	1	67,000	1.078	.075	104,795
		4,591-4,595	4,300	560	42,100	0	298	0	74,000	1.082	.070	121,258
		4,665-4,669	2,600	700	35,500	0	49	0	61,600	1.074	.074	100,449
Pine Mills	Wood	4,700-4,800	1,490	302	31,418	-	799	1,000	50,750	1.060	.086	85,759
		4,700-4,800	1,421	322	30,406	-	756	40	49,850	1.060	.087	82,795
		4,700-4,800	1,382	312	28,612	-	780	48	47,000	1.060	.092	78,134

Field	County	Depth	Constituents, Mg/liter Ca	Mg	Na	Ba-Sr	HCO_3	SO_4	Cl	Sp. Gr.	Resistivity	Total Solids (mg/liter)
			SUB-CLARKSVILLE EAGLE FORD (KGEF) continued									
		4,710-4,776	1,500	230	29,300	0	397	-	48,200	1.062	.088	79,627
		4,797-4,802	1,800	660	27,700	0	500	-	47,500	1.058	.092	78,160
Newsome	Camp	3,850-3,872	1,300	300	25,900	0	463	-	42,900	1.054	.100	70,863
		3,870-3,875	1,400	400	25,900	0	366	0	43,300	1.054	.099	71,366
Nolan Edwards	Wood	4,714-4,744	612	364	27,752	-	1,215	14	44,200	1.054	.099	74,157
		4,658-4,672	1,300	330	26,852	10	1,092	44	44,000	1.052	.098	73,618
		4,692-4,695	1,200	300	27,216	9	1,098	35	44,300	1.053	.097	74,149
		4,763-4,767	1,200	320	27,448	9	1,122	40	44,700	1.053	.098	74,830
Pine Mills, E.	Wood	4,760-4,764	2,000	740	22,100	0	110	-	39,700	1.059	.090	64,650
		4,782-4,786	2,000	700	18,900	0	92	-	34,700	1.059	.090	56,392
Quitman	Wood	4,018-4,217	1,657	415	32,136	-	453	24	53,414			88,102
		-	2,104	638	32,867	-	382	24	56,028			92,046
		4,018-4,217	2,761	239	31,692	-	764	8	53,996			89,461
		-	1,604	462	33,231	-	451	16	55,156			90,929
		-	2,367	638	31,708	-	384	0	54,866			90,197
		-	2,367	558	13,590	-	344	13	26,562			43,435
		-	2,367	558	30,818	-	344	13	53,124			87,225
		-	1,841	239	27,681	-	810	13	46,156			76,744
		-	1,420	383	27,888	-	843	0	46,156			76,718
		-	1,841	319	26,416	-	800	9	44,416			73,864
		-	1,841	399	27,939	-	808	9	47,028			78,028
		-	1,631	399	32,552	-	390	24	53,996			88,993
		-	2,630	558	31,336	-	540	5	54,286			89,366
Quitman	Wood	-	2,235	638	35,963	-	497	21	60,965			100,321
		-	2,104	478	34,947	-	369	8	58,785			96,695
		-	1,972	414	32,946	-	553	22	55,156			90,071
		-	2,104	478	26,567	-	762	10	45,576			75,467
		-	2,630	558	31,844	-	390	3	55,156			90,594
		-	2,235	239	8,799	-	872	6	17,708			29,865
		-	2,235	239	20,282	-	872	6	35,416			59,056
		-	1,631	431	32,925	-	563	19	54,576			90,154

Field	County	Depth	Constituents, Mg/liter Ca	Mg	Na	Ba-Sr	HCO_3	SO_4	Cl	Sp. Gr.	Resistivity	Total Solids (mg/liter)
SUB-CLARKSVILLE (EAGLE FORD) (KGEF) continued												
		-	1,894	415	32,605	-	434	14	54,576			89,941
		-	2,498	399	14,292	-	355	12	27,433			45,036
		-	2,498	399	32,083	-	355	12	54,866			90,260
		-	2,630	399	32,145	-	394	8	55,156			90,747
		-	1,525	462	33,327	-	459	19	55,156			90,955
		-	4,734	638	32,881	-	346	100	60,672			99,391
		-	1,972	399	30,671	-	474	11	51,674			85,222
		-	2,761	399	31,672	-	517	12	54,576			89,938
		-	3,550	638	32,520	-	490	10	58,060			95,372
		-	2,761	399	31,099	-	459	48	53,705			88,484
		-	2,498	319	32,042	-	367	36	54,576			89,858
		-	74	21	3,185	42	-	-	-			89,000
Quitman	Wood	4,232-4,252	1,474	205	31,415	-	137	21	51,287	1.061	.083	84,539
		4,370-4,395	891	159	28,239	-	746	0	45,133	1.054	.093	75,168
Reilly Springs	Hopkins	4,272-4,275	1,467	230	29,788	253	642	-	49,236			81,838
Shirley-Barbara	Wood	5,534-5,540	1,700	540	28,300	0	444	Trace	47,900	1.058	.090	78,884
		5,552-5,556	3,400	660	32,700	Trace	603	-	58,500	1.070	.080	95,863
		5,474-5,488	2,116	194	35,100	0	390	47	58,150	1.067	.083	95,997
		5,600	2,370	389	34,500	13	695	Trace	58,060	1.069	.083	96,014
Slocum, N.	Anderson	5,664-5,828*	532	106	7,450	160	-	-	-			96,700
Slocum, N.	Anderson	5,710-5,720	1,900	900	28,300	0	268	302	49,200	1.065	.086	80,870
Slocum, S.	Anderson	5,958	3,900	350	27,900	Trace	24	556	50,500	1.065	.081	83,230
Trix-Liz	Titus	2,989-3,006	771	255	18,448	-	234	1	30,450	1.036	.121	50,159**
Trix-Liz	Titus	3,003	1,052	239	18,767	-	25	0	31,352			51,667
		-	894	255	17,555	-	167	0	29,320			48,224
		-	842	335	17,415	-	252	0	29,175			48,023
		-	1,073	344	18,966	346	2,238	5	37,179			60,235
Yantis	Wood	4,172-4,196	1,700	800	31,100	-	244	123	53,200	1.059	.092	87,167
		4,185-4,195	2,400	330	27,700	-	48	0	47,900	1.053	.102	78,378
		4,192-4,225	2,000	16	29,400	0	79	0	48,900	1.053	.102	80,395

*Depth Range
**ppm

Field	County	Depth	Constituents, Mg/liter Ca	Mg	Na	Ba-Sr	HCO_3	SO_4	Cl	Sp. Gr.	Resistivity	Total Solids (mg/liter)
COKER SAND (EAGLE FORD) (KGEF)												
Como	Hopkins	4,185	2,100	6	26,400	0	201	0	44,300	1.058	.092	73,007
		4,185	300	40	27,700	55	244	-	43,300	1.056	.093	71,584
		4,202	260	50	29,900	51	134	193	46,500	1.055	.093	77,037
MOORINGSPORT LS. (KCGRU)												
Bethany, NE.	Panola	3,871-3,877	3,034	430	16,382	-	-	1,785	30,406	1.038	.132	52,037
		3,900-3,914	3,944	919	14,398	-	-	1,753	30,406	1.037	.132	51,420
GOODLAND LS. (KCF)												
Longwood	Harrison	2,360-2,398	1,300	440	15,143	0	525	37	26,600	1.033	.154	44,045
		2,369-2,386	2,700	445	15,199	0	52	111	29,400	1.037	.142	47,907
		2,385-2,428	1,500	470	15,101	0	512	152	26,900	1.033	.152	44,635
Panola	Panola	2,500	1,500	286	14,700	0	407	234	25,800	1.032	.158	42,927
		2,500	2,200	409	18,400	0	447	236	33,000	1.040	.135	54,692
		2,500	1,300	46	22,400	Trace	165	469	36,500	1.038	.135	60,880
		2,500	1,400	400	21,300	6	415	0	36,200	1.044	.121	59,715
Waskom	Harrison	2,400	1,050	126	16,400	0	482	508	26,900	1.040	.150	45,466
		2,400	1,330	76	13,300	35	640	0	22,700	1.030	.170	38,046
		2,400	1,600	237	13,000	0	421	0	23,400	1.034	.170	38,658
BUDA LS. (KCW)												
Deer Creek	Falls	1,046-1,068	300	150	7,100	2	268	18	11,700	1.016	.338	19,536
Lott	Falls	1,211	380	160	6,900	28	494	21	11,500	1.017	.328	19,455
		1,230-1,247	390	160	7,200	6	366	20	12,000	1.017	.318	20,136
		1,298	300	160	7,100	0	171	18	11,900	1.017	.318	19,649
FREDERICKSBURG LS. (KCF)												
Shelbyville, E.	Shelby	3,600	3,326	785	27,615	-	201	170	50,529	1.057	.085	82,626

Field	County	Depth	Constituents, Mg/liter							Sp. Gr.	Resistivity	Total Solids (mg/liter)
			Ca	Mg	Na	Ba-Sr	HCO_3	SO_4	Cl			
					WOODBINE (KGW)							
Flagg Lake	Henderson	3,018-3,024	172	70	8,439	-	695	2	13,120	1.018	.275	22,498
		3,042-3,056	140	78	8,419	-	1,196	3	12,765	1.017	.280	22,601
		3,090-3,095	280	100	10,949	-	506	9	17,375	1.021	.266	29,219
Good Omen	Smith	3,950-3,954	1,600	230	25,900	0	634	231	43,000	1.052	.099	71,595
		3,960-3,962	1,500	315	26,200	0	573	201	43,500	1.052	.099	72,289
Grapeland	Smith	6,076-6,087	4,267	594	35,454	-	153	80	63,823	1.074	.072	104,371
Grimes-Percilla	Smith	5,880-5,900	4,087	585	38,601	-	250	104	68,259	1.076	.069	111,886
Gum Springs	Rusk	3,649	800	190	16,800	0	232	0	27,700	1.036	.150	45,722
		3,673-3,714	800	70	16,000	0	256	0	26,200	1.031	.170	43,326
Ham Gossett	Kaufman	3,401-3,406	670	75	16,500	19	37	0	26,900	1.034	.145	44,182
		3,637-3,644	394	72	18,000	1	451	-	28,400	1.034	.143	47,317
		3,704-3,710	388	68	17,900	-	433	29	28,000	1.037	.145	46,818
		3,267-3,271	480	175	14,100	0	262	0	23,000	1.033	.172	38,017
		3,421-3,423	240	68	14,000	-	586	-	22,200	1.028	.174	37,094
		3,983-4,030	530	93	14,600	22	427	-	23,400	1.040	.168	39,050
		5,780-5,785	5,900	1,984	35,400	0	92	948	70,000	1.084	.071	114,324
Ham Gossett, SE.	Kaufman	3,252-3,257	400	24	13,600	0	183	0	21,600	1.028	.182	35,807
		3,256-3,265	370	96	13,000	0	500	0	20,700	1.029	.185	34,666
		3,238-3,244	593	82	14,700	0	531	-	23,600	1.029	.175	39,506
		3,240-3,245	237	70	14,000	0	488	Trace	22,000	1.027	.178	36,795
Hawkins	Wood	4,600-4,650	2,850	530	35,668	3	406	206	61,200	1.070	.073	100,860
		4,790-4,810	2,750	460	35,333	0	470	157	60,300	1.071	.073	99,470
Hawkins	Wood	4,818	2,750	480	35,243	3	290	191	60,300	1.069	.075	99,254
Jacksonville, N.	Cherokee	4,371-4,372	1,740	390	30,900	0	537	204	51,400	1.060	.087	85,171
		4,383-4,402	1,860	400	31,632	0	470	216	52,800	1.062	.085	87,378
		4,432-4,455	1,810	400	30,550	0	628	16	51,100	1.060	.087	84,504
Jacksonville, W.	Cherokee	4,841-4,844	1,500	640	37,289	4	491	181	61,600	1.073	.075	101,701
		4,963-4,968	3,200	600	35,195	5	519	243	61,200	1.070	.076	100,957
Kerens, S.	Navarro	3,371-3,419	290	90	10,685	8	872	61	16,700	1.023	.226	28,698
		3,380-3,385	245	105	12,285	-	857	4	19,200	1.024	.196	32,696**

**ppm

Field	County	Depth	Constituents, Mg/liter Ca	Mg	Na	Ba-Sr	HCO_3	SO_4	Cl	Sp. Gr.	Resistivity	Total Solids (mg/liter)
						WOODBINE (KGW) continued						
Lone Star (Ponta)	Cherokee	3,906-3,932	3,500	660	29,100	0	31	456	52,700	1.068	.077	86,447
		3,978-3,980	3,500	780	29,400	0	37	216	53,600	1.068	.077	87,533
Long Lake	Anderson	5,190-5,250	2,485	442	35,299	0	427	119	59,839	1.066	.074	98,611
		5,190-5,250	2,806	474	36,432	-	376	119	62,232	1.073	.072	102,439
		5,190-5,250	2,798	474	36,460	0	406	139	62,232	1.073	.072	102,509
		5,190-5,250	3,066	493	37,245	0	433	135	64,005	1.075	.071	105,377
		5,322-5,326	3,300	570	37,637	7	424	121	65,200	1.075	.073	107,252
		5,375-5,404	3,355	530	34,814	-	138	135	60,900	1.071	.074	99,872
Long Lake, E.	Anderson	5,320-5,400	3,100	600	37,100	Trace	92	30	64,300	1.075	.073	105,222
		5,340-5,348	3,690	610	37,322	10	329	90	65,600	1.075	.073	107,641
		5,340-5,353	3,400	466	40,400	18	390	0	62,000	1.075	.073	106,656
		5,402-5,417	3,870	1,260	36,488	6	332	123	66,500	1.076	.073	108,573
		5,407-5,424	3,830	620	37,783	5	421	137	66,500	1.076	.071	109,291
Merigale-Paul	Wood	5,237-5,488	3,100	500	35,700	2	110	5	62,000	1.073	.076	101,415
Mexia	Limestone	2,931-3,012	449	150	10,727	-	439	8	17,517	1.021	.212	29,290
		2,932	505	172	11,311	-	439	9	18,581	1.021	.205	31,017
		2,948-3,060	425	147	10,700	-	403	7	17,446	1.020	.216	29,128
		2,970	437	137	10,684	-	445	27	17,375	1.022	.216	29,105
		2,989-3,060	465	150	10,572	-	445	7	17,304	1.020	.216	28,943
		3,027	744	170	11,499	-	284	32	19,361	1.024	.200	32,090
		3,036	485	155	11,273	-	442	5	18,439	1.024	.205	30,799
		3,042	437	153	10,864	-	418	6	17,730	1.022	.212	29,608
		3,065	561	179	11,818	-	290	4	19,573	1.023	.195	32,425
Navarro Crossing	Houston	5,870-5,875	4,100	670	36,470	9	281	109	65,200	1.074	.074	106,830
		5,900	4,400	680	35,813	9	354	115	64,700	1.075	.074	106,062
Neches	Anderson	4,723-4,743	4,300	530	36,300	0	171	376	64,700	1.079	.074	106,377
		4,732-4,738	4,600	350	35,900	0	256	0	64,300	1.076	.075	105,406
		4,749-4,754	3,444	741	36,201	-	259	1	64,000	1.075	.078	104,646
New Hope	Franklin	4,500	1,652	381	30,365	-	257	4	50,704	1.058	.083	83,363
Wortham	Freestone	2,942-2,946	270	100	8,111	14	616	25	12,900	1.019	.280	22,022

Field	County	Depth	Constituents, Mg/liter Ca	Mg	Na	Ba-Sr	HCO_3	SO_4	Cl	Sp. Gr.	Resistivity	Total Solids (mg/liter)
						WOODBINE (KGW) Continued						
Nigger Creek	Limestone	2,830	461	149	9,666	-	317	25	15,957	1.020	.234	26,575
		2,836	453	158	10,567	-	311	9	17,375	1.020	.216	28,873
		2,849	461	144	9,453	-	360	7	15,602	1.020	.238	26,027
		2,856	441	156	8,063	-	299	5	13,474	1.018	.270	22,438
Pine Mills	Wood	5,200	3,600	760	33,900	0	98	183	60,700	1.072	.078	99,241
		5,350-5,400	5,742	354	27,002	-	866	800	51,750	1.064	.085	86,514
		5,270-5,406	3,500	660	32,800	0	275	-	58,500	1.067	.078	95,735
Pleasant Grove (Deep)	Rusk	3,850	1,100	200	18,400	0	537	213	30,500	1.041	.127	50,950
		3,852-3,860	740	120	16,700	0	281	180	27,100	1.034	.165	45,121
		3,880-3,883	1,200	300	17,500	0	481	0	29,800	1.043	.121	49,281
		3,880-3,883	1,840	70	18,500	-	201	170	31,900	1.043	.118	52,681
		3,900	1,215	154	18,400	0	433	267	30,500	1.041	.128	50,969
		4,042-4,728	920	235	17,600	0	79	319	29,100	1.039	.130	48,253
Currie	Navarro	2,888-2,927	65	29	4,378	-	1,403	3	6,135	1.009	.520	12,013
		2,925-3,000	100	45	5,847	6	1,183	50	8,600	1.014	.415	15,825
		2,930-2,957	70	21	3,303	-	1,495	19	4,397	1.008	.680	9,305
Richland	Navarro	2,938-2,949	130	46	5,436	-	725	33	8,300	1.014	.437	14,670
		2,950-2,985	137	48	5,246	-	683	0	8,085	1.011	.440	14,199
		2,950-2,985	124	37	5,654	-	683	0	8,652	1.012	.420	15,150
Rowe and Baker	Henderson	3,137-3,144	341	124	12,475	-	604	-	19,857	1.023	.192	33,401
		3,137-3,144	333	126	12,474	-	586	1	19,857	1.024	.190	33,377
		3,192-3,193	336	120	11,400	14	475	8	18,300	1.026	.209	30,639
Rusk	Cherokee	5,120	4,410	608	34,345	-	189	165	62,304	1.072	.073	102,021
		5,186	4,590	730	33,554	-	281	171	61,700	1.071	.074	101,026
		5,200	3,727	612	37,814	-	238	116	66,486	1.074	.069	108,993
Slocum, S.	Anderson	5,932-5,938	3,300	800	31,000	24	12	325	55,800	1.075	.075	91,237
		5,934-5,945	3,334	778	31,400	-	67	255	56,300	1.074	.075	92,134
		5,950-5,952	3,800	680	35,400	0	268	393	62,900	1.074	.074	103,441
		5,950	3,400	990	35,800	0	311	215	63,800	1.076	.073	104,516

Field	County	Depth	Constituents, Mg/liter: Ca	Mg	Na	Ba-Sr	HCO_3	SO_4	Cl	Sp. Gr.	Resistivity	Total Solids (mg/liter)
					WOODBINE (KGW) Continued							
Slocum, W.	Anderson	5,675-5,686	3,000	430	32,910	0	260	190	57,000	1.068	.081	93,790
		5,750-5,752	3,000	525	32,900	0	43	0	57,600	1.067	.079	94,068
		5,752-5,755	2,700	130	34,300	0	274	421	57,600	1.069	.076	95,425
Stegall	Rusk	3,763-3,766	1,344	113	20,000	-	457	0	33,300	1.042	.128	55,214
		3,799-3,801	1,200	330	20,900	-	366	0	35,100	1.046	.114	57,896
Stewards Mill	Freestone	4,001-4,006	1,300	64	21,700	0	183	372	35,500	1.042	.113	59,119
Stone	Cherokee	3,752-3,753	1,220	170	17,400	0	146	396	29,100	1.042	.118	48,432
		3,752-3,753	1,279	161	19,400	-	464	188	32,300	1.043	.114	53,792
		3,752-3,770	1,300	400	22,000	0	409	0	37,200	1.046	.118	61,309
		3,752-3,770	1,400	33	22,100	0	433	342	36,200	1.046	.114	60,508
Trice	Wood	5,665-5,685	700	43	30,300	0	177	306	60,300	1.073	.074	91,826
Trix-Liz	Titus	3,520-3,530	468	229	23,519	-	343	3	37,600	1.045	.122	62,162**
		3,548-3,574	1,063	331	21,776	-	102	6	36,400	1.043	.125	59,678**
		3,608-3,628	1,169	355	22,584	-	206	1	37,850	1.045	.121	62,165**
		3,826-3,836	1,222	375	23,010	-	222	1	38,650	1.046	.101	63,480**
Van	Van Zandt	2,855-2,948	1,673	120	24,186	-	201	105	40,423	1.048	.102	66,708
		2,864-2,867	1,475	350	25,100	0	73	174	42,200	1.052	.104	69,372
		2,874-2,878	1,180	420	22,600	181	311	174	37,900	1.050	.103	62,585
		2,884-2,912	825	368	27,491	-	536	11	44,600	1.053	.101	73,831
		2,740-2,848	1,360	437	26,200	0	-	50	43,872	1.051	.092	71,919
		2,760-2,880	1,240	414	25,600	0	-	14	43,247	1.050	.099	70,511
		2,797-2,938	1,191	446	26,400	0	-	22	41,023	1.049	.095	69,082
		2,872-2,952	1,388	445	27,800	0	-	68	45,300	1.056	.090	75,001
		2,897-2,963	1,360	437	27,800	0	-	67	45,120	1.053	.090	74,784
		2,936-2,941	1,142	345	23,800	0	-	22	37,410	1.039	.107	62,719
		2,766-2,788	1,160	384	25,700	0	-	10	42,000	1.050	.093	69,254
Van		2,785-2,814	1,080	432	26,200	0	-	31	43,100	1.052	.095	70,843
		2,796-2,802	1,140	444	25,900	0	-	34	44,000	1.052	.095	71,518
		2,826-2,830	1,260	384	26,400	0	-	23	45,400	1.052	.093	73,467
		2,840-2,843	1,120	432	26,100	0	-	15	44,100	1.052	.093	71,767
		2,850-2,854	1,100	444	25,700	0	-	18	42,700	1.051	.098	69,962

**ppm

Field	County	Depth	Constituents, Mg/liter Ca	Mg	Na	Ba-Sr	HCO_3	SO_4	Cl	Sp. Gr.	Resistivity	Total Solids (mg/liter)
					WOODBINE (KGW) Continued							
Walter Fair	Kaufman	4,158-4,165	1,200	14	24,800	0	43	-	40,400	1.048	.105	66,457
		4,170-4,176	1,250	331	22,200	18	317	0	37,200	1.048	.105	61,298
		4,896-4,932	1,410	377	24,200	178	214	0	40,800	1.048	.105	67,001
Powell	Navarro	3,000	62	26	3,964	-	1,393	-	5,462			10,941
		2,500	79	35	4,606	-	1,007	-	6,760			12,525**
		2,500	105	41	5,603	-	1,274	-	8,219			15,287**
		2,500	69	29	4,371	-	993	-	6,267			11,838**
		2,900	217	83	8,428	-	500	-	13,333			22,565**
Ham Gossett	Kaufman	3,254-3,258	364	116	13,481	-	492	7	21,500			39,960**
Hawkins	Wood	4,898-4,903	2,440	340	35,352	-	260	145	59,700			96,277**
E. Texas	Rusk	3,650	1,300	296	24,001	-	452	210	39,800			66,059**
		-	760	284	19,259	0	1,087	37	31,200			52,627
		-	1,150	175	19,837	0	743	414	32,400			54,719
		-	1,050	247	20,111	0	639	382	32,880			55,309
		-	1,020	236	18,407	0	865	429	30,060			50,017
		-	1,300	203	22,694	-	553	338	37,320			62,408
		-	950	223	18,992	0	744	390	30,900			52,199
		-	920	269	17,822	-	799	367	29,160			49,337
		-	1,040	288	19,349	-	805	422	31,740			53,644
		-	760	284	19,259	0	1,087	37	31,200			52,627
		-	1,150	175	19,837	0	743	414	32,400			54,719
	Gregg	3,715	1,140	297	17,951	0	854	420	29,760			50,422
		-	1,190	302	20,443	0	641	240	33,960			56,766
		-	1,120	276	19,300	0	545	311	32,000			53,600
		-	1,360	216	19,694	0	750	199	32,820			55,039
		-	1,030	297	21,100	0	690	454	33,000			55,600
E. Texas	Gregg	-	1,110	229	19,795	-	806	561	32,280			54,781
Newton Branch	Cherokee	5,148-5,151	3,679	642	35,355	-	268	149	62,628			102,720
Fort Trinidad	Houston	8,618-8,641	150	300	4,000	150	-	-	-			71,000
		-	628	42	4,186	0	-	-	-			70,300

**ppm

Field	County	Depth	Constituents, Mg/liter Ca	Mg	Na	Ba-Sr	HCO_3	SO_4	Cl	Sp. Gr.	Resistivity	Total Solids (mg/liter)
					WOODBINE (KGW) Continued							
Navarro Crossing	Houston	-	3,398	531	34,942	-	247	761	61,200			100,435
		5,800	Trace	7	387	0	415	387	376			1,185
		5,727-5,900	5,304	194	38,739	0	126	1,074	67,336			113,440
		5,771-5,781	4,171	634	35,723	-	231	118	64,092			104,973
		5,742-5,744	7,335	705	25,097	-	7	62	54,032			87,438
		5,742-5,744	2,891	504	34,889	-	315	78	58,906			96,783
		5,742-5,744	3,229	539	34,575	-	224	128	60,366			99,061
		5,776-5,780	3,220	582	33,893	0	301	98	59,400			97,493
		5,796-5,806	3,524	504	33,941	0	277	132	59,780			98,158
		5,785-5,805	4,141	567	36,575	0	247	118	65,141			106,788
		5,794-5,796	3,000	485	33,307	0	263	120	57,836			95,011
		5,727-5,900	5,304	194	37,674	-	126	579	67,336			112,880
		5,785-5,805	5,831	560	57,726	-	137	133	31,574			103,995
Buffalo	Leon	5,941-5,400	530	159	4,243	159	-	-	-			85,600
Long Lake	Anderson	5,272	300	3	4,000	500	-	-	-			112,900
Mexia	Limestone	3,020-3,026	528	171	10,156	-	342	0	16,900			28,162
		-	154	409	4,093	31	-	-	-			31,600
Slocum, S.	Anderson	5,934	1,074	161	7,520	215	-	-	-			110,000
William Wise	Cherokee	5,120	3,879	558	35,313	0	190	129	62,729			102,798
Neches	Anderson	-	7,516	215	5,369	215	-	-	-			109,700
		4,732-4,742	3,520	586	35,582	0	274	180	62,520			102,662
Jacksonville, N.	Cherokee	4,376	150	1	4,000	200	-	-	-			87,000
Cayuga	Freestone	3,800-4,100	530	0	8,474	74	-	-	-			85,100
Currie	Navarro	3,000	508	102	1,523	152	-	-	-			19,900
Kerens, S.	Navarro	3,384	409	307	1,534	307	-	-	-			29,700
Powell	Navarro	3,000	303	101	807	101	-	-	-			12,100
Flagg Lake	Henderson	3,100	305	183	2,032	20	-	-	-			23,200
		-	407	204	916	51	-	-	-			21,600
Big Barnett	Rusk	3,746-3,751	156	312	3,116	208	-	-	-			50,600
Walter Fair	Kaufman	4,146	84	420	3,150	63	-	-	-			69,900
Van	Van Zandt	3,080	150	300	4,000	150	-	-	-			73,600

Field	County	Depth	Constituents, Mg/liter Ca	Mg	Na	Ba-Sr	HCO_3	SO_4	Cl	Sp. Gr.	Resistivity	Total Solids (mg/liter)
						WOODBINE (KGW) Continued						
		3,080	528	159	4,227	85	-	-	-			79,500
		3,080	84	210	4,202	42	-	-	-			74,300
Hawkins	Wood	5,100	160	43	5,340	64	-	-	-			101,100
Quitman	Wood	4,351-4,358	64	21	3,183	42	-	-	-			90,100
Wieland	Hunt	2,800	152	304	709	15	-	-	-			14,100
New Hope	Franklin	7,300-8,100	158	42	4,225	75	-	-	-			89,100
Talco	Titus	3,900	1,125	235	21,257	-	171	Trace	35,400			58,188
Trix-Liz	Titus	3,390-3,664	1,123	357	19,035	299	219	0	40,455			61,569
Oakwood	Leon	6,150	-	-	-	-	210	160	67,000			-ppm
		6,150	-	-	-	-	280	10	72,000			-ppm
Ashby-Ramsey	Hunt	3,210-3,226	83	33	5,136	0	796	0	7,700	1.012	.460	13,748
		3,227-3,229	86	40	5,006	0	811	22	7,500	1.012	.475	13,465
Bazette	Navarro	2,947-2,961	190	55	8,000	16	702	32	12,400	1.018	.300	21,379
Big Barnett	Rusk	3,754-3,758	2,000	440	16,660	0	366	230	30,100	1.040	.137	49,796
		3,760-3,766	800	20	18,300	0	653	278	29,100	1.036	.140	49,151
		3,769-3,771	1,200	175	13,700	0	634	458	23,000	1.040	.133	39,167
Boggy Creek	Anderson	3,435-3,487	3,481	580	37,278	-	279	183	65,056	1.076	.071	106,857
		3,547-3,564	3,095	550	36,439	-	336	195	62,950	1.072	.073	103,565
		3,600-3,634	3,451	582	37,615	-	329	184	65,499	1.076	.070	107,660
Buffalo	Leon	5,642-5,645	2,500	430	30,586	9	500	69	52,500	1.064	.089	86,585
		5,722-5,745	1,200	260	27,164	0	753	42	44,300	1.050	.104	73,719
		5,742-5,747	1,700	320	27,659	10	787	46	46,100	1.055	.098	76,612
		5,742-5,750	1,198	431	30,807	-	532	92	50,500	1.061	.084	83,560
Cayuga	Anderson	3,750-3,800	1,412	411	31,362	-	317	163	51,770	1.060	.085	85,435
		3,768	1,443	396	30,900	-	336	157	51,061	1.061	.085	84,293
		4,007-4,014	1,580	380	29,595	2	250	127	49,300	1.059	.089	81,232
		4,009-4,014	1,610	415	30,154	3	262	139	50,300	1.060	.087	82,880
		4,046-4,049	1,620	350	29,833	2	348	118	49,600	1.059	.088	81,869
Cayuga	Anderson	4,077	1,428	305	29,900	-	158	180	49,200	1.058	.086	81,171
Currie	Navarro	2,900-2,950	256	101	7,755	-	628	6	12,340	1.016	.285	21,086
		2,900-2,950	250	160	7,318	17	653	19	11,800	1.017	.318	20,200

Field	County	Depth	Constituents, Mg/liter							Sp. Gr.	Resistivity	Total Solids (mg/liter)
			Ca	Mg	Na	Ba-Sr	HCO_3	SO_4	Cl			
WOODBINE (KGW) Continued												
		2,958	212	91	7,444	-	598	4	11,772	1.015	.295	20,121
		3,168-3,185	276	99	8,059	-	512	4	12,907	1.017	.280	21,857
Dottie Sue	Cherokee	5,083-5,085	800	140	36,000	Trace	171	0	57,200	1.073	.076	94,311
Earl-Lee	Wood	5,518-5,568	3,500	640	31,500	0	177	263	56,300	1.071	.077	92,380
		5,550-5,565	3,500	640	34,100	0	134	373	60,300	1.073	.076	99,047
East Texas	Upshur	3,600-3,800	1,720	85	22,100	-	495	0	37,150	1.048	.115	61,550
		3,600-3,800	1,140	361	20,607	0	596	452	34,200	1.041	.130	57,356
East Texas	Gregg	3,600-3,800	1,260	378	21,622	-	577	298	36,120	1.042	.153	60,255
		3,600-3,800	1,100	295	22,531	-	547	204	37,080	1.045	.137	61,757
		3,600-3,800	1,283	340	23,228	-	603	344	38,470	1.046	.122	64,268
East Texas	Rusk	3,600-3,800	1,300	203	22,694	-	553	338	37,320	1.045	.133	62,408
		3,600-3,800	1,330	227	23,015	-	529	383	37,920	1.047	.135	63,404
		3,600-3,700	1,060	279	16,900	0	588	311	28,200	1.034	.139	47,338
		3,650-3,800	1,140	297	17,951	0	854	420	29,760	1.038	.129	50,422
		3,650-3,800	1,040	288	19,349	-	805	422	31,740	1.040	.154	53,644
		3,650-3,800	930	306	19,627	-	848	198	32,160	1.038	.147	54,069
		3,650-3,800	1,050	247	20,111	0	639	382	32,880	1.040	.144	55,309
		3,650-3,800	1,030	297	20,100	0	690	454	33,000	1.039	.130	55,571
		3,650-3,800	1,100	303	20,100	0	600	334	33,200	1.040	.125	55,637
		3,650-3,800	960	188	20,421	-	739	250	33,120	1.041	.120	55,678
		3,650-3,800	1,270	231	20,600	5	576	312	34,200	1.040	.133	57,189
		3,650-3,800	920	109	21,343	23	610	416	34,200	1.041	.155	57,598
		3,650-3,800	1,230	273	20,793	-	706	420	34,320	1.043	.132	57,742
		3,650-3,800	830	291	21,500	0	360	289	35,000	1.038	.135	58,270
		3,650-3,800	1,110	330	20,926	-	691	147	34,680	1.042	.122	57,884
		3,600-3,800	1,152	307	21,960	-	586	405	36,168	1.042	.113	60,578
		3,600-3,800	1,082	305	22,438	-	476	354	36,877	1.042	.112	61,532
		3,600-3,800	1,232	324	24,564	-	573	352	40,423	1.047	.103	67,468
		3,600-3,800	1,443	146	21,000	-	482	434	34,700	1.046	.115	58,205
		3,600-3,800	1,302	61	16,200	-	476	351	26,900	1.040	.131	45,290

Field	County	Depth	Constituents, Mg/liter: Ca	Mg	Na	Ba-Sr	HCO_3	SO_4	Cl	Sp. Gr.	Resistivity	Total Solids (mg/liter)
					WOODBINE (KGW) Continued							
East Texas	Rusk	3,600-3,800	1,262	98	21,000	-	519	141	34,400	1.042	.125	57,420
		3,600-3,800	1,342	158	16,800	-	409	326	31,900	1.045	.121	50,935
		3,600-3,800	1,443	72	21,100	-	335	49	35,000	1.046	.123	57,999
		3,647-3,668	1,162	308	23,686	-	464	292	39,005	1.045	.106	64,917
		3,659-3,661	1,342	307	23,731	-	500	307	39,351	1.046	.105	65,538
		3,700	1,400	31	20,500	0	768	611	33,300	1.043	.122	56,610
		3,700	1,300	60	17,600	0	506	322	28,400	1.038	.136	48,188
		3,700	1,300	53	15,600	0	353	139	26,200	1.038	.142	43,645
Wieland	Hunt	2,770	97	38	5,716	0	659	17	8,700	1.013	.418	15,227
		2,772-2,801	93	5	5,700	0	506	0	8,700	1.015	.408	15,004
Williams-Ham Gossett	Kaufman	3,228-3,271	530	21	14,600	0	159	0	23,400	1.030	.165	38,710
William Wise	Cherokee	5,093-5,135	3,960	370	36,000	0	256	2,457	60,600	1.074	.076	103,643
		5,117-5,120	3,980	116	33,700	0	67	208	59,200	1.073	.075	97,271
					PALUXY (KCPA)							
Boynton	Smith	7,456-7,461	4,360	933	36,800	0	305	726	66,500	1.079	.070	109,624
Coke	Wood	6,297-6,404	8,900	680	38,800	0	177	497	77,100	1.088	.067	126,154
		6,329-6,333	8,750	895	37,200	0	111	0	74,500	1.088	.068	121,456
		6,370-6,377	8,080	1,030	37,900	Trace	183	477	75,300	1.088	.068	122,970
Dalby Springs	Bowie	4,389-4,390	966	156	9,000	0	357	2,333	14,100	1.022	.249	26,912
Hitt's Lake	Smith	7,131-7,248	4,450	670	37,548	1	311	196	67,400	1.078	.070	110,575
Manziel	Wood	6,300-6,372	7,300	738	44,000	-	34	530	82,500	1.098	.059	135,102
		6,347-6,358	8,239	968	35,768	-	274	476	72,047	1.083	.066	117,772
		6,346-6,358	9,500	950	33,100	13	79	685	70,000	1.094	.065	114,314
		6,367-6,389	9,600	1,400	38,500	0	189	649	79,800	1.096	.064	130,138
		6,375-6,388	9,825	1,182	37,540	-	158	434	78,310	1.092	.061	127,449
		6,375-6,388	9,825	1,200	38,298	-	120	438	79,540	1.094	.060	129,421
Mitchell Creek	Hopkins	4,466-4,542	145	15	4,900	0	896	96	7,300	1.012	.443	13,352
		4,481-4,524	450	22	4,400	0	104	1,409	6,600	1.013	.443	12,985
		4,500-4,525	386	38	4,970	-	364	2,300	6,560	1.010	.441	14,618

Field	County	Depth	Constituents, Mg/liter Ca	Mg	Na	Ba-Sr	HCO_3	SO_4	Cl	Sp. Gr.	Resistivity	Total Solids (mg/liter)
PALUXY (KCPA) Continued												
		4,648	442	85	4,898	-	457	2,249	6,656	1.010	.440	14,787
Mt. Sylvan	Smith	7,339-7,352	3,400	600	31,900	0	177	664	56,300	1.072	.075	93,041
		7,404-7,412	4,260	875	35,300	148	317	810	63,800	1.074	.074	105,362
		7,404-7,412	3,500	640	29,700	17	280	621	53,200	1.070	.074	87,941
Pewitt Ranch	Titus	4,488-4,539	650	42	6,200	0	237	1,210	9,820	1.017	.341	18,159
		4,512-4,592	640	20	6,100	0	61	874	9,930	1.017	.336	17,625
		4,559-4,572	665	110	6,836	-	290	2,550	10,000	1.015	.280	20,451**
Quitman	Wood	6,204-6,310	8,525	732	41,774	-	115	445	81,237	1.096	.059	132,828
		6,220-6,310	9,100	720	41,565	-	84	610	81,787	1.097	.059	133,866
		6,222-6,272	9,116	728	42,107	-	116	580	82,654	1.098	.058	135,301
		6,350-6,372	8,986	712	42,403	-	187	595	82,798	1.098	.058	135,681
Sand Flat	Smith	6,934-7,106	4,200	440	38,700	0	318	355	68,000	1.079	.070	112,013
		7,210-7,239	5,150	700	39,230	0	180	192	71,400	1.082	.068	116,852
		7,540-7,594	3,382	491	38,972	-	107	600	67,000	1.080	.070	110,552
Sugar Hill	Titus	4,377-4,416	810	64	7,000	0	232	62	12,200	1.022	.283	20,368
Sulphur Bluff	Hopkins	4,440-4,500	385	65	4,470	-	437	2,240	5,920	1.009	.440	13,517
		4,483-4,584	376	10	3,800	0	153	354	6,200	1.014	.475	10,893
		4,490-4,561	380	24	4,580	0	528	2,100	6,000	1.014	.523	13,612
		4,500	315	61	5,044	-	476	2,228	6,595	1.012	.400	14,719
		4,514-4,532	384	72	4,510	0	444	2,230	6,000	1.012	.460	13,640
Talco	Titus	4,186-4,342	287	27	6,712	-	542	2,044	9,110	1.014	.345	18,722
		4,239-4,367	600	50	6,800	0	353	2,302	9,800	1.019	.350	19,905
Talco	Franklin	4,252-4,264	430	87	5,849	-	479	2,200	8,080	1.013	.350	17,125**
Tyler	Smith	7,678-7,685	8,300	300	41,300	0	0	492	78,900	1.094	.061	129,292
Walter Fair	Kaufman	4,960-4,975	205	80	4,800	Trace	927	295	7,300	1.017	.440	13,607
		4,970-4,976	229	11	4,400	0	597	300	6,700	1.013	.440	12,237
Birthright	Hopkins	4,741-4,762	270	52	4,281	0	555	2,316	5,200	1.012	.553	12,674
		4,755-4,759	266	49	4,600	0	470	2,369	5,200	1.012	.550	12,954
Bud Lee	Smith	7,564-7,582	4,300	450	33,800	0	49	340	60,700	1.076	.074	99,639
Mitchell Creek	Hopkins	4,546-9,340	336	57	4,630	0	416	2,080	6,140			13,700
		-	552	48	5,308	0	552	2,480	7,257			16,012

**ppm

Field	County	Depth	Constituents, Mg/liter: Ca	Mg	Na	Ba-Sr	HCO_3	SO_4	Cl	Sp. Gr.	Resistivity	Total Solids (mg/liter)
						PALUXY (KCPA) Continued						
		-	473	1,128	4,915	-	455	1,900	7,120			14,994
		-	500	64	5,485	-	403	2,760	7,257			16,470
		-	500	48	5,619	-	413	2,760	7,403			16,743
Mitchell Creek	Hopkins	-	473	96	5,582	-	390	2,640	7,548			16,730
		-	579	80	4,917	-	394	1,840	7,257			15,068
Talco	Titus	4,200-4,230	856	29	6,500	-	317	1,280	7,900			19,932
		-	61	41	1,523	15	-	-	-			16,600
		-	81	41	2,026	25	-	-	-			18,400
		-	41	153	814	8	-	-	-			19,800
Quitman	Wood	6,293-6,301	438	164	4,383	77	-	-	-			153,500
		4,014-4,032	74	16	3,159	42	-	-	-			76,100
		6,316-6,350	438	164	3,284	44	-	-	-			150,200
Chapel Hill	Smith	5,693	155	31	4,145	26	-	-	-			54,600
Shamburger Lake	Smith	7,394-7,430	165	50	85	-	770	3	120			1,193
		7,432-7,437	4,282	481	38,389	-	221	389	67,754			111,113
		7,422-7,500	5,076	518	36,466	-	92	567	66,247			108,966
		-	4,277	945	38,183	-	184	459	68,747			112,795
		-	3,960	557	38,526	0	157	460	67,599			111,258
		-	4,160	630	39,662	0	301	510	69,800			115,062
		-	4,140	543	38,873	0	144	502	68,400			112,603
Shamburger Lake	Smith	6,838-7,670	58	33	6,350	-	295	319	9,540			16,629
		7,550-7,564	413	86	3,735	-	202	328	6,381			11,143
		7,486-7,498	501	50	7,215	-	536	332	11,600			20,233
		-	457	45	6,753	34	35	610	14,136			22,114
		7,361-7,367	665	68	11,045	-	518	360	17,836			30,491
		-	349	51	7,471	0	588	279	11,736			20,472
		7,161-7,167	4,018	714	42,185	-	204	247	73,919			121,308
		-	305	34	6,459	-	124	317	10,400			17,760
		7,336-7,346	4,198	847	36,896	-	197	349	64,801			107,288
		6,838-6,888	284	50	7,268	-	708	337	11,193			19,837
		7,336-7,346	4,301	679	36,878	-	203	257	66,202			108,541

Field	County	Depth	Constituents, Mg/liter Ca	Mg	Na	Ba-Sr	HCO_3	SO_4	Cl	Sp. Gr.	Resistivity	Total Solids (mg/liter)
					PALUXY (KCPA) Continued							
		7,328-7,348	4,936	1,309	4,685	-	614	379	19,130			31,053
		7,352-7,362	3,290	381	5,492	-	458	432	14,818			24,870
		7,314-7,326	235	20	5,763	-	669	365	8,698			15,749
		-	705	110	6,028	-	243	348	10,465			17,898
		7,623-7,670	934	80	14,796	-	493	299	24,205			40,807
Shamburger Lake	Smith	-	200	23	2,540	-	515	93	3,970			7,342
		-	745	269	12,662	-	756	841	20,564			35,836
		-	104	20	4,135	18	780	250	7,546			12,885
		7,288-7,298	438	61	10,562	-	565	458	16,573			28,656
		-	1,518	487	23,420	186	314	775	38,888			65,651
		-	487	63	10,200	-	571	524	16,000			27,840
		-	747	90	11,575	61	461	825	21,205			35,038
		-	1,096	173	16,380	-	356	484	27,137			45,625
		-	1,096	185	16,790	-	401	450	27,800			46,723
		-	1,078	366	13,549	-	512	840	22,950			39,295
		-	940	48	5,162	-	119	200	9,548			16,017
		-	403	44	3,610	-	952	300	5,640			10,948
		-	0	159	6,435	-	742	550	9,547			17,432
		-	915	134	14,176	-	437	452	23,279			39,392
		-	776	28	3,880	195	844	5	7,619			13,373
		-	715	72	14,000	-	505	577	22,300			38,169
		-	627	61	12,249	-	469	340	19,653			33,398
		7,590-7,598	1,080	159	14,772	-	378	468	24,580			41,436
		-	812	108	14,800	-	561	521	23,800			40,604
		-	176	28	5,950	-	804	324	8,870			16,151
		-	255	146	5,847	-	861	36	9,364			16,509
		-	906	120	11,451	79	789	753	20,957			35,129
		-	258	10	6,072	-	708	420	9,078			16,515
		-	1,724	235	22,381	-	402	476	37,656			62,875
		-	257	25	5,230	-	351	298	8,160			14,321
		7,263-7,269	398	97	9,297	-	546	479	14,652			25,469

Field	County	Depth	Constituents, Mg/liter Ca	Mg	Na	Ba-Sr	HCO_3	SO_4	Cl	Sp. Gr.	Resistivity	Total Solids (mg/liter)
PALUXY (KCPA) Continued												
		-	955	182	16,241	0	398	630	26,565			44,971
		7,263-7,269	560	58	10,981	0	535	459	17,441			30,035
		-	882	213	14,154	-	457	572	23,317			39,594
		-	598	80	8,646	60	455	669	17,808			28,379
		-	157	34	5,443	31	902	101	10,190			16,897
		-	1,124	186	17,636	-	392	382	29,214			48,933
Shamburger Lake	Smith	-	1,740	185	24,300	-	361	652	40,399			65,544
		-	58	33	6,350	-	295	319	9,540			16,628
		-	812	108	14,800	-	561	521	23,800			40,602
		7,317-7,318	1,934	315	22,371	-	254	519	38,279			63,673
		-	1,333	134	19,687	0	328	610	32,458			54,549
		-	869	159	15,471	-	334	786	25,083			42,703
Shamburger Lake	Wood	7,256-7,749	353	48	6,006	29	11	325	11,666			18,452
		-	402	91	9,272	52	549	568	14,525			25,483
		-	131	38	5,283	23	315	320	8,116			14,329
		-	552	273	11,549	59	0	340	20,506			33,319
		7,256-7,769	350	44	7,765	-	555	373	12,121			21,207
		7,479-7,489	1,501	207	17,833	0	155	631	30,195			50,522
		-	250	33	4,602	27	463	270	7,433			13,094
		-	552	121	9,303	39	446	450	16,233			27,175
		-	301	91	5,173	27	244	320	8,544			14,719
		7,503-7,522	199	31	4,203	-	635	221	6,389			11,677
		7,486-7,498	365	60	6,414	-	699	1,119	10,219			17,867
		-	80	10	2,055	11	696	180	3,952			7,071
		-	602	137	9,939	47	244	700	17,516			29,286
		-	402	151	9,236	29	489	469	14,738			25,542
		7,590-7,598	619	160	12,785	-	531	28	20,948			35,071
		-	1,456	324	21,114	88	303	750	35,671			59,789
Sand Flat	Smith	7,220	2,161	216	4,321	22	-	-	-			120,600
Bud Lee	Smith	7,560	4,304	523	37,634	-	244	487	66,766			110,071
		-	4,161	582	38,706	-	156	458	68,307			112,370

Field	County	Depth	Constituents, Mg/liter							Sp. Gr.	Resistivity	Total Solids (mg/liter)
			Ca	Mg	Na	Ba-Sr	HCO_3	SO_4	Cl			
PALUXY (KCPA) Continued												
		-	200	200	4,000	50	-	-	-			48,000
Hitt's Lake	Smith	7,299-7,305	4,444	551	39,604	-	259	513	70,000			115,371
		7,219-7,239	4,605	915	39,381	193	73	720	67,721			113,730
		7,203-7,270	4,709	730	34,615	-	231	221	65,532			104,037
		-	4,143	571	40,290	-	243	647	70,486			116,375
		7,294-7,312	4,467	209	39,375	-	245	649	68,605			113,549
		7,233-7,268	4,121	685	37,809	0	203	628	67,158			110,775
		7,233-7,268	3,969	450	38,388	-	295	632	66,882			110,615
Hitt's Lake	Smith	-	4,315	503	37,566	0	192	419	66,600			109,595
		7,294-7,312	4,247	581	38,912	0	179	631	68,803			113,535
		-	4,538	661	37,322	-	191	257	67,198			110,167
		7,232.5-7,272.8	5,036	665	42,321	-	93	840	75,429			255,240
		7,140-7,210	4,540	765	36,670	0	126	207	66,741			109,230
		7,202-7,212	4,383	724	40,240	-	238	622	69,200			115,407
		7,308-7,318	3,963	537	37,069	-	409	634	65,027			107,639
		-	4,138	576	35,303	-	201	540	62,916			103,673
		-	4,450	577	37,962	-	90	450	67,703			111,231
		-	4,519	618	37,110	-	127	459	66,605			109,438
		-	4,507	579	37,424	-	170	729	66,729			110,136
		-	4,759	647	35,545	-	204	227	64,821			106,202
Lindale, E.	Smith	7,841	5,840	1,020	38,741	351	234	560	73,000			119,925
Walter Fair	Kaufman	5,380	406	152	609	10	-	-	-			15,600
Quitman	Wood	6,211-6,352	9,731	1,388	39,627	-	96	460	82,009			133,373
		-	11,309	1,435	12,063	-	65	352	42,529			67,801
		-	11,309	1,435	39,645	-	65	352	85,058			137,912
		-	10,651	1,356	40,998	-	129	476	85,638			139,325
		-	11,966	1,834	39,655	-	96	352	87,380			141,335
		-	10,651	1,196	40,160	-	104	444	83,896			136,495
		-	6,443	2,073	41,192	-	67	352	80,704			130,897
		-	11,700	798	40,632	-	83	460	85,348			139,115
		-	11,572	1,595	40,407	-	96	38	87,380			141,145

Field	County	Depth	Constituents, Mg/liter Ca	Mg	Na	Ba-Sr	HCO_3	SO_4	Cl	Sp. Gr.	Resistivity	Total Solids (mg/liter)
					PALUXY (KCPA) Continued							
		-	11,966	1,750	39,599	-	102	305	87,090			140,875
		-	11,046	1,435	39,576	-	104	352	84,478			137,065
		-	10,257	717	37,911	-	104	396	78,381			127,824
		-	10,520	1,914	40,259	-	100	43	86,218			139,111
		-	10,257	1,276	41,582	-	86	444	85,638			139,332
		-	10,914	1,435	40,531	-	102	424	85,348			138,618
		-	4,333	460	25,676	-	34	0	48,742			79,503
		-	11,835	1,435	39,933	-	65	360	86,509			140,318
Manziel	Wood	6,306-6,346	9,468	1,914	39,222	-	106	444	82,444			133,634
Manziel	Wood	6,337-6,347	9,472	1,187	39,068	0	106	296	80,177			130,306
		6,345-6,357	9,541	1,059	39,143	-	99	318	80,033			130,192
		6,345-6,357	8,756	1,260	38,621	0	96	299	78,459			127,470
		-	9,200	1,333	43,431	0	107	400	86,772			141,242
		6,347-6,358	8,929	1,046	38,753	-	293	516	78,077			127,619
					RODESSA (KCGRL)							
Pokey	Limestone	6,338	16,646	2,158	47,259	-	63	290	108,359			174,775
McBee	Leon	-	539	43	273	0	0	Trace	1,705			2,602
		-	15,200	1,290	54,100	0	42	287	114,000			185,005
		8,703-8,716	14,201	1,457	51,141	-	12	150	108,111			175,073
		8,707-8,720	11,652	1,331	37,461	-	67	275	82,014			132,799
		8,703-8,716	12,959	1,575	50,484	-	164	280	105,062			170,524
		8,762-8,770	13,731	1,417	53,597	-	19	250	110,870			179,883
		-	12,416	1,410	43,546	843	200	325	104,651			165,026
		-	11,640	1,816	39,548	-	302	230	86,524			140,060
		8,703-8,716	12,849	1,439	45,582	-	94	314	96,924			157,200
		-	212	8	442	-	7	0	1,080			1,752
		-	251	6	240	-	Trace	0	833			1,330
		8,660-8,663	16,970	1,514	39,085	-	406	337	94,218			152,530
		8,650-8,663	17,952	1,411	43,503	-	479	273	102,473			166,091

Field	County	Depth	Constituents, Mg/liter Ca	Mg	Na	Ba-Sr	HCO_3	SO_4	Cl	Sp. Gr.	Resistivity	Total Solids (mg/liter)
RODESSA (KCGRL) Continued												
		8,955-8,979	853	132	8,265	-	345	579	14,018			24,191
Teague, W.	Freestone	6,702	4,915	123	5,578	-	98	126	18,091			29,302
Tennessee Colony	Anderson	8,882-9,700	11,052	553	6,631	221	-	-	-			152,000
Fairway	Henderson	9,516-9,540	19,860	1,442	56,113	-	32	329	125,275			204,245
		9,517-9,523	22,127	1,922	49,003	-	0	269	120,116			193,437
		9,517-9,523	19,042	1,971	50,359	-	79	322	116,802			188,575
		9,517-9,523	19,164	1,976	52,593	-	114	211	120,540			194,590
		9,474-9,485	3,085	481	33,336	-	145	1,840	56,818			95,704
Tyler, S.	Smith	9,520-9,560	1,074	85	1,891	-	74	9	5,022			9,003
Chapel Hill	Smith	-	30	15	3,035	76	-	-	-			18,400
		7,704-7,712	22,927	2,497	60,177	-	83	247	140,399			226,329
Wright Mountain	Smith	7,586	220	10	4,503	-	397	7,742	1,335			14,274
Hitt's Lake	Smith	9,305-9,320	20,676	1,800	50,753	-	Trace	283	119,879			193,390
Lansing, N.	Harrison	6,957-6,965	16,700	1,760	49,600	8	102	262	111,000			179,000
		-	578	25	258	0	62	0	1,100			1,820
		-	571	17	221	0	37	68	1,356			2,236
		-	478	46	423	0	48	423	1,590			2,610
		-	5,050	262	13,113	0	275	102	29,100			48,502
		-	630	24	484	0	72	0	1,890			3,100
		-	475	18	129	0	70	8	1,296			2,193
		-	14,800	1,580	41,100	0	102	157	94,000			152,000
		-	14,900	1,340	40,100	25	96	172	92,000			149,000
		-	15,300	1,760	42,100	0	156	170	97,000			156,500
		-	15,600	1,640	43,300	14	49	180	99,000			160,000
		-	19,900	365	2,940	36	6	113	40,800			64,100
		-	17,800	243	2,870	44	30	102	36,600			57,600
		-	21,500	3,650	3,820	0	12	48	54,600			83,600
		-	1,710	43	501	5	30	16	3,900			6,200
		-	2,960	36	870	0	102	48	6,600			10,600
		-	2,720	24	880	0	180	60	6,100			10,000

Field	County	Depth	Constituents, Mg/liter Ca	Mg	Na	Ba-Sr	HCO_3	SO_4	Cl	Sp. Gr.	Resistivity	Total Solids (mg/liter)
RODESSA (KCGRL) Continued												
		-	4,100	304	4,150	0	120	32	14,500			23,200
		-	246	7	512	0	36	0	870			1,670
		-	3,452	377	3,180	0	152	47	12,000			19,200
		-	5,400	122	4,960	0	146	41	17,500			28,100
		-	1,090	67	895	0	48	0	3,480			5,580
		-	2,600	546	34,200	70	113	0	58,800			96,200
		-	448	18	182	0	30	0	1,110			1,790
		-	238	8	637	0	132	0	1,350			2,360
		-	580	58	1,580	0	65	0	3,600			5,890
		-	370	12	86	0	134	4	744			1,350
		-	270	4	272	0	95	0	855			1,500
		-	226	4	150	0	24	0	630			1,030
		-	1,600	61	3,860	0	85	12	8,900			14,500
Lansing	Harrison	-	206	2	521	0	43	0	1,150			1,920
		-	100	36	2,470	0	0	8	4,080			6,690
		-	120	6	270	0	180	0	540			1,120
		-	130	46	553	0	30	0	1,200			1,960
		-	6,557	147	2,005	-	0	101	15,086			28,307
		-	2,210	41	824	-	11	38	5,279			10,393
		6,634-6,645	6,098	608	22,725	-	98	3,781	44,756			78,066
		-	2,681	98	1,246	-	46	46	6,906			13,694
Quitman	Wood	8,409-8,425	657	48	1,405	-	56	21	3,484			5,765
		-	4,997	80	36,858	-	52	80	65,898			108,095
		-	22,620	2,455	56,396	-	92	420	132,252			219,555
		-	24,722	2,711	53,054	-	10	88	133,538			214,371
		-	1,446	191	6,062	-	10	27	12,483			20,295
		-	815	16	2,022	-	75	0	3,193			6,195
		-	28,798	4,306	64,806	-	6	128	163,438			261,637
		-	30,040	3,300	63,601	-	229	172	160,734			258,309
		-	12,210	183	9,768	110	-	-	-			335,700
		-	1,000	500	5,000	350	-	-	-			324,900

Field	County	Depth	Constituents, Mg/liter Ca	Mg	Na	Ba-Sr	HCO_3	SO_4	Cl	Sp. Gr.	Resistivity	Total Solids (mg/liter)
					RODESSA (KCGRL) Continued							
Blackfoot	Anderson	9,030-9,050	20,000	1,778	58,100	910	251	233	129,800	1.148	.048	210,162
		9,034-9,052	17,400	2,200	61,100	0	0	367	131,200	1.150	.048	212,267
Cayuga, NW.	Henderson	7,436-7,444	22,800	1,930	59,447	5	122	225	137,400	1.154	.046	221,924
Cornersville	Franklin	7,753-7,759	32,800	2,193	62,900	368	50	216	161,300	1.180	.046	259,459
Fairway	Henderson	9,565-9,585	32,200	610	34,020	0	30	400	111,000	1.122	.049	178,260
Haynes	Cass	6,000-6,003	22,920	3,200	55,800	8	31	104	135,800	1.152	.042	217,855
		6,000-6,004	25,800	2,440	56,800	0	61	327	140,000	1.161	.046	225,428
		6,051-6,064	23,200	3,100	57,400	Trace	50	100	138,500	1.159	.042	222,350
		6,081-6,083	26,300	3,400	52,600	2	37	89	137,700	1.157	.042	220,126
Kildare	Cass	5,591-6,037	17,200	6,900	46,500	0	0	2,305	120,500	1.142	.052	193,405
LaRue	Henderson	7,762-7,772	22,100	2,600	59,600	6	110	289	138,300	1.157	.047	222,999
		7,800-8,000	20,100	3,000	59,000	12	67	364	134,700	1.157	.047	217,231
Malakoff, S.	Henderson	7,462-7,471	17,900	2,200	52,484	5	58	258	118,800	1.135	.048	191,700
		7,478-7,520	18,100	3,500	49,800	5	64	249	118,800	1.137	.049	190,513
		7,510-7,520	16,800	1,940	52,476	4	55	229	116,600	1.130	.049	188,100
Mound Prairie	Anderson	10,046-10,068	13,620	1,255	48,083	-	68	290	101,800	1.114	.050	165,116**
New Hope	Franklin	7,302	23,233	2,306	83,181	-	71	242	175,877	1.156	.048	284,910
		7,364	26,800	2,970	61,486	-	40	237	150,692	1.170	.048	242,225
		7,364	25,004	2,691	87,773	-	62	234	187,224	1.168	.045	302,988
		7,350-7,400	25,597	2,376	54,136	-	0	344	135,446	1.155	.047	217,899
		7,350-7,400	24,699	2,918	61,948	-	35	287	147,501	1.166	.046	237,388
Rodessa	Marion	6,062-6,091	20,195	2,699	62,711	-	79	310	140,063	1.152	.045	226,057
		6,068-6,090	21,157	2,839	61,332	-	67	297	140,063	1.155	.045	225,755
		6,077-6,122	20,997	2,909	61,391	-	73	307	140,063	1.155	.045	225,740
Rodessa	Cass	5,986-6,004	22,840	2,621	60,929	-	-	279	141,836	1.155	.044	228,505
		5,999-6,025	21,478	2,455	61,672	-	-	313	140,063	1.154	.044	225,981
		6,033-6,077	23,321	2,673	60,285	-	-	291	141,836	1.158	.044	228,406
		5,981-5,986	21,197	2,503	59,569	-	24	219	136,517	1.149	.046	220,029
		6,008-6,030	21,397	2,298	62,062	-	-	314	140,063	1.153	.046	226,134
		6,024-6,049	23,160	2,551	60,700	-	-	292	141,836	1.157	.046	228,539
Rodessa	Marion	6,096-6,107	15,788	3,101	65,841	-	49	299	138,290	1.155	.045	223,368

**ppm

Field	County	Depth	Constituents, Mg/liter Ca	Mg	Na	Ba-Sr	HCO_3	SO_4	Cl	Sp. Gr.	Resistivity	Total Solids (mg/liter)
						RODESSA (KCGRL) Continued						
Sand Flat	Smith	9,332-9,342	19,744	1,735	45,669	-	107	154	110,240	1.121	.050	177,649
Teague, W.	Freestone	6,940-6,949	16,342	1,814	50,349	-	126	464	111,600	1.123	.049	180,695**
Tennessee Colony	Anderson	8,930-8,971	20,600	2,060	54,259	0	46	267	125,900	1.141	.049	203,132
		8,950-9,004	16,800	1,480	43,556	0	37	248	101,000	1.116	.055	163,121
		9,046-9,058	20,100	2,153	54,700	15	159	269	125,900	1.143	.049	203,281
Tri-Cities	Henderson	7,680-7,750	10,260	6,570	51,900	0	24	524	117,000	1.137	.049	186,278
Winnsboro	Wood	8,260-8,280	28,286	2,327	53,777	0	6	172	140,067	1.160	.047	224,635
		8,265-8,281	25,000	3,038	49,225	0	79	151	129,074	1.150	.044	206,567
		8,265-8,281	20,000	1,000	67,300	0	0	351	141,800	1.167	.046	230,451
		7,845-7,862	32,400	2,200	86,500	36	0	634	161,300	1.188	.044	283,034
Kildare	Cass	-	11,052	332	3,316	67	-	-	-			168,800
		6,032-6,038	700	100	4,000	300	-	-	-			131,000
Douglass	Nacogdoches	8,210-8,296	14,559	1,714	53,658	-	110	410	113,300			183,731**
Tennessee Colony	Anderson	-	11,904	1,183	37,677	0	82	208	82,445			133,533
		8,976-9,000	17,828	1,805	49,450	-	38	184	113,100			182,405**
		-	7,246	729	19,122	0	149	104	44,325			71,848
Willow Springs	Gregg	-	5,400	213	4,120	0	12	62	16,500			26,300
Willow Springs	Gregg	6,650	1,040	103	2,720	0	38	12	6,300			10,200
Lansing, N.	Harrison	-	17,500	1,400	14,300	0	314	204	107,200			172,300
		6,965	8,900	243	7,660	0	94	65	28,200			45,200
		-	11,900	912	6,490	0	49	181	33,600			53,100
		-	4,500	182	11,400	0	0	28	26,100			42,200
		-	8,600	243	10,700	28	48	56	32,400			52,100
		-	30,700	3,830	5,690	0	6	195	76,000			116,400
		-	3,050	134	1,000	0	348	50	7,100			11,700
		-	730	24	268	0	146	16	1,680			2,860
						JAMES LS. (KCGR)						
Fairway	Henderson	9,819-9,829	16,688	1,407	47,234	-	244	520	106,025	1.117	.049	172,118
		9,899-10,024	17,400	1,760	46,840	0	76	240	108,000	1.120	.049	174,316

**ppm

Field	County	Depth	Constituents, Mg/liter							Sp. Gr.	Resistivity	Total Solids (mg/liter)
			Ca	Mg	Na	Ba-Sr	HCO_3	SO_4	Cl			
						JAMES LS. (KCGR) Continued						
		10,164-10,285	20,700	1,880	38,930	0	80	240	102,000	1.148	.054	163,830
Frankston	Henderson	10,050-10,064	23,100	1,887	56,000	10	129	223	132,600	1.160	.046	213,939
Tyler, S.	Smith	9,920-10,000	15,300	1,500	70,900	0	0	835	140,100	1.158	.047	228,635
						PETTET (KCGRL)						
Tennessee Colony	Anderson	9,700	521	48	1,417	0	57	9	3,216			5,273
Trawick	Nacogdoches	7,945-8,035	18,295	1,820	60,364	-	92	265	131,000			211,936**
Lansing, N.	Harrison	7,595	22,800	1,820	54,300	30	378	256	129,000			209,000
		7,595	7,950	420	7,860	89	92	109	27,300			43,700
		7,595	24,700	121	14,600	0	18	132	66,600			106,000
		7,595	17,800	912	8,630	0	0	163	47,400			74,900
Danville	Gregg	7,320	17,900	2,370	53,300	-	45	224	114,000			188,036**
		7,320	15,300	1,570	39,000	-	50	125	93,500			149,714**
		7,320	14,900	1,600	27,000	-	0	45	73,600			117,395**
		7,320	14,500	1,500	31,300	-	135	125	79,000			126,697**
Tennessee Colony Colony	Anderson	-	2,023	708	2,023	152	-	-	-			17,800
		9,654-9,684	-	-	-	-	-	-	-			51,000
Elysian	Harrison	5,960	4,120	309	7,211	82	-	-	-			45,200
Kildare	Cass	-	348	581	4,644	81	-	-	-			246,400
		6,618-6,620	1,500	150	5,000	350	-	-	-			248,000
Carter-Gragg	Navarro	6,832-6,842	20,500	2,070	66,076	81	49	213	108,100	1.127	.052	197,008
Cornersville	Franklin	8,260-8,282	35,800	2,123	61,900	350	18	138	164,900	1.185	.046	264,879
Groesbeck	Limestone	5,604-5,762	11,147	1,452	42,663	-	106	478	89,352	1.103	.057	145,198
Henderson	Rusk	7,262-7,270	20,700	2,300	50,900	0	0	538	121,400	1.133	.049	195,838
Kildare	Cass	6,686-6,690	30,300	2,590	57,200	0	64	363	149,000	1.162	.046	239,517
Longwood	Harrison	5,626-5,646	13,000	1,810	46,210	0	110	232	99,300	1.114	.052	160,662
Manziel Brothers	Smith	8,050-8,060	24,200	6,600	36,400	173	61	297	117,900	1.136	.053	185,458
New Hope	Franklin	7,386	26,935	1,870	63,670	-	120	227	151,053	1.167	.045	243,875
		8,072	29,476	2,524	58,982	-	52	228	150,300	1.169	.044	241,562

Field	County	Depth	Constituents, Mg/liter							Sp. Gr.	Resistivity	Total Solids (mg/liter)
			Ca	Mg	Na	Ba-Sr	HCO_3	SO_4	Cl			
PETTET (KCGRL) Continued												
Pittsburgh	Camp	7,885-8,020	26,700	1,900	55,600	0	0	2,700	136,500	1.162	.048	223,400
		7,970-8,111	22,000	2,100	44,400	0	0	0	113,500	1.135	.052	182,000
		7,838-7,923	32,840	Trace	56,700	-	200	285	145,000	1.157	.047	235,025
		7,956	29,580	2,280	58,750	-	354	220	149,200	1.160	.046	240,384
Teague, W.	Freestone	7,340-7,424	21,492	2,255	61,949	-	38	440	140,000	1.138	.042	226,174
Waskom	Harrison	5,820-5,830	19,950	2,620	59,160	-	24	337	133,900	1.150	.046	215,991
		5,824-5,830	18,650	2,430	62,742	0	122	355	136,500	1.151	.046	220,799
Woodlawn	Harrison	6,673-6,786	24,000	2,150	50,900	163	30	304	127,000	1.148	.047	204,384
		6,773-6,786	24,700	2,540	55,565	345	122	298	136,500	1.155	.045	219,725
		6,788-6,796	23,600	2,320	56,613	200	43	263	135,600	1.152	.046	218,439
TRAVIS PEAK (KCTP)												
Carthage	Panola	6,081-6,090	19,255	1,598	77,000	-	-	325	119,000	1.145	.042	217,178
		6,094-6,100	20,210	2,171	80,055	-	-	254	123,645	1.151	.042	226,335
		6,101-6,108	20,609	1,930	78,865	-	-	280	121,835	1.149	.042	223,519
		6,102-6,105	20,041	1,508	79,307	-	-	307	122,493	1.149	.042	223,656
		6,103-6,105	20,234	1,870	80,200	-	-	302	123,900	1.151	.042	226,506
		6,104-6,108	19,426	1,809	83,500	-	-	272	128,800	1.155	.042	233,807
		6,118-6,122	19,495	1,930	77,500	-	-	258	119,700	1.133	.042	218,883
		6,133-6,147	19,754	1,870	79,300	-	-	304	122,500	1.149	.042	223,728
Fruitvale	Van Zandt	8,552-8,570	31,300	2,850	64,549	182	Trace	171	163,100	1.183	.044	261,970
		7,263-7,269	20,900	2,000	57,600	151	0	246	131,500	1.154	.047	212,246
		7,500-8,000	22,500	2,110	61,137	212	49	282	140,000	1.157	.042	226,078
Minden	Rusk	7,461-7,475	20,300	2,100	62,500	627	0	0	138,300	1.162	.045	223,200
Waskom	Harrison	6,100-6,200	18,328	1,866	60,622	0	112	335	131,025	1.141	.043	212,288
		6,101-6,170	14,800	1,930	56,700	586	0	320	119,000	1.134	.050	192,750
		6,193-6,239	16,700	1,840	43,100	76	293	237	101,000	1.116	.055	163,170
		6,188-6,194	18,100	2,040	55,300	581	0	230	123,000	1.137	.049	198,670
		6,236-6,246	20,750	2,210	59,561	1,069	67	355	134,700	1.154	.046	217,643
		6,236-6,246	20,240	1,871	64,135	-	67	273	140,067	1.158	.049	226,653

Field	County	Depth	Constituents, Mg/liter Ca	Mg	Na	Ba-Sr	HCO_3	SO_4	Cl	Sp. Gr.	Resistivity	Total Solids (mg/liter)
TRAVIS PEAK (KCTP) Continued												
McBee	Leon	10,039-10,204	4,058	332	16,081	0	119	70	33,679			55,280
Reka	Navarro	6,960	23,066	577	8,073	231	-	-	-			256,000
Henderson, S.	Rusk	7,550-7,568	22,428	2,234	65,386	145	196	530	146,664			237,590
Henderson	Rusk	7,475	15,390	1,440	46,685	-	25	154	104,076			168,218
Carthage	Panola	6,086-6,092	197	14	377	-	60	4	935			2,244
		6,414	19,865	1,325	70,077	-	12	237	146,387			239,425
		6,243-6,264	27,380	2,194	68,466	-	309	943	159,453			258,745
		6,672-6,690	22,677	1,222	67,456	1,360	29	398	149,847			244,341
Waskom	Harrison	6,184-6,195	17,380	1,128	53,828	-	27	489	116,095			190,638
Lansing, N.	Harrison	-	520	55	1,743	-	400	120	3,450			6,288
		7,800	21,603	1,684	62,180	-	100	392	138,656			218,915
		-	1,377	109	3,776	-	61	40	8,523			15,238
		-	3,043	72	1,946	-	414	76	8,318			16,681
Bethany	Harrison	6,241-6,265	600	100	3,000	200	-	-	-			125,000
		5,760	10,820	541	5,410	325	-	-	-			126,600
		-	11,421	343	9,137	171	-	-	-			238,100
Fruitvale	Van Zandt	8,552-8,570	39,368	2,153	81,127	-	90	260	200,774			323,772
		-	4,734	473	9,469	473	-	-	-			331,300
Manziel	Wood	8,009-8,915	25,640	2,790	63,268	-	179	212	152,238			246,599
		-	22,749	1,675	46,681	-	8	58	117,280			188,783
		8,886-8,903	19,725	1,115	37,343	-	100	64	95,758			154,307
Bryan's Mill	Cass	7,915-8,155	24,192	2,590	47,049	-	221	500	122,522			197,254
Linden, E.	Cass	7,689-7,724	22,061	2,030	46,130	-	247	1,968	114,431			186,866

Appendix B. Pressure/Depth Data from saline formations, East Texas Basin.

Raw data from Petroleum Information, Inc.

East Texas Waste Isolation

Deep Basin Hydrology

The raw data displayed in Appendix B were purchased as Proprietary Data under agreement with Petroleum Information Corporation and cannot be shown in the final report. However, interpretations of these data are included in the body of this report. For further information contact the Bureau of Economic Geology.